BIOMASS FAST PYROLYSIS
IN A FLUIDIZED BED
Product cleaning by in-situ filtration

Cover design: Xiaoquan Wang
Front cover is a prototype of filter-assisted fluidized bed reactor

BIOMASS FAST PYROLYSIS IN A FLUIDIZED BED
Product cleaning by in-situ filtration

Proefschrift

ter verkrijging van
de graad van doctor aan de Universiteit Twente,
op gezag van de rector magnificus,
prof. dr. W.H.M. Zijm,
volgens besluit van het College voor Promoties
in het openbaar te verdedigen
op donderdag 9 februari 2006 om 13.15 uur

door

Xiaoquan Wang

geboren te Xishui, Hubei China

Dit proefschrift is goedgekeurd door de promotor:

prof.dr.ir. W.P.M. van Swaaij

en de co-promotoren:

dr.ir. W. Prins
dr. S.R.A. Kersten

To my beloved family

Contents

Summary and Conclusions

The use of biomass as a renewable source of energy has been stimulated strongly by governments and international donor agencies during the last decennia for a number of different reasons, the main ones being:

- the desired reduction of green house gas emissions to the atmosphere;
- the threat of depletion of traditional fossil fuels;
- national policies to secure the energy supply by diversification of the resources.

To replace fossil fuels in the production of heat, power, transportation fuels, and chemicals, various biomass conversion routes are possible. Apart from the physical (pressing of seeds or fruits) and biochemical (anaerobic digestion, fermentation) ones, they all start with biomass combustion and gasification as a first step in the conversion chain. Since the early eighties of the past century, a new thermo-chemical conversion technique is being developed which is meant especially as a biomass pre-treatment step to facilitate its transport over long distances and to simplify its combustion and gasification. This technique is called "fast pyrolysis". While slow pyrolysis is known already for ages as a technique to produce charcoal, fast pyrolysis is meant for the conversion of biomass to an intermediate, liquid bio-fuel that has a significantly increased volumetric energy density and a much lower ash content than the original biomass. The principle of fast pyrolysis is rapid heating of relatively small biomass particles (> 5 mm) to approx. $500^{o}C$ in absence of oxygen. Like in slow pyrolysis, the biomass is decomposed to three products, viz. charcoal, condensable vapors and permanent gases. However, the product distribution is completely different in a sense that the production of condensable vapors is maximised at fast-pyrolysis conditions. Up to 75 wt % of liquid product (bio-oil) can be collected, by passing the hot vapors and permanent gas through an efficient condenser.

This thesis is dedicated to the subject of fast pyrolysis in a fluid bed reactor. A large part of the work is related to reactor design aspects of fast pyrolysis, a subject that has not been considered sufficiently. Past research efforts were focussed mainly on the kinetics of wood pyrolysis and the testing of different reactor types by measuring the bio-oil yield as a function of the reactor temperature. To enable a proper reactor and process design, more knowledge is required concerning the relations between the biomass feedstock type and the various reactor operating conditions (temperature,

1

biomass particle size, mixing conditions, residence times etc.) on the one hand, and the yield and quality of the bio-oil on the other.

Special attention is paid in this thesis work to the removal of particulates from the hot pyrolysis vapors. The presence of solid particles (char and minerals) in the condensed liquid product is highly undesired because it increases the ash content of the oil and promotes its instability, both hindering in the storage and in the application in e.g. diesel engines or gas turbines. In this thesis, the concept of in-situ filtration of hot vapors is explored. The use of cylindrical filter elements submerged in the fluid bed reactor is investigated in a number of both, cold and hot-flow experiments, and also by studying the consequences for the process design.

The literature review of Chapter 2 reveals that the information needed for reactor calculations on basis of single-particle pyrolysis rates, is insufficient. A fluid bed set-up was made to measure such rates for (mainly) cylindrical wood particles of different sizes. These measurements are described in Chapter 3. Results are interpreted with a generalized single-particle model, presented in Chapter 2 and designed to understand the influence of the most important variables. It is first of all important to recognize that biomass is a natural material with always differing features, which makes it very difficult to reproduce decomposition measurements. Despite all the experimental results and models published, the pyrolysis rate of biomass particles, and the related product selectivity, can still not be predicted very well. Only in case of heat transfer control the single particle pyrolysis rate can be calculated quite well. The yield and quality of the products however, still remain related to the biomass nature, and can therefore not be completely predicted.

The above observations explain why it is useless to apply complicated and detailed models for the prediction of single-particle pyrolysis rates, pyrolysis times and product yields, apart from learning. A simple one-dimensional model, accounting for the pyrolysis decomposition kinetics and the heat transfer to and through the biomass particle, provides sufficient accuracy for engineering calculations. From the literature it also appeared that the relation between the pyrolysis conditions and the precise composition of the products, either being charcoal, condensed vapors (bio-oil) or permanent gases, has never been investigated systematically in a single research work. To validate the various model simulations and explore the effects of pyrolysis conditions on the product composition, an extensive experimental program has been carried out using a small fluid bed as a pyrolysis reactor. Conversion times, product yields, and product compositions were measured as a function of the biomass (pine and beech wood, demolition wood and, bamboo) type, biomass particle size (up to 17

2

mm), the vapor residence time, the reactor temperature (350 - 800°C) and the biomass position in the fluid bed. The following main conclusions could be drawn.

1. Existing single particle models have a limited predictive power with respect to the product distribution and the conversion time of small particles (< 3 mm), due to a wide variation in reported decomposition kinetics.

2. The pyrolysis time of biomass particles in the size range of 1 to 5 mm, usually applied in full-scale reactors at 500°C, is influenced by all three mechanisms: the pyrolysis kinetics, the heat transfer from the bulk of the reactor to the particle, and the intra-particle heat conduction. Model calculations further show that the external heat transfer rate affects the pyrolysis time and product yields just slightly if α > 250 W/m^{2}K and d_p >1 mm.

3. Variations in bio-oil quality (e.g. water content of liquid) cannot yet be predicted by existing single particle models. Product quality is however an important design parameter. Optimal process conditions for a maximal liquid yield may differ from those for a certain desired bio-oil quality. A model is suggested that can potentially deal with these problems.

4. Product yields of pine and beech wood are similar. The bio-oil yield is maximal (65 wt % on wet basis) between 450°C and 550°C, when the water content of the bio-oil is minimal (30 to 35 wt %).

5. In the set-up used, the residence time of the pyrolysis vapors is not very critical with respect to the possible loss of condensable products; τ < 5 s seems acceptable at 500°C.

6. Both, theory and experiments show that the particle size has only a minor effect on the total liquid yield up to a diameter of 20 mm. However, for particles larger than 3 mm the water content of the produced bio-oil increases substantially.

Chapter 4 deals with the effects of in-situ filtering on the fluid bed hydrodynamics. The experimental work reported was out carried at ambient conditions in laboratory-scale equipment, and had an explorative nature. Glass beads in the size range of 100 to 300 μm were used as fluid bed particles. The purpose of the work was to study cake formation (stagnant zone around the filter) and solids mixing under gas extraction conditions.

A two dimensional air-fluidized bed of plexi-glass (12 x 3 cm cross sectional area) was used to find the conditions for which cake formation around a cylindrical filter element (sintered glass; 12 mm diameter; pore size 10 or 30 μm) is avoided. And in a second cold flow model, i.c. a cylindrical air-fluid bed (10 cm intern. diameter) made of glass, experiments were carried out to determine the influence of extraction of the

fluidizing gas through submerged filter elements (ceramic, pore size 6 μm) on the fluid bed appearance and solids mixing. In these tests a vertically oriented filter element has been used as well, next to horizontal ones. While the appearance of the fluid bed was observed visually (bubble behavior, type of fluidization), the solids mixing has been studied by measuring time dependent axial temperature profiles inside the bed after adding a certain amount of hotter bed particles to the surface of the bed at time zero.

Main conclusions of this chapter are:

1. Filter cake formation can be prevented in a fully fluidized bed;
2. If the velocity at the top of the fluid bed is used to correlate the solids dispersion coefficient to, heat transport (solids mixing) in the tested fluid beds shows the same dependency of the superficial gas velocity, with or without extraction of gases through the filters. At equal top velocity, the heat-dispersion coefficient with flow through the filter is ca. 2.5 times lower than without.

Chapter 5 describes how the concept of extracting and cleaning pyrolysis vapors by means of filters immersed in a fluid bed has been tested experimentally. For this, a batch-wise fed lab-scale fluid bed (20 g per batch) and a continuous bench-scale fluid bed (1 kg/h) have been equipped with an immersed filter (pore size between 6 and 15 micron). In short batch experiments of approx. 2 minutes, pyrolysis oils have been produced that did not contain any particles, magnesium or sodium.

While using the continuous bench-scale FB, approximately 5700 g of non-filtered oil and 3000 g of filtered oil was produced. Filtered oil contained two times less particles and 5 times less ash components than the non-filtered oil. The ash content of the filtered oil was only 0.01 wt % resulting in a very low aging rate expressed as the increase in viscosity per unit time. Silica was found on the inner walls of the filter and the downstream tubing indicating that sand fines (bed material) slipped trough the filter during long-term operation. There is evidence that the particles found in the filtered bio-oil have different origins. Part of them slipped simply through the filter, while others were formed by secondary processes (polymerization of vapors) occurring after the filter.

The last chapter of this thesis (Chapter 6 contains preliminary design calculations of a full-scale fast pyrolysis unit of 10 tons biomass per hour based on the principle of a fluid bed reactor with submerged filter elements. Based on knowledge, gained in Chapters 2 to 5 of this thesis, an engineering model has been developed to estimate the volume of a FAFB reactor. For small particle sized feedstocks (≤ 1 mm), the

required reactor volume of a FAFB is 13 m^3 including the freeboard, compared to 22 m^3 for a regular FB. For larger sized feedstocks intensification is hardly possible, because the lower reaction rate and therewith the hold-up of reacting particles dominates the reactor design. Extracting large parts of gases and vapors through the immersed filters does not result in significantly large intra-bed temperature gradients due to less intense solids mixing.

Samenvatting en Conclusies

Het gebruik van biomassa als hernieuwbare energiebron wordt de laatste decennia om verschillende redenen sterk gestimuleerd door nationale en internationale overheidsinstanties. De belangrijkste redenen zijn:

– de wens om de uitstoot van broeikasgassen te verminderen,

– de verwachting dat fossiele bronnen uitgeput raken,

– diversificatie van energiebronnen als nationaal beleid.

Er zijn verschillende mogelijkheden bekend, en reeds operationeel, om fossiele brandstoffen te vervangen door biomassa bij de productie van warmte, elektriciteit, transportbrandstoffen en chemicaliën. Voor de productie van warmte en elektriciteit is verbranding of vergassing vaak de eerste conversie stap. Mechanische (uitpersen van zaden of vruchten) en biochemische (anaerobische vergisting en fermentatie) routes worden gebruikt voor de productie van transportbrandstoffen. Sinds het begin van de jaren tachtig, is er een nieuwe thermo-chemische conversie methode in ontwikkeling. Deze conversie methode wordt aangeduid met de term "snelle pyrolyse" en is bedoeld als voorbehandeling van biomassa om het transport over lange afstanden efficiënter te maken en de verbranding en vergassing te vereenvoudigen. Langzame pyrolyse is al eeuwen bekend als een techniek om houtskool te produceren. Met snelle pyrolyse kan een vloeibare biobrandstof worden gemaakt met een veel hogere energie-inhoud per volume eenheid, en veel minder as, dan de oorspronkelijke biomassa. Het principe behelst het snel opwarmen van kleine biomassa deeltjes (< 5mm) tot circa 500 °C in afwezigheid van zuurstof. Net als bij langzame pyrolyse, wordt biomassa omgezet in drie producten: houtskool, condenseerbare dampen en permanente gassen. De verhouding van de producten verschilt echter in die zin dat de productie van condenseerbare dampen wordt gemaximaliseerd bij snelle pyrolyse. Door de hete dampen door een efficiënte condensor te leiden kan tot circa 75 gewicht % vloeibaar product (bio-olie) uit de grondstof worden gevormd.

Dit proefschrift is gewijd aan snelle pyrolyse in een wervelbed. Een groot deel van het werk heeft betrekking op aspecten van het reactorontwerp voor snelle pyrolyse, een onderwerp dat tot nu toe onvoldoende aandacht heeft gekregen. Het onderzoek was in het verleden vooral gericht op de kinetiek van hout pyrolyse, en het testen van verschillende reactor types door meting van de bio-olie opbrengst als functie van de reactortemperatuur.

7

Om de reactor en het proces goed te kunnen ontwerpen is er meer kennis nodig, enerzijds met betrekking tot de relatie tussen het soort biomassa en de verschillende bedrijfscondities van de reactor (temperatuur, grootte van de deeltjes biomassa, menging, verblijftijd, etc.), en anderzijds de kwaliteit van de bio-olie.

Het proefschrift besteedt ook aandacht aan de afscheiding van vaste stof deeltjes uit het hete pyrolyse gas. De aanwezigheid van zulke deeltjes (koolstof en mineralen) in het gecondenseerde vloeibare product is ongewenst omdat het daardoor minder stabiel wordt en tot problemen leidt bij toepassingen van het product in bijvoorbeeld motoren en turbines. In dit proefschrift wordt het concept van iin-situ filtratie onderzocht. Het gebruik van een cilindrisch filterelement ondergedompeld in een fluid-bed pyrolyse reactor is onderzocht aan de hand van experimenten uitgevoerd bij kamertemperatuur en bij verschillende pyrolyse temperaturen, en door bestudering van de gevolgen voor het procesontwerp.

Uit het literatuuronderzoek van hoofdstuk 2 blijkt dat de kennis die nodig is voor reactor berekeningen op basis van de pyrolyse snelheid van een enkel deeltje, onvoldoende is. Daarom is er een fluid bed testopstelling gebouwd om de pyrolysesnelheid voor (hoofdzakelijk) cilindrische houtdeeltjes van verschillende afmetingen te meten. De metingen worden beschreven in hoofdstuk 3 en de resultaten zijn geïnterpreteerd met het algemene rekenmodel voor enkele deeltjes dat in hoofdstuk 2 is beschreven. Het model is speciaal ontworpen om de invloed van belangrijke parameters te leren begrijpen. Het blijkt van het grootste belang te onderkennen dat biomassa een natuurlijk materiaal is met steeds verschillende eigenschappen, waardoor het erg moeilijk is om pyrolyse metingen te reproduceren. Ondanks al het experimentele werk en de gepubliceerde modellen, kan de pyrolysesnelheid van biomassa deeltjes en de bijbehorende productverdeling nog steeds niet erg goed worden voorspeld. Alleen als de pyrolysesnelheid gelimiteerd wordt door warmte overdracht, kan deze snelheid voor één enkel deeltje wel redelijk goed worden berekend. Maar, de opbrengst en de kwaliteit van de producten blijven steeds gerelateerd aan het type biomassa en kunnen ook in dat geval niet goed worden voorspeld.

Het blijkt dus zinloos om ingewikkelde en gedetailleerde modellen toe te passen voor het voorspellen van de pyrolysesnelheid van enkele deeltjes, van de pyrolysetijden, en van de productopbrengst, behalve dan om van te leren. Een eenvoudig 1-dimensionaal model dat rekening houdt met de pyrolysekinetiek en de warmteoverdracht naar en door de biomassa, is voldoende nauwkeurig voor reactor en proces

8

ontwerpberekeningen. Uit de literatuur is bovendien gebleken dat het verband tussen de toegepaste pyrolysecondities en de precieze samenstelling van de producten nooit systematisch is onderzocht, of het nu gaat om houtskool, gecondenseerde damp (bio-olie) of permanente gassen.

Er is tenslotte besloten om een uitgebreid experimenteel programma uit te voeren met als doel om verschillende modellen te valideren en om onderzoek te doen naar de effecten van pyrolysecondities op de productsamenstelling. Daarvoor is een meetopstelling gebruikt met een klein fluid bed als pyrolysereactor. Conversietijden, productopbrengst en productsamenstellingen zijn gemeten als functie van het soort biomassa (grenen- en beukenhout, plus bamboe), de grootte van de deeltjes (tot 17 mm), de verblijftijd van de damp, de temperatuur van de reactor (350 tot 800°C) en de positie van de biomassa in het fluid bed. Hieruit zijn de volgende hoofdconclusies getrokken:

1. Door grote verschillen in de gerapporteerde pyrolysekinetiek kunnen de productverdeling en de conversietijden voor kleine deeltjes niet goed met bestaande modellen voor een enkel deeltje worden voorspeld

2. De pyrolysetijd van biomassadeeltjes met een grootte van 1 tot 5 mm, zoals gebruikt in commerciële reactoren die worden bedreven bij 500°C, wordt bepaald door drie factoren, n.l.: de pyrolysekinetiek, de warmteoverdracht van het reactor bed naar het deeltje en de warmtegeleiding binnen het deeltje. Modelberekeningen laten zien dat de externe warmteoverdracht een kleine invloed heeft op de pyrolysetijd en de productopbrengst zolang $\alpha > 250$ W/m^{2}K en $d_p > 1$ mm.

3. Variaties in de bio-olie kwaliteit (bijvoorbeeld het watergehalte) kunnen niet worden voorspeld door bestaande modellen voor enkele deeltjes. Maar de productkwaliteit is wel een belangrijke ontwerpparameter. Optimale procescondities voor een maximale olieopbrengst kunnen afwijken van de optimale procescondities voor een gewenste oliekwaliteit.

4. De productopbrengst uit grenen- en beukenhout zijn gelijk. De bio-olieopbrengst is maximaal (65 gew. % op natte basis) bij een temperatuur tussen de 450 en 550°C, waarbij het watergehalte van de bio-olie minimaal is (30 tot 45 gew. %).

5.   In de gebruikte opstelling (met een lage houtskool inventaris) is de verblijftijd van de pyrolyse dampen in verband met het mogelijke verlies aan condenseerbaar product niet erg kritisch; $t < 5\,s$ lijkt acceptabel bij een temperatuur van 500°C.

6.   Zowel de theorie als de experimenten laten zien dat de deeltjesgrootte tot 20 mm slechts een kleine invloed heeft op de totale vloeistofopbrengst. Echter, voor deeltjes groter dan 3 mm neemt het watergehalte in de bio-olie wel substantieel toe.

Hoofdstuk 4 gaat over de effecten van in-situ filtratie op de hydrodynamica van het wervelbed. De gerapporteerde experimenten zijn uitgevoerd op laboratoriumschaal onder normale omgevingscondities. Glasparels met afmetingen van 100 tot 300 μm zijn toegepast als deeltjes voor het wervelbed. Het doel was de bestudering van de vorming van filterkoek, en van de menging van deeltjes terwijl gas wordt onttrokken. Een 2-dimensionaal, door lucht gefluïdiseerd wervelbed van plexiglas (12 x 3 cm in dwarsdoorsnede) is gebruikt om de condities te vinden waarbij de vorming van een filterkoek rond een cilindrisch filterelement (gesinterd glas; 12 mm diameter; poriegrootte 10 of 30 μm) wordt vermeden. In een tweede opstelling, een door lucht gefluïdiseerd cilindrisch wervelbed (10 cm interne diameter) van glas, zijn experimenten uitgevoerd ter bepaling van de invloed van gas onttrekking door filters in het bed (keramisch, poriegrootte 6 μm) op het zichtbare fluïdisatiegedrag van het bed en de deeltjesmenging. In deze test zijn er naast verticale filters ook horizontale filters getest. Terwijl het gedrag van het wervelbed visueel is beoordeeld (bellen gedrag, type fluïdisatie), is de menging van deeltjes bestudeerd door meting van tijdsafhankelijke temperatuurprofielen in het bed na toevoeging op tijdstip nul van een bepaalde hoeveelheid deeltjes met een hogere temperatuur via het bedoppervlak.

De belangrijkste conclusies van dit hoofdstuk zijn:

1.   De vorming van een filterkoek kan worden vermeden door het instellen van de juiste fluïdisatiecondities (bv. de snelheid aan het bed oppervlak moet groter zijn dan 7 maal de minimum fluidisatiesnelheid).

2.   Wanneer de snelheid boven in het wervelbed wordt gebruikt om de dispersiecoëfficiënt van de deeltjes te correleren, dan zal het warmtetransport (menging van deeltjes) met en zonder extractie van de gassen door de filters dezelfde correlatie met oppervlaktesnelheid van het gas vertonen. Er blijkt dat als de snelheid van het gas boven in het bed dezelfde is, de

warmtegeleidingcoëfficiënt voor het geval met filter circa 2.5 keer lager is dan zonder filter.

Hoofdstuk 5 beschrijft hoe het concept van de onttrekking en reiniging van pyrolysedampen door middel van filters onder het oppervlak van een wervelbed experimenteel is onderzocht. Voor dit onderzoek zijn er twee pyrolyseopstellingen gebruikt waarbij de wervelbedreactor was uitgevoerd met een filter (poriegrootte 6 en 15 μm) onder het bedoppervlak. In de eerste opstelling werd het wervelbed discontinu gevoed (20 g voeding per batch), en de tweede opstelling werd continu bedreven (1 kg/h). In korte discontinue experimenten van ongeveer 2 minuten is er pyrolyse olie geproduceerd die geen deeltjes, magnesium of natrium bevatte.

Bij het gebruik van het continue wervelbed is er ongeveer 5700 g ongefilterde en 3000 g gefilterde olie geproduceerd. De gefilterde olie bevatte een factor 2 minder deeltjes en een factor 5 minder ascomponenten dan de niet gefilterde olie. De gefilterde olie bevatte slechts 0.01 gew. %. Een laag asgehalte resulteert in stabiel product dat slechts langzaam veroudert. (De veroudering is waarneembaar als een toename van de viscositeit in de tijd.)

Op de binnenwand van het filter en de buizen stroomafwaarts is silicium gevonden, hetgeen laat zien dat fijne zanddeeltjes (bedmateriaal) het filter kunnen passeren. Vaste-stofdeeltjes die zijn teruggevonden in de bio-olie hebben een verschillende oorsprong. Een deel is eenvoudigweg door het filter geslipt, terwijl andere deeltjes zijn gevormd door secundaire processen (polymerisatie van dampen) die plaatsvinden na het filter.

Hoofdstuk 6 van dit proefschrift bevat verkennende ontwerpberekeningen voor een grootschalige installatie. Het betreft de pyrolyse van 10 ton biomassa per uur volgens het principe van een wervelbed met ondergedompelde filters. Met de vergaarde kennis beschreven in hoofdstukken 2 t/m 5 van dit proefschrift, is een ontwerpmodel ontwikkeld om het volume van een FAFB (Filter Assisted Fluid Bed) reactor te bepalen. Voor biomassa met kleine deeltjes (< 1mm), is het benodigde reactorvolume van een FAFB 13 m^3 inclusief de ruimte boven het bedoppervlak, in vergelijking met 22 m^3 voor een gewoon wervelbed. Voor biomassa met grotere deeltjes is reactor verkleining nauwelijks mogelijk, omdat de lagere reactiesnelheid, en de bijbehorende langere verblijftijd, het reactorontwerp bepalen. Onttrekking van een groot aandeel van de gassen en dampen via ondergedompelde filters veroorzaakt geen grote temperatuurgradiënten in het bed als gevolg van minder intensieve deeltjesmenging.

概要与结论

近几十年来用生物质作为可再生能源受到各级政府及国际捐赠机构的大力推动有各种各样的原因，其中主要有：
— 期望减少温室气体向大气中的排放；
— 传统化石燃料日益枯竭的威胁；
— 通过资源多样化确保能源供应安全的国家政策。

为了替代用于供热、发电、车用燃料及制造化学品的化石燃料，有多种可能的生物质转化路线。除了物理的（植物种子或果实的压榨）及生物化学的（厌氧消化，发酵）方法外，其它的都把生物质燃烧或气化作为生物质转化链中的第一步。自上世纪八十年代初，一种新兴的热化学转化技术得到开发，它特别适合作为生物质预处理步骤来弥补长途运输带来的不便，以及简化燃烧和气化工艺。这种技术称为快速热解。尽管用来制造木炭（半焦、焦炭）的慢速热解技术已有很长的历史，但快速热解的主要目标却是将生物质转化成液态中间燃料，它能够显著提高能量密度，并降低原始生物质中的灰含量。快速热解的原理是将相对较小的生物质颗粒（≤5毫米）在无氧的条件下迅速加热到 500°C 左右。和慢速热解一样，生物质会被分解成三种产物，即半焦、可凝性蒸汽以及永久性气体。然而两者的产物分布完全不同，可凝性蒸汽的收率在快速热解条件下最高。让热的蒸汽及永久气体通过高效冷凝器可收集到高达 75%（重量）的液体产物（生物质油）。

本论文研究流化床反应器中的快速热解技术。本工作的主要部分涉及快速热解反应器的设计，这一课题在以前的研究工作中尚未得到充分地考虑。以往的研究工作主要集中在木材热解动力学及在各类反应器中生物质油的收率与反应器温度的关系。为了恰当地设计反应器及其工艺，一方面需要更多地了解生物质原料种类和各种反应器操作条件（温度、生物质颗粒大小、混合状况、停留时间等）的影响，另一方面还需要了解收率和油品质量的关系。

本论文还特别探讨了如何从热的热解蒸汽中除去固体粒子。在冷凝液体产物中存在固体粒子（半焦及矿物质）是非常有害的。因为它会增加油品的灰含量，加剧了生物质油的不稳定，这两点都会妨碍油品储存及其在柴油机或燃气轮机中的应用。本文探讨了就地过滤热解蒸汽的概念。通过大量的冷、热态试验考察了将圆柱形过滤管插入流化床反应器后的行为，并且研究了它对工艺设计造成的影响。

第二章文献综述揭示了基于单颗粒热解速率进行反应器设计计算所需的信息是不够的。为此设计了一套流化床装置来测定不同大小的柱状木材颗粒的反应速率。这些测量在第三章中作了阐述。实验结果用在第二章中描述的通用单颗粒模型作了解释，并由此来理解一些重要操作变量带来的影响。首先要认识到生物质是一种某些性质常在变化的天然材料，这一点使得很难重复热分解测量结果。尽管已经有很多测量结果和模型发表，但生物质颗粒的热解速率以及相关产物的选择性还是不能得到很好地预测。只有在传热控制的条件下才能很好地计算单颗粒热解速率。但是热解产物收率及其品质，依然和生物质自然属性相关，因而难以得到圆满地预测。

上述观察结果说明了为什么复杂而详尽的数学模型来预测单颗粒热解速率、热解时间及产品收率除了学习之外并无多大用处。简单的、包含热分解动力学以及生物质颗粒间粒内传热的一维模型足以达到工程计算所需的精确度。从现有的文献可知：热解条件和产物的精确组成，无论是半焦、可凝结性蒸汽（生物质油）还是永久气体的关系从未得到系统地研究。为了验证各种模型的模拟结果以及热解条件对产物组成的影响，采用一小型流化床作热解反应器作了大量实验，分别对转化时间、产品收率以及产物组成与生物质种类（松木、山毛榉及竹材）、生物质颗粒大小（达 17毫米）、蒸汽停留时间、反应器温度（350°C～800°C）以及生物质在流化床中的位置的关系作了测量，得出的主要结论如下：

1. 由于文献报道的动力学参数变化范围过宽，现有的单颗粒模型对产物分布及小颗粒（<3毫米）生物质的转化时间的预测能力有限。
2. 通常在满负荷反应器内采用的粒子大小在 1～5 毫米之间、反应温度为 500°C，生物质颗粒的热解时间受三种机理控制：热解动力学、反应器主体部分向粒子部分的热量传递、颗粒内部的热传导。模型计算结果进一步表明当外部传热系数大于 250W/m^{2}K 时，颗粒大于 1 毫米时，外部传热速率对热解反应时间以及产品收率的影响很小。
3. 生物质油的品质（即液体中的水分含量）变化不能通过现有的单颗粒模型预测。然而产品质量又是一个重要的设计参数。基于最高的液体产物收率的最优工艺条件可能有别于满足特定油品质量的条件，这些问题有望通过新建模型得以解决。

13

4.	松木（软木）和山毛榉（硬木）的产品收率相近，生物质油的收率在 450℃ 至 550℃ 之间最高（湿基收率为 65％），并且此时生物质油中的水分含量最低（30wt% 至 35wt%）。
5.	在所用的装置中，热解蒸汽的停留时间造成的可凝性产物的可能损失并不重要，反应器在 500℃ 时，停留时间低于 5 秒是可以接受的。
6.	理论和实验都表明颗粒大小（达 20 毫米）对全液体的收率影响很小，然而当粒子大于 3 毫米时产物油中的水分含量显著增加。

第四章探讨流化床中的流体动力学对就地过滤的影响。试验工作是在室温条件下于一小型设备中进行的，具有探索性。用于流化的玻璃珠大小介于 100 至 300 微米之间。实验目的是要研究在有气体不断被移出的条件下滤饼的形成以及固体粒子的混合特性。

用有机玻璃制成的二维流化床（截面为 12 厘米乘 3 厘米）来考察圆柱状过滤元件（烧结玻璃，直径为 12 毫米，孔径为 10 或 30 微米）的周围免生滤饼的条件。在另一冷态装置中，即由玻璃制成的圆柱状流化床（内径为 10 厘米）中考察由浸没在流化床中的过滤管元件（陶瓷质，孔径为 6 微米）抽出气体后对流化床行为的影响以及固体混合状况。在这些试验中除了采用水平放置的过滤管，还用到了垂直放置的过滤管。自某零时刻向床面添加一定量的热的床料，通过测量床内与时间相关的轴向温度分布来考察固体混合状况。本章主要结论如下：
1.	在完全流化的床内可以防止过滤管周围滤饼的生成；
2.	如果用流化床顶部的气体速度来关联固体粒子的轴向热扩散系数（表征固体混合），无论有还是没有从过滤管抽出气体均表现出相同的表观气速依赖关系。在相同的顶部气速条件下，有气体从过滤管抽出时的热扩散系数要比没有气体抽出时低 2.5 倍。

第五章阐述了通过浸没在流化床中的过滤管抽出热解蒸汽及其净化的实验过程。为此，分别在一间歇式操作的小型流化床（每批处理 20 克）及一套连续操作的流化床（1kg/h）中装配了过滤管（孔径在 6 至 15 微米之间）。在短时间（约 2 分钟）间歇式试验中，热解制得的生物质油几乎不含任何固体粒子、镁或钠离子。

但是在连续操作的小型流化床中制备了 5700 克未过滤油及 3000 克过滤油。过滤油中所含的固体粒子要比未过滤油低 2 倍，灰含量要低 5 倍。过滤油中灰含量只有 0.01wt%，使得以单位时间内粘度增加值为指标的油品老化速率很低。在过滤管内壁及其下游管道中发现硅的存在表明部分微细的砂质会由于长时间操作穿透过滤管。有迹象表明过滤油中所含的固体粒子起源不尽相同。一部分仅仅是简单地穿透过滤管，另一部分则是由于过滤后地二次作用（热解蒸汽发生聚合作用）。

论文的最后一章（第六章）涉及满负荷为每小时处理 10 吨生物质带过滤管的流化床的初步设计。基于本论文第二至第五章所获得的知识，发展了一套用于估算过滤管辅助流化床（FAFB）体积的工程模型。对于细小的原料粒子（≤1mm），所需的 FAFB（含沉降段）体积为 13 立方米。相比之下，所需常规的流化床则要求原料粒子 22 立方米。对于比较大的原料粒子，这种强化作用几乎不太可能。因为低得多的反应速率以及由此带来的反应粒子含率限制了这种可能。通过浸没在床内的过滤管抽出大部分气体并不会带来由于减弱的固体混合而产生的明显的床内温度梯度。

Chapter 1

General Introduction

Biomass and its Conversion

Biomass, one of the renewable resources, is a material of recent biological origin. Examples of biomass are wood waste from the timber industry, agricultural, forestry and plantation residues, animal waste (manure), and the organic components of municipal and industrial waste. Ever since mankind obtained the control over fire, biomass has been used as fuel. At present about 10% of the world's need for energy is directly derived from biomass, mainly in the developing countries and via traditional methods [1-3].

A large fraction of the world population already relies on biomass as a main source of energy. Nowadays renewable biomass, produced in a sustainable way, is recognized as an attractive alternative to fossil fuels for which the resources are finite and in some cases geographically restricted (e.g. crude oil). In principle biomass derived energy has no net carbon dioxide (CO_2) impact on the atmosphere and is therefore advantageous in offering resistance to a climate change due to the greenhouse effect. The bio-energy production chain is relatively labour-intensive and may provide many local jobs, skilled and unskilled, also in developing countries. Moreover, biomass can play a role in improving the countries' energy security as part of a diversification strategy. In recent decades, the need to meet the increasing energy demands, without sacrificing the world's resources too quickly and damaging the environment, gave an important stimulus to the development of technologies for biomass conversion to modern energy carriers such as electricity, liquid biofuels, syngas and hydrogen.

There are several ways to transfer the energy contained in biomass, ranging from traditional combustion to gasification and liquefaction. Production of gaseous and liquid fuels can be done by thermo-chemical and biological methods (methane, alcohol). Here, only the thermo-chemical routes are discussed.

Direct combustion is the traditional way of using biomass and is widely practiced to provide heat and power. The technology is commercially available and presents minimum technological risks to investors. In combustion, the biomass is completely transformed to heat, which must then be consumed or used for power generation immediately, because storage is not a viable option. Overall efficiencies to power tend to be rather low: typically 15% for small plants up to 35% for large modern plants. Biomass combustion systems are currently only competitive when wastes are used as feedstock material such as residues from the pulp and paper industry (black liquor), plantations (bagasse), agriculture (malasse, rise husk), and forestry (thinnings). Emissions and ash disposals need to be controlled carefully. Fluid bed and grate combustors are, however, widely implemented throughout Asia, North America and Europe, frequently utilizing forestry, agricultural and industrial wastes. Next to stand-alone systems fuelled with biomass only, also co-combustion in coal fired furnaces of power plants is practiced increasingly.

Biomass can be gasified at temperatures below 900°C by different technologies [4-6] to produce a gas containing carbon monoxide (CO), hydrogen (H_2), methane (CH_4), and a small amount of hydrocarbons including tars. If air is used as a gasification agent the gas will be diluted with nitrogen and cannot be transported economically over large distances, nor stored, and has to be used at once. Direct coupling of such an air-blown gasifier to a combustor provides advantages in emissions and process control, and allows for co-firing of biomass in existing fossil fuel based furnaces.

In principle it is also possible to produce syngas (an undiluted mixture of H_2 and CO) from biomass by entrained-flow gasification with pure oxygen or oxygen/steam mixtures at high temperature (> 1300°C) en pressure (40 to 80 bar). Although for coal, mineral oil, and natural gas many large-scale gasification plants have been built and operated successfully over decades [7], the same technology is not yet available for full-scale biomass operation. However, a start has been made with the development of entrained-flow biomass gasifiers. Recently, successful runs at pilot and demonstration scale have been carried out [8-10]. Indeed, methanol or Fischer-Tropsch diesel could in principle be produced from biomass derived syngas [11,12]. For economical

18

reasons however, the existing Fischer-Tropsch and methanol plants have capacities of over 10^6 ton/year. In case low-density (~ 100-300 kg/m^3) agricultural or forestry waste would be considered as a feedstock material, the collection, transport and storage of the required large quantities represent a huge challenge. From an ecological point of view, the withdrawal and movement of the minerals from the biomass production areas to the industrials sites could become a serious threat to the sustainability of this conversion route.

In the distant future, such large-scale plants based on solid biomass might be possible and economically viable [13-15]. For the near future a simple and cheap liquefaction process to be applied in the biomass production areas as a pre-treatment step, offers many advantages.

Decentralized Liquefaction of Biomass

Biomass derived from agricultural and forestry waste, and consisting mainly of lignocellulose, is typically produced in quantities of around 10 tons dry material per hectare per annum [13,16] depending on various factors. Biomass grown especially for energy production (miscanthus, willow, poplar, etc.) can have higher yields, viz. up to 20 tons/ha. The highest potential is in the utilization of waste and residues, which are cheap and altogether represent an energy content of half the crude oil production [17]. Such resources are indeed abundant but dispersed over large areas, depending on the soil condition and climate.

Biomass liquefaction to an intermediate energy carrier, at a scale that matches the local logistics of collection and storage, seems to be beneficial in case it:

- has an energy density of up 10 times higher than the biomass bulk material of which it has been made;
- can be handled and stored easily as a uniform low-viscosity liquid without any risk of natural degradation;
- can be collected from various production areas and shipped easily over long distances to central sites for further applications;
- can be traded in large quantities as a world wide commodity through the existing infrastructure of bulk tankers and harbour facilities;
- can be pressurized and pumped through pipelines;
- can be used as a liquid fuel in modern conversion equipment (gas turbines, diesel engines, oil and gas furnaces);
- can be used as a source of oxygenated chemicals;

- can be converted to syngas by the proven technology of oil gasification;
- can be co-fed to a traditional crude oil refinery after a proper pre-treatment (de-oxygenation).

Such a liquefaction process should preferably:
- be safe, simple and easy to operate at atmospheric pressure and moderate temperatures;
- produce a stable non-toxic uniform liquid, with a high energy density and favorable transport, storage and combustion properties;
- have a high liquid yield and high thermal efficiency;
- have favorable economics even at low production capacities (10,000 - 50,000 ton/year);
- be omnivorous, accepting all kinds of biomass and residues;
- recover the minerals and allow them to be returned to the soil as essential nutrients belonging to the production area.

A liquefaction process for biomass fulfilling all these wishes is not (yet) available. Biological production of alcohol is very successful in countries like Brazil, the US and Canada [18,19], but at industrial scale, only sugars and carbohydrates can be converted in this way. New developments [20,22] have led to enzymatic conversion of cellulose into sugars suitable for alcohol production. Future efficiencies, yields, economics and scale of operation are not yet known. Recently, lingo-celluloses materials have been converted successfully to bio-ethanol in the pilot facility of the IOGEN company (EcoEthanol™ process) [23].

Hydrothermal liquefaction is process converting water/biomass slurries into light and heavy products that contain significantly less oxygen than the original biomass due to formation of H_2O and CO_2 during conversion. The process conditions are pretty severe as high pressures are required (150 - 200 bar) and moderately high temperature (250 - 350°C). In the hydrothermal liquefaction process, the products are called light biocrude and heavy biocrude respectively. Without further treatment the products are at least partially solid at ambient conditions. In The Netherlands, the process is being developed since 1998 by a company called Biofuel BV [24], on pilot scale.

Fast pyrolysis is a liquefaction process that at least fulfils a large part of the list of wishes given above. While still under development it is approaching the commercial

20

application. The present thesis is focused on further improvement of this process, which will now be discussed in more detail.

Pyrolysis

Pyrolysis is a conversion technique in which biomass is transformed to gaseous, liquid and solid products that can be used as improved fuels or intermediate energy carriers. Essentially the method consists in heating the biomass in an inert atmosphere up to a certain desired temperature. Both, during heating and at the final temperature, decomposition of biomass takes place in a complex interaction of mass and heat transfer with chemical reactions, resulting in the evaporation of water and vapors and production of some non-condensable gases. A solid matrix (char) consisting of carbon mainly, but including most of the minerals, is left. A large part of the produced vapors can be condensed to a brown liquid, leaving the non-condensable gases as a combustible fuel for immediate use. The precise distribution of products depends on many factors like heating rate, final temperature, operating pressure, residence times of the vapors and the converting biomass and their states of mixing. Moreover, several feedstock properties like particle size, water and ash content, composition, structure related properties, etc., are influencing the process and product compositions.

Mankind has used pyrolysis of biomass for ages, perhaps from shortly after gaining the full control of fire making. In the past, pyrolysis processes were focussed on char production in for example sand covered piles of wood, brick kilns and retorts, with tars as a second product. Over the last two centuries pyrolysis processes for fuel gas production from coal or biomass have been practiced on a rapidly increasing scale. Also the production of wood chemicals (methanol, acetic acid) has been practiced in the past.

Pyrolysis processes directed to the production of liquid fuels or intermediate energy carriers became subject of study in the last quarter of the former century and during the nineties the first pilot plants were realized [25-27].
They were based on the notion that for the production of mainly liquid fuels, biomass should be heated up rapidly ("fast pyrolysis") or even extremely fast ("flash pyrolysis") and that vapor products should be rapidly cooled to avoid secondary conversion to carbon and permanent gases in consecutive reactions. Temperatures applied were in the range of 400 - 600°C and different reactor types were used (see Figure 1).

The work of this thesis is focussed on "fast pyrolysis" which is usually carried out at atmospheric pressure in the temperature range of 400 - 600°C. For research purposes a wider range of operation conditions is sometimes explored. There are two special routes described in the literature for pyrolysis oil production, basically different from the common type of process, vacuum pyrolysis and ablative pyrolysis. A German company called Pytec is currently scaling up the ablative pyrolysis technique [28]. Vacuum pyrolysis was invented at the Laval University and has been scaled up by Pyrovac, a Canadian company [29]. Application of vacuum enhances the release of vapors from the biomass particles and therefore enables coarser materials to be used as a feedstock.
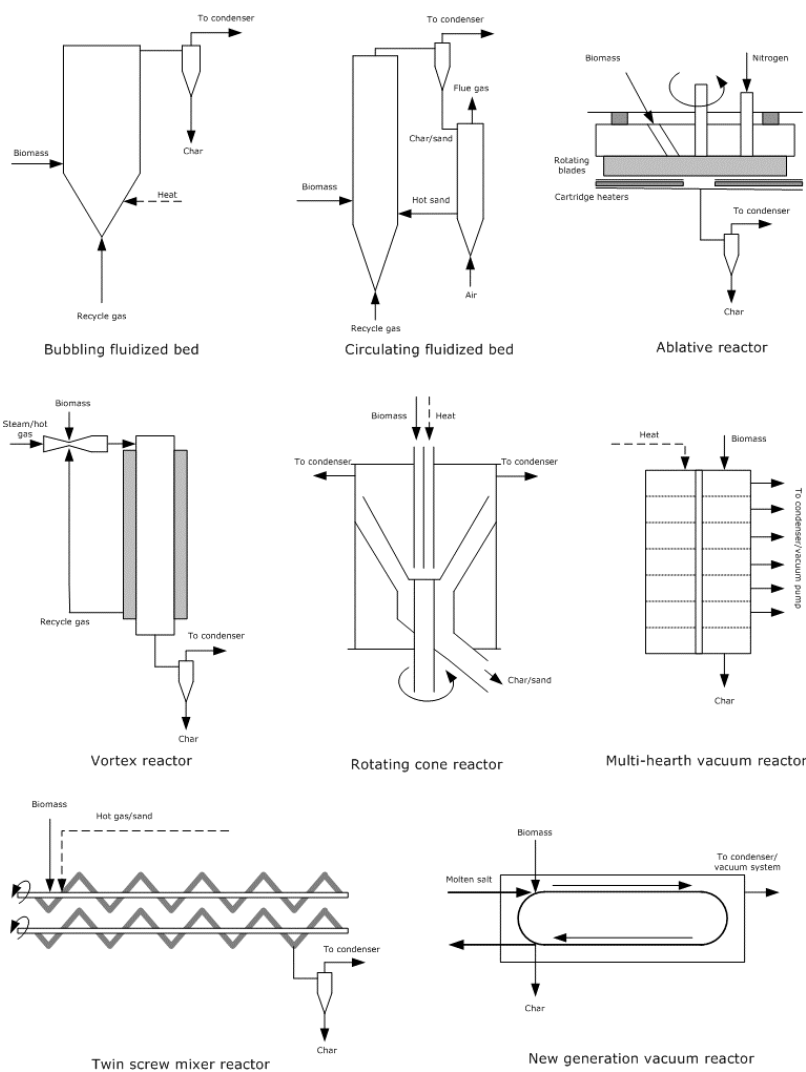

Figure 1. Various reactor types used in biomass pyrolysis processes.

The biomass is conveyed over a moving belt and heated indirectly by molten salts. The application of vacuum and the way of heating make the process quite complex. There is also an increased risk for explosion or fire as oxygen may be sucked into the reducing atmosphere from outside in case of any leakage.

In ablative pyrolysis, which is based on the principle to press large biomass particles (usually wood) against a moving heated wall, it is attempted to continuously remove the product layers that are supposed to be formed at the surface of the biomass particle during its conversion. In this way the resistance for rapid heating, otherwise caused by the presence of a char product layer, is eliminated [30,31]. For regular fast pyrolysis various pilot plants have been built, often based on dense or circulating fluid beds. Table 1 provides an overview.

Table 1. Overview of various pyrolysis technologies at pilot-plant scale.

Plant owner / Location	Reactor type	Capacity kg/h
BTG/NL	Rotating cone	200
Wellman/UK	BFB	250
	BFB	500
Dynamotive/CA	CFB	400
Ensyn/USA	CFB	1000
ENEA/IT	CFB	650
Union Fenosa/ES	BFD	150
Pyrovac/CA	Vacuum	50

Another special case is the rotating cone reactor. In this technology first developed by the University of Twente [32,33]. The biomass is brought into intimate contact with a heat carrier (for example sand) in the centre of a spinning cone from where the mixture is swept along the wall in upward direction. Vapors escape from a thin solids layer and flow towards the condenser as a consequence of the resulting pressure increase. Since no inert carrier gas is required in the reactor, a dilution of the vapors is avoided which facilitates the condensation of pyrolysis liquid. The heat carrier plus the produced char are transported to a separate section for reheating by combustion of the char. BTG (Biomass Technology Group B.V.) further developed this technology,

23

and after a few years of pilot plant testing (5 ton/day intake), they recently delivered the first commercial unit for the conversion of 50 tons/day palm plantation residues to a client in Malaysia. At the time of writing this thesis, the first successful runs were completed.

Apart from the small but attractive market for flavor production (commercial bio-oil production by Ensyn for Red Arrows [34]), a bulk market for pyrolysis oil is still to be developed. Important barriers are the lack of a completely demonstrated technology, the fluctuating energy market for fossil fuels and some real and/or perceived problems related to the bio-oil quality. The latter refers to phenomena like a high acidity (corrosion), instability caused by re-polymerisation reactions, separation of a water phase, and the presence of particulates (entrained char and ash particles).

The presence of solid particles in the oil may affect the oil quality by:

- promoting the instability due to settling;
- promoting the instability by the formation of nuclei/catalysts for polymerisation or cracking reactions;
- increasing the ash content of the oil;
- hindering the combustion in e.g. diesel engines;
- reducing the re-evaporation properties in case of secondary processes (reforming of bio-oil to hydrogen, combustion in gas turbines).

Filtering

Of course, the pyrolysis oil can in principle be filtered to remove the particles. This however, is not an easy process. Part of the condensed bio-oil will stick to the particles leading to losses, and filter cakes may cause problems in decreasing the permeability (high pressure drops required) and complicating the washing. Moreover, the ash removal efficiency may suffer from dissolved minerals (due a high water content) passing through the filter anyway. A better approach might be high temperature filtration of the vapors immediately after their formation. This could be done in a separate unit, for example an assemblage of candle filters, placed between the pyrolysis reactor and the bio-oil condenser. Hot gas filtration is under development for advanced power generation systems and appears to be quite a challenge, mainly because the filter materials need to withstand severe conditions easily leading to corrosion, erosion, blocking, and rupture or cracking. Filter cleaning is a particular problem that needs to be solved as well. In case of pyrolysis vapors an

additional difficulty is the presence of entrained char and aerosols that may condense on the filter and cause sticky deposits.

Part of this thesis will be on integration of the production and filtration operation. It may save a separate filtration unit and lead to intensification of the production operation in case of a fluid bed pyrolyser.

The idea is to remove the produced gas and vapors mainly through an assemblage of filter units submerged in the fluid bed, and just for a small part through the upper surface area of the fluid bed. The filtered stream of gases and vapors are then sucked away through a manifold to the condenser. An additional advantage could come from the shorter residence time of the pyrolysis vapors which are largely by-passing (part of) the bed, the entire freeboard and the cyclone(s) in this new concept.

The set-up of such a unit requires a careful and special design in which the fluidization at each level in the bed is maintained by the formed vapors. Controlled removal of product gases over the bed height is essential and dilution with additional fluidization gases should be avoided.

Outline of the Thesis

The literature review included in Chapter 2 revealed that the information needed for reactor calculations on basis of single particle conversion rates, is insufficient. Therefore a special experimental set-up was made to measure such conversion rates for (mainly) cylindrical wood particles of different sizes. The measurements are reported in Chapter 3. Results are interpreted with a generalized particle model (described in Chapter 2) and designed to understand the influence of the most important variables. This model predicts the conversion rates of individual wood particles with sufficient accuracy for design and engineering purposes.

To allow the study of filtering in a fluid bed, various measuring/visualisation set-ups have been constructed and operated. Some filter design rules for the filters and the limits for cake formation have been determined. The influence of the filtering on the hydrodynamics of the fluid bed (including back mixing in the fluid bed) has been considered. Results and first attempts on modelling are presented in Chapter 4.

Finally, a small pilot plant for continuous production of bio-oil from about 1 kg biomass per hour has been designed and constructed in order to demonstrate the concept of fluid pyrolysis with integrated filtration. Eventually, the production of filtered and ash free pyrolysis oil succeeded; the results are given in Chapter 5.

The last chapter of this thesis (Chapter 6) contains the elements of a preliminary design of a full-scale fast pyrolysis unit of 10 tons biomass per hour based on the principle of a fluid bed reactor with submerged filter elements. The design considerations reveal both the potential and the limits of the concept. Reactor intensification is possible if the fast pyrolysis process is fast enough to keep the biomass/char hold-up below reasonable limits.

References

1. World Energy Supply Scenario: 200-Year Picture Sustained Growth Scenario, Royal Dutch Shell, 1995.

2. IEA, World Energy Outlook 1998, IEA/OECD, Paris, France, 1998.

3. Solantausta, Y., Podesser, E., Beckman, D., Ostman, A., Overend, R.P., IEA Bioenergy task 22: Techno-economic assessments for bioenergy applications, Final report, Technical Research Centre of Finland: Espoo, 2000.

4. Bridgwater, A.V., Ed. Thermo-Chemical Processing of Biomass; Butterworths: London, UK, 1984.

5. Bridgwater, A.V., Toft, A.J., Brammer, J.G., A techno-economic comparison of power production by biomass fast pyrolysis with gasification and combustion; Renewable and Sustainable Energy Rev., 2002. 6, pp. 181-248.

6. Beenackers, A.A.C.M., Maniatis, K., Gasification technologies for heat and power from biomass; In Biomass gasification and pyrolysis: state of the art and future prospects, Kaltschmitt M., Bridgwater, A.V., Eds., CPL Press, UK, 1997, pp. 24-52.

7. Higman, C., van der Burgt, M., Gasification; Gulf Professional Publishing, Boston, USA, 2003, 391.

8. Henrich, E., Weirich, F., Pressurized Entrained Flow Gasifiers for Biomass; Envir. Eng. Sci., 2004. 21, pp. 53-64.

9. Henrich, E., Dinjus, E. Tar-free, high pressure synthesis gas from biomass; In Expert meeting on Pyrolysis and Gasification of Biomass and Waste, Strasbourg, France: CPL Press, UK, 2002.

10. CHOREN, Electricity and heat from biomass: Carbon-V process.

11. Calis, H.-P., Haan, J.P., Boerrigter, H., van der Drift, A., Peppink, G., van den Broek, R., Faaij, A.P.C., Venderbosch, R.H., Preliminary techno-economic analysis of large-scale synthesis gas manufacturing from imported biomass; In Expert meeting on Pyrolysis and Gasification of Biomass and Waste, Strasbourg, France, CPL Press, UK, 2002.

12. Boerrigter, H., den Uil, H., Calis, H.-P., Green diesel from biomass via Fischer-Tropsch synthesis: new lights in gas cleaning and process design; In Expert meeting on Pyrolysis and Gasification of Biomass and Waste, Strasbourg, France: CPL Press, UK, 2002.

13. Junginger, M., Faaij, A., van den Broek, R., Koopmans, A., Hulscher, W., Fuel supply strategies for large-scale bio-energy projects in developing countries. Electricity generation from agricultral and forest residues in Northeastern Thailand, Biomass and Bioenergy, 2001, 21, pp. 259-275.

14. Hamelinck, C.N., Faaij, A.P.C., den Uil, H., Boerrigter, H., Production of FT transportation fuels from biomass: technical options, process analysis and optimisation, and development potential; Utrecht University, Utrecht, The Netherlands, 2003.

15. Ouwens, C.D. Faaij, A. A comparison of the production costs and the market introduction of Fischer-Tropsch oil and Ethanol; In Twelfth European Biomass Conference: Biomass for Energy, Industry and Climate Protection, Amsterdam, The Netherlands: ETA-Florence and WIP-Munich, 2002.

16. Toft, A.J., A comparison of integrated biomass to electricity systems, Ph.D. Thesis, University of Aston, Birmingham, UK, 1996.

17. Groeneveld, M., personal communication with Michiel Groeneveld; Shell Global Solutions, Amsterdam, 2004.

18. Rosillo-Calle, F., Cortez, L.A.B., Towards ProAlcool II - a review of the Brazilian bio-ethanol programme; Biomass & Bioenergy, 1998, 14, pp. 115-124.

19. Ward, O.P., Singh, A., Bio-ethanol Technology: Developments and Perspectives; Adv. Appl. Microbiology, 2002, 51, pp. 53-80.

20. Tassinari, T., Macy, C., Differential speed two roll mill pre-treatment of cellulosic materials for enzymatic hydrolysis; Biotechnology and Bioengineering, 2004, 19, pp. 1321-1330.

21. Schell, D.J., Farmer, J., Newman, M., McMillan, J.D., Dilute-Sulfuric Acid Pretreatment of Corn Stover in Pilot-Scale Reactor: Investigation of Yields, Kinetics, and Enzymatic Digestibilities of Solids; Applied Biochemistry and Biotechnology, 2003, 105-108, pp. 69-85.

22. Palonen, H., Role of lignin in the enzymatic hydrolysis of lignocellulose; Helsinki University of Technology: Espoo, Finland, 2004.

23. Lawford, H.G., Rousseau, J.D., Cellulosic Fuel Ethanol: Alternative Fermentation Process Designs with Wild-Type and Recombinant Zymomonas mobilis; Appl. Biochem. Biotechn., 2003, 106, pp. 457-470.

24. Naber, J.E., Goudriaan, F., van der Wal, S., Zeevalkink, J.A., van de Beld, B., The HTU Process for Biomass Liquefaction: R&D Strategy and Potential Business Development; In The 4th Biomass Conference of the Americas. Oakland, CA, USA, 1999.

25. Bridgwater, A.V., Bridge, S.A., A review of biomass pyrolysis and pyrolysis technologies; In Biomass pyrolysis liquids upgrading and utilisation; Elsevier Science Publishing Co., New York, 1991, pp. 11-92.

26. Bridgwater, A.V., Czernik, S., Diebold, J., Meier, D., Oasmaa, A., Peacocke, C., Piskorz, J., Radlein, D., Eds., Fast Pyrolysis of Biomass. A handbook. CPL Press, UK, 1999.

27. Kersten, S.R.A., Wang, X., Prins, W., van Swaaij, W.P.M., Biomass pyrolysis in a fluidized bed reactor: Part I. literature review and model simulations; Ind. Eng. Chem. Res., 2005, pp. 8773-8785.

28. Meier, D., Schoell, S., Klaubert, H., New ablative pyrolyser in operation in Germany; PyNe newsletter, 2004, Issue 17.

29. Roy, C., Morin, D., Dube, F., The biomass pyrocycling[TM] process; In Biomass gasification and pyrolysis: state of the art and future prospects; Kaltschmitt, M., Bridgwater, A.V., Eds., CPL Press, UK, 1997, pp. 307-315.

28

30. Lede, J., Comparison of contact and radiant ablative pyrolysis of biomass; J. Anal. Appl. Pyrolysis, 2003, 70, pp. 601-618.

31. Lede, J., Panagopoulos, J., Li, H.Z., Villermaux, J., Fast Pyrolysis of Wood: direct measurement and study of ablation rate; Fuel, 1985, 64, pp. 1514-1520.

32. Wagenaar, B.M., The rotating cone reactor: for rapid thermal solids processing; Ph.D. Thesis, University of Twente, Enschede, The Netherlands, 1994.

33. Janse, A.M.C., A heat integrated rotating cone reactor system for flash pyrolyisis of biomass; Ph.D. Thesis, University of Twente, Enschede, The Netherlands, 2000.

34. Freel, B.A., Graham, R.G., Method and apparatus for a circulating bed transport fast pyrolysis reactor system; US Patent 5,792,340, 1998.

30

Chapter 2

Biomass Pyrolysis in a Fluidized Bed Reactor. Part I: Literature Review and Model Simulations

Abstract

The literature on biomass pyrolysis regarding kinetics, models (single particle and reactor), and experimental results is reviewed from an engineering point of view. Predictions of existing single particle models derived from a detailed description of the transport phenomena and literature data on measured intrinsic chemical kinetics are presented. The main conclusions from the literature and modeling studies can be summarized as follows: 1) the available knowledge on kinetics and transport phenomena has not been integrated properly for reactor design, 2) complex two-dimensional single particle models do not provide more accurate, or otherwise better, information for engineering calculations than do the simple one-dimensional models, and 3) single particle models predict (for all available kinetics) that the influence of the particle size on the liquid yield is limited. This effect can be explained with the effective pyrolysis temperature, a parameter that represents the particle's average temperature at which the conversion is essentially taking place.

1. Introduction

Biomass is becoming increasingly important as a renewable source. Fast pyrolysis is one of the possible technologies facilitating the fuelling of biomass into a wide variety of energy production installations. It is a high temperature (ca. 500°C) process in which biomass is rapidly converted, in the absence of oxygen, to vapors, gases, and charcoal. After cooling and condensation, a dark brown liquid is formed that is often called bio-oil. The process is optimized toward maximal bio-oil production. Apart from direct combustion in boilers or prime movers for the production of heat, shaft power, or electricity, bio-oil is also considered for upgrading to blending components for transportation fuel through either hydrogenation [1,2] or gasification followed by Fischer-Tropsch or methanol synthesis [3–7].

From pyrolysis handbooks and overview papers [8-15], it is learned that for optimal fast pyrolysis in terms of liquid yield, the temperature required is approximately 500°C, the biomass particle size should be small ($\leq$ 2 mm), and the produced vapors should be separated from the char and condensed immediately to prevent secondary cracking to gaseous products.

The last two statements are insufficiently supported by theoretical or experimental evidence. In some cases, even contradictory experimental findings have been reported in the literature. These statements are, however, crucial for reactor and process design. For instance, a reevaluation of the most suitable reactor configuration would be required if larger biomass particles could be used. Moreover, it is insufficiently recognized that the process temperature for a maximum liquid yield may differ from the one for a specific bio-oil quality.

This research includes two separate parts. Part I is concerned with a literature review and modeling studies, while part II [16] contains the experimental validation of model results. It is meant to study fast pyrolysis in fluid beds and to clarify the reference points for reactor design. Although the research is dealing mainly with pyrolysis in a fluidized bed, application of the results presented is not restricted to it. The fluid bed experiments reported in part II are representative for pyrolysis carried out under known and spatially isotherm external conditions, and high heat transfer rates to the particle. Apart from fluidized beds, those conditions prevail in many other reactor types such as a circulating fluid bed, a transported bed reactor, a rotating cone, or a cyclonic reactor. Fixed bed type reactors, screw reactors, and ablative reactors are, however, of a different nature [17].

32

The behavior of the individual biomass particles inside the reactor is important for the design of a pyrolysis reactor. Parameters such as the conversion time (reaction rate), the time-averaged bio-oil yield and quality, and the particles' residence time and spatial distribution are essential. They are determined by the feedstock type and dimensions, as well as by the prevailing reactor conditions (e.g., the external heat transfer coefficient). The conversion time and the time-averaged yields can be predicted with single particle pyrolysis models. Once the particles' devolatilization rate is known, the required hold-up of reacting particles (ranging from fresh biomass to charcoal) in the reactor can be calculated for a certain biomass throughput. The required hold-up of reacting particles determines, amongst others, the volume of the reactor. Knowledge of the product selectivity observed for single particles, data on secondary cracking of the vapor products, the overall mixing state of the gas phase, and the char hold-up (tar cracking) are all required to determine the optimal process temperature for a maximum bio-oil yield and/or a desired bio-oil quality.

In part I (this paper), the literature on biomass pyrolysis concerned with experimental results, in particular the effect of the operating conditions, kinetics, and models is reviewed from an engineering point of view. Predictions of existing single particle models derived from a detailed description of the transport phenomena and literature data on measured intrinsic chemical kinetics are presented. In part II [16] (subsequent paper), experimental results of fluid bed pyrolysis are presented and compared with predictions of these models.

2.   Literature Review

The literature on biomass fast pyrolysis is quite extensive, and excellent technology reviews [8-15] are available. In the following subsections, the available literature with respect to the parameters important for reactor design will be briefly discussed. Four types of investigations are especially relevant in this respect. Quite a number of publications are dedicated to the intrinsic kinetics of primary and secondary decomposition reactions and product distribution. A second type of published papers is concerned with the development of single particle models in which the reaction kinetics are combined with intraparticle transport phenomena and heat transfer from the bulk to the particle. The third series of investigations deals with laboratory and pilot-plant measurements of product distributions as a function of the reactor

temperature, the type/size of feedstock, and (occasionally) the vapor residence time. We will focus here on results obtained for fluid beds, because the experimental part of this work (part II [16]) also deals with fluid bed pyrolysis. Finally, a few publications on reactor design that appeared recently in the literature will be discussed.

2.1.   State of the Art of Fast Pyrolysis Technology

Although laboratory studies regarding the thermal decomposition of various organic substances have been carried for a much longer period, the technology development of "fast" and "flash" pyrolysis started only some 20 years ago when the advantages of liquefying biomass in such a simple way were gradually recognized. During the 1980s and the early 1990s, research was focused on the development of special reactors such as the Vortex reactor [18,19], rotating blades reactor [20,21], rotating cone reactor [22,23], cyclone reactor [24,25], transported bed reactor [26], vacuum reactor [27,28], and the fluid bed reactor [26,29,30].

Since the late 1990s the process realization emerged, resulting in the construction of pilot plants in Spain (Union Fenosa) [31,32], Italy (Enel) [26], UK (Wellman) [33], Canada (Pyrovac, Dynamotive) [34,35], Finland (Fortum) [36], and The Netherlands (BTG) [23]. In the U.S. and Canada, Ensyn's entrained flow bed process [37] is applied at a scale of around 1 ton/hr for commercial production of a food flavor called "liquid smoke". Dynamotive and BTG announced demonstration installations of 2 - 4 tons biomass throughput per hour to be under construction. These companies aim at the utilization of bio-oil for energy production and, in a later stage, chemicals. Many pilot-plant projects have stopped, soon or late after the initial testing. At the time of writing (March 2005), the plants of Union Fenosa, Enel, Wellman, Fortum, and Pyrovac's large-scale installation in Jonquiere, Canada, were not in operation any more. This may be caused by a lack of confidence in economic prospects and markets, or by legislative limitations.

A successful co-firing test with 15 tons of bio-oil has been conducted in a 350 MWe power station in The Netherlands [38]. Entrained flow gasification (high pressure, oxygen blown) of bio-oil and bio-oil/char slurries has been demonstrated also on a substantial scale [4].

2.2. Kinetics and Rate Expressions

A general concern in the measurement of pyrolysis kinetics is the exclusion of heat transport limitations. Wagenaar et al. [39,40] concluded that the application of a thermogravimetric analysis (TGA) is therefore limited to ca. 450°C. At higher temperatures, he used small particles in a drop tube furnace. TGA is the most frequently used tool for kinetic analysis of biomass conversion. Grønli et al. [41] report on a Round-Robin study in which eight laboratories with access to five different types of thermogravimetric analyzers performed pyrolysis experiments at heating rates of 5 and 40°C/min while using Avicel PH-105 cellulose as feedstock. The eight laboratories measured char yields in the range of 2.9 - 10.5 wt % (at 40°C/min). For a certain fixed value of the weight loss, the scatter in the temperature measurement was about 17°C. Grønli et al. ascribed the differences in results primarily to variations in the thermal lag of the instruments used, and to the different heating rates applied. The thermal lag is defined as the difference between the temperature of the direct environment of the sample, which is controlled by the TGA, and the actual temperature of the sample [42]. This Round-Robin concludes that i) biomass pyrolysis kinetics are inherently difficult to measure by any technique, but that TGA gives the most reliable data, and ii) differences between studies using the same feedstock are still significant and caused by systematic errors in the applied methods. Similar discussions on the impact of systematic errors during the determination of pyrolysis kinetics are reported by Antal and Várheghi [43-45]. Kinetic expressions describing merely the weight loss of biomass have been published frequently in the literature [43, 46-51]. For woody biomass, however, kinetics including the selectivity to the products are determined only by Wagenaar et al. [40], Chan et al. [52], Thurner and Mann [53], and Di Blasi and Branca. [54]. In Table 1, the details of the experimental apparatuses and conditions used by these researchers are summarized.

Table 1. Experimental details of reported kinetic measurements.

	Wagenaar et al.	Chan et al.	Thurner and Mann	Di Blasi and Branca[a]
Feedstock	pine 100 - 125 μm	undefined sawdust (compressed)	oak sawdust 650 μm	Beech < 80 μm (TGA) 100 - 500 mm (TF)
Reactor	TGA drop tube (DT)	single particle Pyrex reactor	tube furnace (TF)	TGA Tube furnace
Temperature/^{o}C	280 - 400 (TGA) 500 - 600 (DT)	not indicated	300 - 400	300 - 435 (TGA) 300 - 435 (TF)

[a] To determine their kinetic expressions, Di Blasi and Branca used experimental data of various origins, besides the results of their own measurements with beech wood.

The experimental data on which these kinetic expressions are based vary a lot with respect to both the product distribution and the reaction rate, possibly due to the fact that different types of wood were used. In Figure 1, the yields and conversion time as predicted by these intrinsic kinetics are plotted. Intrinsic kinetics can be used to predict pyrolysis experiments when heat transfer to and within the particle is much faster than the chemical kinetics. Provided that the enthalpy of reaction is zero or negligible relative to the heat required to heat the biomass, the chemical reactions inside the particle take place at the reactor temperature. In case of a significant endothermic reaction enthalpy, the reaction temperature is always (somewhat) lower than the reactor temperature.

Clearly there is a lot of difference between the predictions of the various kinetic data sets, and trends are sometimes not even uniform (see Figure 1).
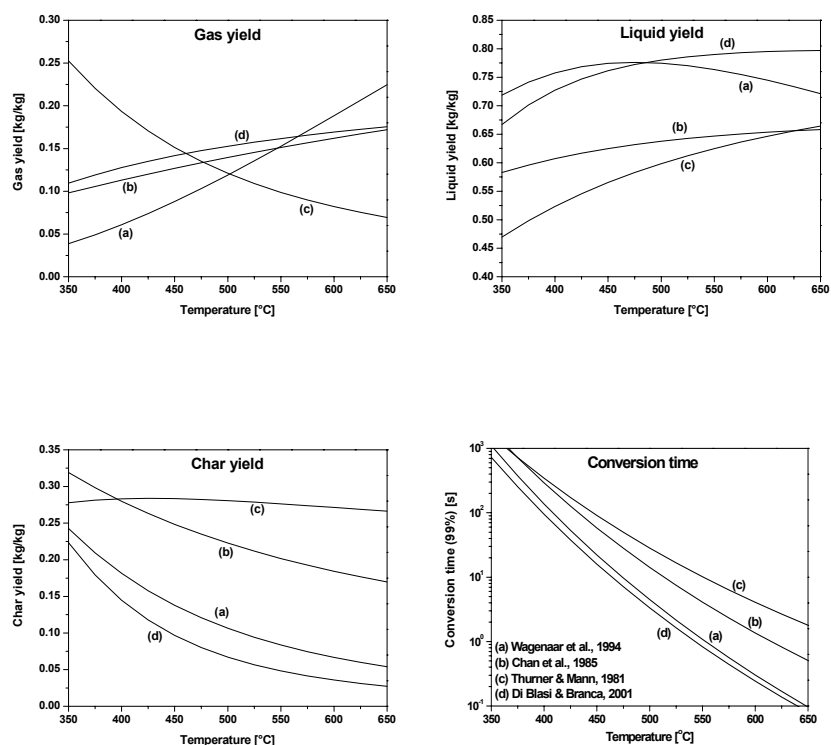
Figure 1: Product yields and conversion time (99% conversion) as predicted by the intrinsic kinetics of (a) Wagenaar et al. [40], (b) Chan et al. [52], (c) Thurner and Mann [53] and (d) Di Blasi and Branca [54].

The kinetic parameters of Wagenaar et al. [40], Chan et al. [52], Thurner and Mann [53], and Di Blasi and Branca [54], were derived while assuming a single process for the decomposition of wood, including three parallel first-order decay reactions for the formation of the product classes. This is the so-called "Shafizadeh" scheme [55]. The three lumped product classes are: permanent gas, liquids (bio-oil, tar), and char; a classification that has become standard over the years. Dried wood was used as feedstock in all four kinetic studies mentioned. All of the condensable organic products, including the formed water, were indicated as liquids. However, the amount of water in the produced liquid phase was never reported. Hence, the available kinetics cannot predict the moisture content of the produced liquid. In a practical pyrolysis process with a feed stream of 10 to 15 wt % moisture content, the water in the liquid phase has two origins, moisture from the feedstock and water produced by chemical reactions. Char does not only represent a carbonaceous solid, but can also

37

include high-molecular-weight tar components [56-61] and minerals. It should be noticed that the kinetic selectivity expressions are obtained by regression of yield versus temperature data. In the absence of any underlying mechanistic model, extrapolation outside the experimentally validated regime is basically impossible. Stenseng et al. [62] validated several reaction rate expressions against experimental data of wheat straw pyrolysis, for conditions outside the range they were derived from. They concluded that none of the rate expressions could be extrapolated outside the range of applied conditions, and that a widely applicable kinetic model for pyrolysis is still missing. In their analysis, they included: a first-order decay reaction, a three parameter nucleation model, a distributed activation energy model, and a superposition model based on first-order reactions. Of these reaction rate equations, the distributed activation energy model showed the best performance. The others failed completely when applied outside the validated regime, while the distributed activation energy model could still predict trends. Distributed activation energy models have also been discussed by Varhegyi et al. [63], Wojtowicz et al. [64] and Rostami et al. [65]. They found again a good agreement between model predictions and experimental results. Unfortunately, the reported kinetics using the distributed activation energy approach only considered the total conversion of biomass and not the selectivity toward the products.

The kinetic constants of tar conversion are determined by Antal [66], Diebold [67], Liden et al. [68] and Boroson et al. [69,70]. Diebold, Liden et al., and Boroson et al. interpreted their experimental results with a single first-order rate equation for the cracking of tar to permanent gases. Antal, however, proposed a scheme of two parallel (competing) first-order reactions to permanent gases and refractory condensable materials. Antal [66], Diebold [67], Liden et al. [68] did measurements for different limited temperature ranges. On the basis of these measurements Wagenaar et al. [39,40] derived a rate expression for a much wider temperature range, from of 450 - 800°C. As explained further in section 2.4 "Vapor Residence Time", char catalyzes the decomposition of tar.

To conclude, there is wide variation in data published for combined values of the pre-exponential factor and activation energy. Published rate and selectivity expressions may be valuable in describing trends, but they can hardly ever be used for reliable quantitative prediction of anything else than the corresponding original data. The scatter in the reported results is caused by systematic errors in the measurement technique, the type of biomass, and by the employed interpretation models. In view of

the complex reaction network including even catalytic effects of minerals, it is indeed unrealistic to expect that the thermal degradation of biomass can be described accurately with a simple set of rate/selectivity equations.

2.3.   Single Particle Models

During the last 60 years, many models have been published concerning the thermal degradation of a single biomass particle. In 1946, Bamford [71] formulated the first model for the weight loss of wooden sheets being exposed to gas flames. Many researchers subsequently used this basic model. Roberts et al. [72], for instance, modified the model by incorporating the effect of internal convection. Publications concerned with detailed modeling of biomass pyrolysis on particle level are those by, for example, Di Blasi [73-75] and Bellan and co-workers [76]. These detailed models include chemical kinetics, moisture evaporation, particle shrinkage, heat transfer to and through the particle (conduction, convection and radiation), and convective mass transfer inside the particle. It has been concluded by several researchers that the contribution of the diffusion flux of the produced vapors, as compared to convective flow, can be neglected [77-79]. In the single particle models, moisture evaporation is described with an Arrhenius-type equation [77,80,81].

Pyle and Zaror [82] showed that it is relatively easy to identify the controlling steps of wood pyrolysis. They gave guidelines for the simplification of a one-dimensional pyrolysis model to models for 1) "kinetically controlled", 2) "external heat transfer controlled" (uniform particle temperature), and 3) "internal heat transfer controlled" (shrinking core) pyrolysis. Py and Py' numbers were proposed, which can be used to determine whether heat transfer or reaction is the faster mechanism. The model results were validated successfully against experimental pyrolysis data of large cylindrical pine wood particles with a high l_p/d_p ratio. The cooling effect of the outward flowing vapors has been studied and quantified by Di Blasi [73,74], Janse [81], and Kersten [77].

Most model results reported in the literature are difficult to apply directly with respect to reactor design because they are focused on the description of intraparticle phenomena rather than on the prediction of reaction rates and product distributions as function of the operating conditions prevailing in practical pyrolysis reactors.

2.4. Continuous Laboratory Experiments in Fluid Beds

The first results of fluidized bed pyrolysis were those by Scott and his co-workers. In a series of publications [12,29, 83-86], they presented data obtained in their Waterloo bench-scale plant (~ 20 g/h) and pilot-plant (max 3 kg/h). The experimental program involved variation of the feedstock, reactor temperature, vapor residence time, and particle size. In the Waterloo plants, liquid yields (organics plus water) ranging from 60 - 85 wt % on moisture free feedstock basis were reported, depending on the biomass type and the operating conditions. A selection of later publications concerned with fluidized bed pyrolysis are those by Agblevor et al. [87], Horne and Williams [88], Peacocke et al. [20,89,90], Hague [91], Bilbao et al. [92], Luo et al. [93], and Olazar et al. [94]. Regarding the trends, the results obtained are in good agreement with those reported in the original work of Scott et al. However, in later investigations, the highest liquid yields of Scott and co-workers (> 80 wt %) could never be reproduced anymore. In the following subsections, the reported effects of the operating conditions are discussed. While analyzing the effect of the operating conditions, it must be realized that the reported mass balance closure is typically around 90 - 95%. Hence, rather small difference (say 3%) in results (e.g., yields) cannot be interpreted as a distinct trend.

Reactor Temperature

Quite some experimental results can be found in the literature [12,20,29, 83-94] regarding the influence of the fluid bed temperature on the product distribution, particularly the bio-oil yield. As a function of temperature, the liquid yield goes through a maximum. For a variety of feedstock types, it has been observed that the maximum yield of bio-oil is obtained at temperatures of around 400 - 550°C. However, taking into account the experimental errors, it can be argued that many researchers actually observed a plateau in the liquid yield over several decades of degrees centigrade within the range of 400 - 550°C. Over the whole temperature range, generally, a monotonic decrease in char yield and corresponding increase in gas yield was found.

According to Scott et al. [85], the best bio-oil quality in terms of caloric value and hydrogen over carbon ration is also achieved at the maximum yield temperature. Over the past decade, a number of authors, including Scholze et al. [95,96], and Oasmaa et al. [97,98], discussed the quality of bio-oil in some more detail [99-101].

40

Biomass Particle Size

Surprisingly, the biomass particle size has hardly been a systematically varied parameter in fluidized bed fast pyrolysis research. The attention was focussed mainly on "flash" pyrolysis requiring heating rates over $1000^oC/s$ and, consequently, very small particles ($d_p < 1$ mm). The published work regarding the influence of the particle size on the yield and quality of bio-oil was limited to the size range from 44 μm to 2 mm [29,83,102]. In this range, no significant influence of the particle size on the product yields has been reported.

In fixed beds, the particle size has been varied over a wider range [61,103]. Fiqueiredo et al. [61] observed that oil yields of holm oak wood chips did not vary as a function of the particle size in the range from 0.4 to 2 mm. Roy et al. [103] reported that a yield of almost 74 wt % of bio-oil (total liquids including water) was obtained from air-dried aspen saw dust at 450^oC, while a yield of 67 wt % was achieved for 1 cm aspen wood chips. Kelbon et al. [104] did experiments with single particles heated by an arc lamp at constant flux (W/m^2). At a flux of 8.4 x 10^4 W/m^2, they found that the liquid yield of 1.5, 1 and 0.5 cm (length) wood cylinders was 65, 48, and 38 wt %, respectively. For fluxes of 16.8 and 25.2 W/m^2, they observed nearly identical liquid yields for all particle sizes.

Unfortunately, literature results regarding the effect of the particle size over a wide range in a single reactor are not available. One could try to derive a relation on basis of data from different reactor types. However, this relation would be very difficult to interpret because of the fundamental differences between the reactors used, particularly concerning the intra-reactor temperature gradients, the external heat transfer coefficient, extra-particle vapor residence time, and the hold-up of char being a cracking catalyst.

For this paper (part I), the particle size has been varied therefore over a wide range (d_p = 0.01 - 20 mm) in simulations with single particle models. In part II [16] these model predictions are compared with results of real pyrolysis experiments in a fluid bed (d_p = 0.7 - 17 mm).

In some publications, the effect of the particle size on the conversion time [81, 105-107] is discussed on basis of both measurements and modelling. Particle sizes up to a few centimeters were used in the experiments. It was found that the observed conversion times and intraparticle temperature gradients, as a function of the particle size, could be well understood from simple one-dimensional single particle models (Bamford's model [63]).

Heating Rate and Heat Flux

The effect of the heating rate has only been studied: i.) in (semi-)batch fixed bed reactors installed in a laboratory oven [108,109], ii.) by heating single particles in an oven [105,110,111], iii.) by heating single particles with a lamp [104,112]. In all experiments, the heating rate (°C/s) or the heat flux (W/m^2) of the biomass sample is controlled and monitored accurately. The general conclusion from the batch tests is that the applied heating rate has a significant effect on the pyrolysis process, particularly on the oil yield, which is reported to drop in case of lower heating rates at otherwise constant conditions. Theoretical analysis of the effects of the heating rate are also available in literature, for example in the work by Lede [113-115].

In practical pyrolysis reactors like fluid beds, neither the heating rate nor the heat flux are independent variables. They are in fact nonstationary and dependent on local conditions. It is not clear how experiments under "controlled" heating conditions can be translated to continuous reactors.

Vapor Residence Time

Scott et al. [12] and Liden et al. [68] measured the effect of the vapor residence time in a fluid bed reactor in the range of 0.2 - 0.9 s. At 525°C, they found that in this range the liquid yield dropped from 75 to 60 wt %. Lower oil yields at prolonged vapor residence time are ascribed to cracking and polymerization reactions of vapors to gases and solids, respectively. On the basis of their measurements, Liden et al. [116] derived the kinetic constants for tar cracking while assuming a first-order decay reaction. Besides by Liden et al., cracking reactions of pyrolysis vapors have been studied and quantified also by Boroson et al. [69], Antal [66], and Diebold [67]. However, they measured homogeneous tar cracking, whereas Liden at al. [116] used a fluid bed with a considerable char hold-up. The first order kinetic constants (k) vary between ~ 0.04 and 0.20 (s^{-1}) at 500°C. This range is rather large; the lowest value allows a vapor residence time of 5 s to keep the loss of primary tar limited to 10%, the highest value only 1 s.

Vapor cracking rates cannot be compared on residence time and temperature basis only, because also the amount of char in the reactor is reported to have a significant effect on the extent of cracking. Boroson et al. [117] performed controlled experiments in which they led pyrolysis vapors over a char bed. They found that already at 400°C a fraction of wood tar is very reactive in the presence of wood char. No "catalytic" rate equations, containing specific information on the char used, are available in the literature.

42

An interesting observation was reported by Freel at al. [118], who showed that, at 650 and 850°C, the liquid yield decreased due to homogeneous gas-phase cracking for vapor residence times increasing from 0.1 to 1 s. It remained, however, constant for any longer residence times. This behavior cannot be explained with a single first-order decay reaction for tar cracking. However, with the scheme of Antal [66] that includes parallel reactions of primary tar to gases and refractory (less reactive) tar, it can be explained indeed. According to this mechanism, primary tar can be converted rapidly to gases and less reactive refractory tar that does not, or very slowly, decompose. The explanation further assumes that primary tar and refractory tar form a single liquid upon condensation.

Both the single reaction and the competing reactions scheme plea for a reactor design in which the produced vapors are quenched rapidly as this maximizes the liquid yield. In addition, the competing reactions scheme predicts that at increased vapor residence time the composition of the liquid is changing from primary tar to refractory tar. This adds an oil quality aspect to the discussion of the vapor residence time. If primary tar would be a better bio-liquid constituent than refractory tar, short residence times would be preferred even though the total liquid yield remains unaffected. Unfortunately, there are no studies available that analyze the composition of the recovered liquid as function of the vapor residence time.

2.5. Reactor Design and Modeling

The number of publications concerning fluid bed design and modeling is limited. Di Blasi [74,107] presented a fluid bed model in which the emphasis is completely on the single particle behavior. A reactor model is introduced via the external heat transfer coefficient and an extra-particle residence time of the gas phase to account for vapor cracking in the bulk. On the other hand, Lathouwers and Bellan [119] developed a fluid bed reactor model based on a multi-fluid approach including the kinetic theory of granular flow. In this model, a computational fluid dynamics description of a fluid bed is coupled with the devolatilization characteristics of discrete particle classes. The results of this comprehensive model are, however, not straightforward to interpret and to use for reactor design. It is not clear how the energy required is brought into the reactor and how, in practice, a preheated biomass feed (up to 225°C) could be created. Gerhauser [120,121] employed CFD modeling to study fluidized bed reactor scale-up. He concluded that the heat input into the fluidized bed is a major concern for pyrolysis reactors with a size of 100 tons per day or larger.

3.   Single Particle Model Calculations

Two models, adopted from the literature, are used in this work. Results of simulations will be presented and compared with experimental results (part II [16]), to evaluate the descriptive and predictive power of such single particle models.

1)   The first is a two-dimensional (2D) model as described by Di Blasi [75]. In this model, both conductive and convective heat transport are taken into account and the physical properties (e.g., permeability, conductivity) can be anisotropic. The convective fluxes of vapors and gases are modeled with Darcy's law. For more information regarding the model, the reader is referred to the original publications [75,77].

2)   The second is a one-dimensional (1D) model as proposed by Bamford [71] that assumes the heat transfer within the particle to occur by conduction only.

The major assumptions of both models are that i) cylindrical particles are considered, ii) the volume of the particle does not change during devolatilization, iii) there is thermal equilibrium between the vapors and the solid matrix, and iv) the enthalpy of the pyrolysis reaction is zero (the effects of an endothermic reaction will be discussed to a certain extent). The pyrolysis reaction is described by the scheme proposed by Shafizadeh [55]. As mentioned before, the liquid phase predicted by the used pyrolysis kinetics includes, next to organics, all the water produced. The applied kinetics were derived for dry wood, while wood with a moisture content of ca 7.5 wt % was used in the experimental part of this work (part II [16]). Therefore, evaporation of this moisture has been incorporated in the single particle models. Moisture evaporation is described by an Arrhenius rate equation as proposed by Bryden and Hagge [80]. The liquid yield resulting from the single particle models is thus made up out of liquid predicted by the primary kinetics, plus the moisture evaporated from the feed. The actual moisture content of this liquid cannot be predicted because the formed water was not separately taken into account in the kinetic studies (see section 2.2). Cracking of vapors to gas is modeled as a first order reaction. In the model the conversion time (τ) was defined as the time at which 99% (wt) of the initial biomass is decomposed. The conversion is calculated using the equation below:

$$X = \frac{W_0 - W}{W_0 - W_\infty} \qquad\qquad (1)$$

The coupled system of partial differential equations describing the model is solved by applying the method of lines in a DAE solver environment in MATLAB$^{©}$. Tests were performed to ensure that the obtained results were grid independent and convergent. For the 2D model, usually a grid of 40x40 spatial grid cells showed sufficient accuracy. Table 2 gives the physical properties of the particles used in the calculations. Dimensionless numbers used in this paper (e.g., Bi, κ) are always based on initial values of the involved parameters (e.g., λ, ρ, C_p).

Table 2: Properties used for the (base-case) model simulations.

Property	Unit	Value
Moisture content biomass	wt %	7.5
Particle density biomass	kg/m^3	660
Skeletal density biomass	kg/m^3	1500
Enthalpy of reaction	J/kg	0
Molar mass gas	g/mole	20
Molar mass vapors	g/mole	224
Specific heat biomass	J/(kg.K)	$10^3 \times (1.5 + 10^{-3}T)$ [a]
Specific heat char	J/(kg.K)	$10^3 \times (0.42 + 2.09 \times 10^{-3}T - 6.85 \times 10^{-7} \times T^2)$[a]
Specific heat gas and tar	J/(kg.K)	$1560 + 0.567(T-298)$ [b]
Viscosity gas and tar	Pa s	3×10^{-5}
Heat conductivity gas and vapors	W/(m^2.K)	$0.0688 + 1.61 \times 10^{-4}(T-298)$ [b]
Heat conductivity biomass (axial)	W/(m.K)	0.25
Heat conductivity biomass (radial)	W/(m.K)	0.15
Heat conductivity char (axial)	W/(m.K)	0.20
Heat conductivity char (radial)	W/(m.K)	0.10
Permeability biomass (axial)	m^2	10^{-16} (10^{-14})[c]
Permeability biomass (radial)	m^2	10^{-12} (10^{-14})
Permeability char (axial)	m^2	10^{-12} (10^{-12})
Permeability char (radial)	m^2	10^{-14} (10^{-12})
Pyrolysis kinetics		Wagenaar et al. [40], Chan et al. [52], Thurner and Mann [53], and Di Blasi and Branca [54].
Vapor cracking kinetics		Liden et al. [116], Diebold [67], Boroson et al. [69], and Wagenaar et al. [39,40].
Fluid bed heat transfer coefficient	W/(m^2.K)	Prins et al. [122]
Initial temperature	^{o}C	25

[a] From Grønli [123]; T in Kelvin.

[b] Derived for pyrolysis gas on basis of the polynomials in Reid et al. [124]; T in Kelvin.

[c] Values between brackets are for isotropic particles.

46

4. Simulation Results and Discussions

In the first subsection, 4.1, the results of the 1D and 2D model will be compared. The effects of the external heat transfer coefficient and the particle size will then be discussed in subsections 4.2 and 4.3, respectively. In part II [16], more simulation results will be presented to allow a proper comparison with experimental results of fluid bed pyrolysis. In this work, we focus on the conversion time (reaction rate) and the product yield. These particle-related parameters are important for reactor design. The importance of a good estimate of the conversion time for reactor design becomes clear when realizing that at a given feed rate the required hold-up of reacting particles (from fresh biomass to char) is approximately proportional to the conversion time. The hold-up of reacting particles determines, amongst others, the total reactor volume and is important from an operational point of view. The amount of char in a fluid bed in case of 3 mm biomass particles, for instance, is limited to ca. 5 wt % of the total bed [125,126]; higher fractions cause fluidization problems (e.g., heavy segregation). The product yield, in particular the oil yield, is important because the pyrolysis process aims at a maximum oil production.

4.1. Comparison between 2D or 1D Models

Table 2 shows the predicted conversion time and product yields for a dry wood particle with a diameter of 5mm that was supposed to be converted at a reactor temperature of 527°C (800 K). Simulation results of the 2D- and 1D-model are compared. The corresponding conversion time and yields of kinetically controlled pyrolysis are also included in Table 3. With the 2D-model, the effects of isotropic versus anisotropic permeability and the l_p/d_p has been analyzed. The 1D-model, obviously, represents a particle with infinite l_p/d_p. The typical anisotropic structure of wood causes all the produced vapors to flow out of the particle in axial direction near the reaction front, parallel to the fibers. In case of particles with an isotropic structure, the produced vapors flow out over the whole surface of the particle (see Di Blasi et al. [75] and Kersten [77]). As a consequence of this difference in outflow pattern of produced vapors, heating of anisotropic particles will not be counteracted so much by the cooling effects of these vapors. Hence, when comparing identical particles with different permeability orientation, the isotropic particle will have a longer conversion time. For gasification conditions (T > 800°C), the difference in conversion time between particles with isotropic and anisotropic permeability can be up to 50% (see

Kersten [77]). At pyrolysis conditions (say T < 550°C), however, this effect is limited to 10% (see Table 3 and Kersten [77]), which is small in comparison with the uncertainties in the chemical kinetics. The simulations indicate that, for typical pyrolysis temperatures, the cooling effect of the out flowing produced vapors does not have an important influence on the pyrolysis time. With respect to the product yields, the influence of the permeability orientation is marginal (see Table 3). Kersten [77] concluded on the basis of simulations with a full 2D model, including vapor cracking kinetics [39], that under pyrolysis conditions (~500°C) intraparticle tar cracking does not proceed to a significant extent.

Simulations with the 2D and 1D model give nearly identical conversion times in case of particles with large aspect ratio ($l_p/d_p \geq 3$) (see Table 3 and Figure 2). The effect on the product distribution is marginal, and the conversion time is over predicted slightly by the 1D model. This conclusion has been put forward also by Miller and Bellan [127]. Particles with $l_p/d_p < 3$ require two-dimensional models for accurate prediction of the conversion time because below this value a significant amount of heat penetrates into the particle through the flat surface (see Figure 2). However, analysis of the data in Figure 2 shows that for engineering purposes also a one-dimensional model combined with a correction factor to account for the effect of l_p/d_p gives good results. In this case, the one-dimensional model is used to calculate the conversion time at $l_p/d_p = \infty$, where after Fourier's linear conductive heat equation is used to scale the results to finite length over diameter ratios. With the Fourier equation, the heating time (τ_H) of a particle with given l_p/d_p can be compared with the heating time of a particle with the same diameter for $l_p/d_p = \infty$ at otherwise identical conditions. The ratio of these heating times is used as correction factor (P) to scale the conversion time calculated with the 1D model to finite l_p/d_p ratios. Analytical solutions of the Fourier equation are available (see, e.g., Carlslaw and Jaeger [128]) to enable quick calculation of P.

$$\tau(L_p/d_p) = \tau_{L_p/d_p=\infty}(\text{1D model}) \cdot P(L_p/d_p) \qquad (2)$$

$$P(L_p/d_p) = \frac{\tau_H(L_p/d_p, d_p, \kappa, Bi)}{\tau_H(L_p/d_p = \infty, d_p, \kappa, Bi)} \qquad (3)$$

As mentioned before, the thermal diffusivity κ and the dimensionless number Bi are based on initial conditions and can have different values for the radial and axial

direction. The scaling procedure described above includes only the effect of the l_p/d_p ratio. The influence of the cooling outflow of the vapors is not included in the one-dimensional model. However, as stated before, for typical pyrolysis temperatures the effect of convective heat transport is limited.

Concluding, for engineering calculations that should provide estimates on the conversion time and the product yields a 1D model provides sufficient accuracy for particles with $l_p/d_p > 3$, and for particles with $l_p/d_p < 3$ the results of a 1D model can be scaled with a correction factor (P).

The analysis above has been presented while using the intrinsic kinetics of Wagenaar [39,40]. For the other kinetic data sets, similar qualitative results have been obtained.

Table 3: Model predictions of the 1D and 2D model for pyrolysis of a wood particle with d_p = 5 mm at 527°C (800 K)[a].

l_p/d_p Permeability	Intrinsic Kinetics	2D model			1D model
		1 isotropic	1 anisotropic	3 anisotropic	∞
τ, s	2	22	20	34	35
Gas yield, kg/kg	0.14	0.1	0.1	0.09	0.09
Liquid yield	0.77	0.77	0.78	0.76	0.76
Char yield	0.09	0.13	0.12	0.15	0.15

[a] Conditions are listed in Table 2. Primary decomposition kinetics and tar cracking (intra particle) kinetics are adapted from Wagenaar [39,40]. Deviations from Table 1: biomass density = 600 kg/m^3, heat conductivity biomass in radial direction = 0.1 W/(m.K), moisture content = 0 wt %, external heat transfer coefficient = 400 W/(m^2.K).
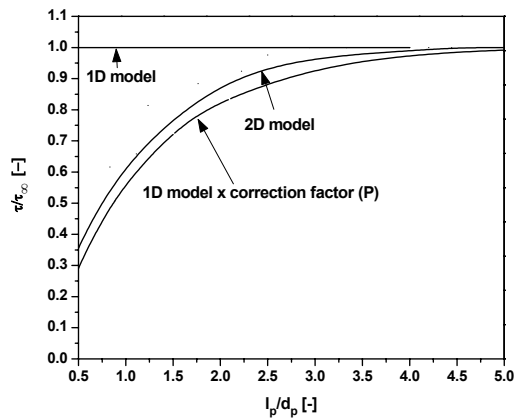
Figure 2: Effect of l_p/d_p on the conversion time, τ. τ_∞ stands for the conversion time at infinite l_p/d_p. Reactor temperature is 527°C (800 K). Other conditions/properties are listed in Table 2.

4.2. External Heat Transfer Coefficient, α

For a given particle, α is determined by the reactor type and by the operating conditions. In fluid beds, high external heating rates can be reached ($\alpha \approx 1000$ W/(m^2.K)), whereas for instance in fixed beds and rotary kilns external heating is much slower ($\alpha \approx 100$ W/(m^2.K)). Figure 3 show results of simulations (1D model) of pyrolysis at 500°C in which the external heat transfer coefficient has been varied over the range of 50 - 1200 W/(m^2.K). Conversion times and product yields are plotted against α for four different particle sizes. For small particles of 1 - 3 mm, the external heat transfer coefficient has a clearly noticeable effect on the conversion time. In a fluid bed, the conversion is about 1.5 times faster as compared to for slow heating conditions (see Figure 3a). In fact, in a fluid bed such small particles approach the kinetically controlled regime. A factor 1.5 difference in the estimate of the conversion time (reaction rate) is important for reactor design, as it corresponds to a factor 1.5 in the hold-up of reacting particles.

For larger particles of 5 - 10 mm, the influence of the external heat transfer coefficient on the conversion time is small. Because of the relatively low thermal conductivity of wood, heat conduction in the particle is the limiting step in the heating process of large particles. Model simulations indicate that for particles larger than 5 mm the

50

effect of α on the conversion time is never more than 20% in the practical range of α = 100 - 1200 W/(m^2.K). The impact of the external heating on the product yield is small. Figure 3b shows the influence of α on the liquid yield. The influence of α on the gas and char yield is just as low as for the liquid yield.
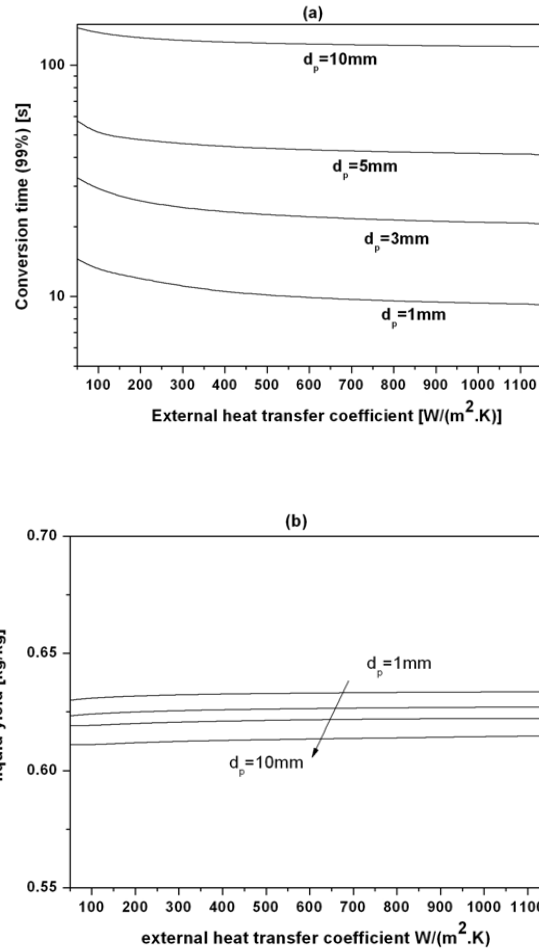

Figure 3: Effect of the external heat transfer coefficient on the conversion time (a) and the liquid yield (b). Simulations were performed with the 1D model. Primary decomposition kinetics of Chan [52] were used. Reactor temperature is 500°C; other conditions/properties as in Table 1.

4.3. Particle Size Effect

In Figure 4a, the predicted liquid yield (1D model) is plotted versus the particle size for a reactor temperature 500^oC. Such a curve is of importance for fast pyrolysis because it predicts at which particle size the liquid yield starts to decrease. The calculations show a constant or nearly constant liquid yield at 500°C as a function of the particle size up to 20 mm (see Figure 4a), irrespective of the kinetics applied. This can be explained by combining the measured intrinsic kinetics with the knowledge about the heat transport to and inside a pyrolyzing particle. To clarify this, an effective pyrolysis temperature (Π) is defined that can explain the product distribution for heat transfer limiting conditions on basis of the intrinsic kinetics (measured for small particles). In analogy with the Thiele modulus concept [129], the effective pyrolysis temperature Π allows using intrinsic kinetics, after a correction for transport limitations, for predicting the product yields at the temperature of the bulk. Hence, Π is the temperature at which the decomposition reactions are actually taking place with respect to the product distribution. It turns out that the volume-averaged value of the local temperature at which the reaction rate is maximal (T^*) is a good estimator for Π.

$$T^*(\mathbf{x}, \mathbf{y}, \mathbf{z}) = \max(-\frac{\partial \rho_{bio}}{\partial t}, T) \qquad (4)$$

$$\Pi = \frac{\int_V T^*(\mathbf{x}, \mathbf{y}, \mathbf{z}) \partial V}{V} \qquad (5)$$

The analysis on the effective pyrolysis temperature is similar to an earlier analysis by Lede [114] regarding the reaction temperature of solid particles undergoing volatilization. Lede did simulations for ablative and chemically controlled conditions. In the first case, the reaction is taking place in a very thin layer close the surface of a big particle, while in the second case the particle temperature is uniform. He concluded that the temperature at which the reaction starts varies within narrow limits, while the temperature at which the reaction proceeds stabilizes as a function of the conversion degree. This was ascribed to both the endothermicity of the reaction and the fact that the reaction is fast as compared to heat penetration. Apparently, the latter effect must be dominant because simulations with $\Delta H = 0$ also yielded a nearly constant temperature during the conversion. The observed stabilized reaction temperature, with a range of ca. 100^oC between the beginning and end of the

52

conversion, was compared with a phase change. Several authors saw "phase-change" like behavior in pyrolysis experiments [113,115]. On the basis of model calculations, Narayan and Antal [42] have shown that, in a TGA experiment, the temperature at which the conversion actually takes place remains nearly constant (like in a phase-change), irrespective of the values of model parameters such as the heating rate of the environment, the enthalpy of reaction, and the heat transfer coefficient. In the present work, the temperature at which the reaction actually takes place has been analyzed in the presence of intraparticle temperature gradients instead of at a spatial uniform particle temperatures or ablative conditions. For this, a particle average reaction temperature has been defined.

Figure 4b shows this effective pyrolysis temperature versus d_p, calculated with the 1D single particle model for the kinetic data sets (a – d). In Figure 4a, the intrinsic liquid yields evaluated at Π corresponding to its value at d_p (hence at Π (d_p)) are presented, next to results of the full model. Clearly, there is good quantitative agreement between these two yields. Only the liquid yield is plotted. For char and permanent gas, the agreement was found to be just as good. Obviously, for small particles Π equals nearly the reactor temperature. Π then decreases when the particle size increases due to transport limitations. Model simulations show that for a typical pyrolysis temperature of 500^oC, the drop in Π is restricted to ca. 100^oC for particles up to 20 mm (see Figure 4b). This observation is in line with simulation results of Narayan and Antal [42] and Lede [114], which showed that the actual reaction temperature did not vary as a function of the degree of conversion for TGA and ablative conditions.

Such a small difference between the reactor temperature and the effective reaction temperature (Π) explains why the cooling effect of out flowing vapors (see section 4.1 and Kersten [77]) is not that important for a typical pyrolysis temperature of 500^oC. If Π is close to the bulk temperature, the additional energy required to heat the produced gases and vapors to bulk conditions is small. The effect of the used kinetic data set on the curves of Π versus d_p is limited, because the activation energy does not vary much for these data sets. According to Wagenaar's [40] and Chan's [52] intrinsic decomposition kinetics (see Figure 1), the oil yield is hardly dependent on the temperature in the range between 500^oC and 400^oC. Therefore, the oil yield predicted by the particle model including these kinetic data remains practically constant up to d_p = 20 mm at a reactor temperature of 500^oC, despite the fact that the characteristic reaction temperature decreases due to heat transport limitations. The intrinsic kinetics

53

of Di Blasi and Branca [54] and Thurner and Mann [53] show a more profound effect on the oil yield in this temperature range, resulting in a slightly decreased bio-oil yield for larger particles pyrolyzed at 500°C.

As mentioned before, single particle models predict that at 500°C the influence of intraparticle cracking of tars can be neglected for all the available tar decomposition kinetics. These tar decomposition kinetics were determined in gas-phase reactors or in a fluid bed with a relatively low char hold-up. Inside a reacting particle, however, the produced vapors flow outward via a char matrix with a high specific area, which is known to have catalytic activity towards tar cracking. If this char layer is extremely active (much more reactive than in the gas-phase cracking of tars), then three effects could occur upon increasing the particle size and, accordingly, the vapor residence time inside the particle: 1) the liquid yield decreases because primary tar is converted to gasses only (e.g. Liden [68]), 2) the composition of the liquid changes because primary tar decomposes to other liquid compounds [66], and 3) a combination of 1) and 2) occurs. Experimentally it has been found now that the liquid yield remains more or less constant in the range of d_p = 0.7 - 17 mm in a fluid bed reactor. However, the water content of the recovered liquid appeared to increase with increasing particle size (see Part II [16]).

To conclude, up to particles of 20 mm the effective pyrolysis temperature drops maximally 100°C, which, according to the intrinsic kinetics, results in a just marginal decrease in the liquid yield, a decrease in gas yield of about 5 wt % and a corresponding increase in char yield.
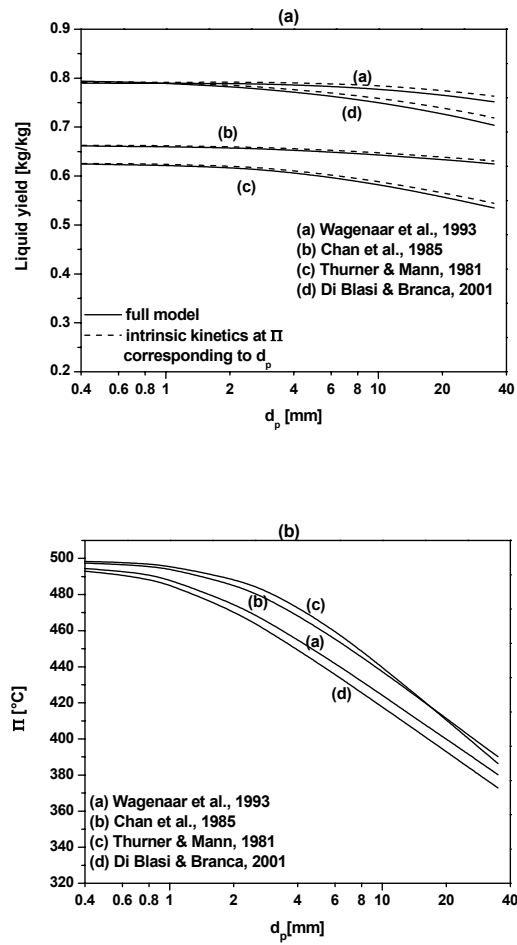
Figure 4. a) Predicted oil and char yield versus the particle size for the kinetic data sets (a - d). Next to the results of the full 1D-model (—), also the intrinsic oil yields evaluated at Π corresponding to its value at d_p are presented (---). b. Effective pyrolysis temperature versus the particle size for the kinetic data sets (a - d). Reactor temperature = 500°C; other conditions/properties are as in Table 1.

5   Conclusions

The main conclusions can be summarized as follows:

(1)   The literature on biomass pyrolysis has been reviewed. Many excellent studies have been reported with a high level of detail. However, it appears to be rather difficult to extract reliable quantitative information on conversion rates and product yields required for process design.

(2)   For kinetic studies, the pyrolysis products have been lumped into the classes gas, liquid, and char. But the quality/composition of these classes (e.g., the water content of the liquid) depends strongly on the operating conditions. For practical application and optimization, kinetics should also be able to predict the product quality. Such kinetic schemes are not available yet.

(3)   There is a lot of scatter in the reported biomass kinetics and selectivity data. For exactly the same feedstock, significant differences already occur because of systematic errors in the experimental methods. Intrinsic reaction rates published for different biomass types vary up to a decade, and even trends are sometimes not uniform. This is probably related to differences in composition and structure.

(4)   For a given set of kinetics, one-dimensional single particle pyrolysis models provide sufficient accuracy for engineering calculations. For particles with $l_p/d_p > 3$, the one-dimensional will do, and for particles with $l_p/d_p < 3$ the results of a 1D model can be scaled with a correction factor, P. P is the ratio of the heating time of a particle with finite l_p/d_p over a particle with infinite l_p/d_p at otherwise identical conditions. Also, the cooling effects of out flowing vapors, the influence of anisotropy, and intraparticle tar cracking can be neglected at fast pyrolysis conditions.

(5)   Model calculations show that the external heat transfer coefficient (related to the reactor type) has little influence on the product yields at typical fast pyrolysis temperatures. Only for small particles (say ≤ 3 mm), and low values of α, the influence of α on the conversion time is clearly notable.

(6)   Contrary to the common belief, single particle models predict (for all available kinetics) that the influence of the particle size on the liquid yield is very limited. This phenomenon can be explained with an effective pyrolysis temperature, a parameter that represents the temperature at which the conversion is essentially taking place averaged over the particle's volume.

(7)   While the influence of the biomass particle size, its effective pyrolysis temperature, and the vapor residence time, on the liquids yield is limited, the liquid composition may change substantially.

56

Acknowledgement

Notation

T	Temperature	K
C_p	Specific heat capacity	$J/Kg \cdot K$
P	Correction factor	-
d_p	particle diameter	m
Bi	Biot number $\quad Bi = \dfrac{\alpha \cdot L_c}{\lambda}$, L_c is the characteristic length of the particle	
Py	Pyrolysis number $\qquad p_y = \dfrac{\lambda}{\kappa \cdot \rho \cdot C_p \cdot L_c^2}$	
Py'	Pyrolysis number (external) $\qquad p_{y'} = \dfrac{\alpha}{\kappa \cdot \rho \cdot C_p \cdot L_c}$, $\; p_{y'} = Bi \cdot p_y$	
$1D$	One-dimensional	
$2D$	Two-dimensional	
DAE	Differential Algebraic Equation	
MWe	Million Watts equivalent	
l_p	Particle length	m
t	Time	s
V	Volume	m^3
X	Conversion, defined as $X = \dfrac{W_0 - W}{W_0 - W_\infty}$	
W	Mass of the biomass particle	kg

Greek Symbols

Π	Effective pyrolysis temperature	^oC
λ	Heat conductivity	$J/(m \cdot s \cdot K)$
ρ	Density	Kg/m^3
κ	Thermal diffusivity	$\kappa = \dfrac{\lambda}{\rho \cdot C_p}$

57

τ	Conversion time	s
τ_H	Heating-up time	s
α	External heat transfer coefficient	$J/(m^2 \cdot s \cdot K)$

Subscripts

H	Heating up
p	Particle
x, y, z	Coordinates
∞	Infinite or final state
bio	Biomass
0	Initial state

58

References

1. Baker, E.G., Elliott, D.C., Catalytic Hydrotreating of Biomass-Derived Oils; ACS Symposium Ser., 1988, 376, pp. 228-240.

2. Baldauf, W., Balfanz, U., Upgrading of fast pyrolysis liquids at VEBA OEL AG; In Biomass gasification and pyrolysis: state of the art and future prospects, Kaltschmitt, M., Bridgwater, A.V., Eds., CPL Press, UK, 1997, pp. 392-398.

3. Boerrigter, H., den Uil, H., Calis, H.-P., Green diesel from biomass via Fischer-Tropsch synthesis: new lights in gas cleaning and process design; In Expert meeting on Pyrolysis and Gasification of Biomass and Waste, Strasbourg, France, CPL Press, UK, 2002.

4. Henrich, E., Dinjus, E., Tar-free, high pressure synthesis gas from biomass; In Expert meeting on Pyrolysis and Gasification of Biomass and Waste, Strasbourg, France, CPL Press, UK, 2002.

5. Venderbosch, R.H., van de Beld, L., Prins, W., Entrained flow gasification of bio-oil for synthesis gas; In Twelfth European Biomass Conference: Biomass for Energy, Industry and Climate Protection, Amsterdam, The Netherlands: ETA-Florence and WIP-Munich, 2002.

6. Van Swaaij, W.P.M., Prins, W., Kersten, S.R.A., Strategies for the future of biomass for energy, industry and climate protection; In The 2nd World Conference and Technology Exhibition on Biomass for Energy, Industry and Climate Protection, Rome, Italy, 2004.

7. Van Swaaij, W.P.M., Kersten, S.R.A., van den Aarsen, F.G., Routes for methanol from biomass; In International 2-Day Business Confence on Sustainable Industrial Developments, Delfzijl, The Netherlands, 2004.

8. Bridge, S.A., Flash pyrolysis of biomass for liquid fuels; Master's Thesis, The University of Aston, Birmingham, UK, 1990.

9. Bridgwater, A.V., et al., Eds., Fast pyrolysis of biomass: A handbook; CPL Press, UK, 1990.

10.   Bridgwater, A.V., Meier, D., Radlein, D., An overview of fast pyrolysis of biomass; Org. Geochem., 1999, 30, pp. 1479-1493.

11.   Meier, D., Faix, O., State of the art of applied fast pyrolysis of lignocellulosic materials - a review; Bioresource Technology, 1999, 68, pp. 71-77.

12.   Scott, D.S., et al., A second look at fast pyrolysis of biomass - the RTI process; J. Anal. Appl. Pyrolysis, 1999, 51, pp. 23-37.

13.   Bridgwater, A.V., Peacocke, G.V.C., Fast pyrolysis processes for biomass; Renewable and Sustainable Energy Rev., 2000, 4, pp. 1-73.

14.   Bridgwater, A.V., Ed., Fast pyrolysis of biomass: A handbook; CPL Press, UK, vol. 2, 2002.

15.   Bridgwater, A.V., Renewable fuels and chemicals by thermal processing of biomass; Chem. Eng. J., 2003, 91, pp. 87-102.

16.   Wang, X., et al., Biomass pyrolysis in a fluidized bed reactor: Part II. Experimental validation of model results; Ind. Eng. Chem. Res., 2005, pp. 8786-8795.

17.   Van Swaaij, W.P.M., van der Ham, A.G.J., Kronberg, A.E., Evolution patterns and family relations in G-S reactors; Chem. Eng. J., 2002, 90, pp. 25-45.

18.   Diebold, J., Scahill, J., Production of primary pyrolysis oils in a Vortex reactor; In ACS Symposium Series 376: Pyrolysis oils from biomass producing, analyzing, and upgrading; Soltes, E.J., Milne, T.A., Eds., 1988, pp. 31-40.

19.   Diebold, J.P., Scahill, J.W., Improvements in the Vortex reactor design; In Developments in thermochemical biomass conversion, Bridgwater, A.V., Boocock, D.G.B., Eds., 1997, Blackie Academic & Professional, London, UK, 1997, pp. 242-252.

20.   Peacocke, G.V.C., Ablative pyrolysis of biomass; Ph.D. Thesis, Aston University, Birmingham, UK, 1994.

21.   Boutin, O., et al., Temperature of ablative pyrolysis of wood. Comparison of spinning disc and rotating cylinder experiments; In Biomass gasification and

pyrolysis: state of the art and future prospects, Kaltschmitt, M., Bridgwater, A.V., Eds., CPL Press, UK, 1997, pp. 336-344.

22.   Wagenaar, B.M., Prins, W., van Swaaij, W.P.M., Pyrolysis of biomass in the rotating cone reactor: modeling and experimental justification; Chem. Eng. Sci., 1995, 49, pp. 5109-5126.

23.   Prins, W., Wagenaar, B.M., Review of the rotating cone technology for flash pyrolysis of biomass; In Biomass gasification and pyrolysis: state of the art and future prospects, Kaltschmitt, M., Bridgwater, A.V., Eds., CPL Press, UK, 1997, pp. 316-326.

24.   Bramer, E.A., Brem, G. A novel technology for fast pyrolysis of biomass: Pyros reactor; In Twelfth European Biomass Conference: Biomass for Energy, Industry and Climate Protection, Amsterdam, The Netherlands: ETA-Florence and WIP-Munich, 2002.

25.   Lede, J., Verzaro, F., Antoine, B., Villermaux, J., Flash pyrolysis of wood in a cyclone reactor; Chem. Eng. Process., 1986, 20, pp. 309-317.

26.   Rossi, C., Graham, R., Fast pyrolysis at ENEL, in Biomass gasification and pyrolysis: state of the art and future prospects; Kaltschmitt, M., Bridgwater, A.V., Eds., CPL Press, UK, 1997, pp. 300-306.

27.   Roy, C., Lemeuix, R., de Caumia, B., Blanchette, D., Processing wood chips in a semi-continuous multiple hearth reactor; In Pyrolysis Oils from Biomass, Producing, Analyzing and Upgrading. ACS, Washington, DC, 1988.

28.   Amen-Chen, C., Softwood bark vacuum pyrolysis oils-phenol-formaldehyde resols for bonding oriented strand board (OSB); Ph.D. Thesis, Laval University, Quebec, Canada, 2001.

29.   Scott, D.S., Piskorz, J., The flash pyrolysis of Aspen-Polar wood; Can. J. Chem. Eng., 1982, 60, pp. 666-674.

30.   Lappas, A.A., et al., Biomass pyrolysis in a circulating fluid bed reactor for the production of fuels and chemicals; Fuel, 2002, 81, pp. 2087-2095.

31.   Report of the EU project, Production, Treatment and Utilization of Bio-Oils from Pyrolysis, for Energy and Alternative Fuels and Chemicals; Contract No. AIR2-CT93-1086; 1996.

32. Matas, A., Union Electrica Fenosa; In Pyrolysis Network Newsletter, Issue No. 6, 1998, pp. 8-9.

33. McLellan, R., Wellman integrated fast pyrolysis pilot plant; In Pyrolysis Network Newsletter, Issue No. 10, 2000, pp. 12.

34. Roy, C., Morin, D., Dube, F., The biomass pyrocycling[TM] process; In Biomass gasification and pyrolysis: state of the art and future prospects, Kaltschmitt, M., Bridgwater, A.V., Eds., CPL Press, UK, 1997, pp. 307-315.

35. Dynamotive. BioTherm[TM]: A system for continuous quality, fast pyrolysis bio-oil; In The 4th Biomass Conference of the Americas, Oakland, CA, USA, 1999.

36. Gust, S., Nieminen, J.-P., Liquefied wood fuel could soon replace heavy oil!; In Wood Energy, 2002, No. 6, pp. 24-34.

37. Freel, B.A., Graham, R.G., Apparatus for a circulating bed transport fast pyrolysis reactor system; U.S. Patent 5,961,786. 1999.

38. Wagenaar, B.M., et al. Bio-oil as coal substitute in 600MWe power stations; In Twelfth European Biomass Conference: Biomass for Energy, Industry and Climate Protection, Amsterdam, The Netherlands, ETA-Florence and WIP-Munich, 2002.

39. Wagenaar, B.M., The rotating cone reactor: for rapid thermal solids processing; Ph.D. Thesis, University of Twente, Enschede, The Netherlands, 1994.

40. Wagenaar, B.M., Prins, W., van Swaaij, W.P.M., Flash pyrolysis kinetics of pine wood; Fuel Process. Techn., 1993, 36, pp. 291-298.

41. Gronli, M., Antal, M.J., Varhegyi, G., A round-robin study of cellulose pyrolysis kinetics by thermogravimetry; Ind. Eng. Chem. Res., 1999, 38, pp. 2238-2244.

42. Narayan, R., Antal, M.J., Thermal lag, fusion, and the compensation effect during biomass pyrolysis; Ind. Eng. Chem. Res., 1996, 35, pp. 1711-1721.

43. Antal, M.J., Jr., Varhegyi, G., Cellulose pyrolysis kinetics: the current state of knowledge; Ind. Eng. Chem. Res., 1995, 34, pp. 703-717.

44. Antal, M.J., Jr., Varhegyi, G., Impact of Systematic Errors on the Determination of Cellulose Pyrolysis Kinetics; Energy & Fuels, 1997, 11, pp. 1309-1310.

45. Antal, M.J., Jr., Varhegyi, G., Jakab, E., Cellulose pyrolysis kinetics: Revisited; Ind. Eng. Chem. Res., 1998, 37, pp. 1267-1275.

46. Knight, J.A., Gorton, C.W., Kovac, R.J., Oil production by entrained flow pyrolysis of biomass; Biomass, 1984, 6, pp. 69-76.

47. Nunn, T.R., Howard, J.B., Longwell, J.P., Peters, W.A., Product composition and kinetics in the rapid pyrolysis of sweet gum hardwood; Ind. Eng. Chem. Prod. Res. Dev., 1985, 24, pp. 836-844.

48. Reina, J., Velo, E., Puigjaner, L., Thermogravimetric study of the pyrolysis of waste wood; Thermochim. Acta, 1998, 320, pp. 161-167.

49. Samolada, M.C., Vasalos, I.A., A kinetic approach to the flash pyrolysis of biomass in a fluidized bed reactor; Fuel, 1991, 70, pp. 883-889.

50. Lanzetta, M., Di Blasi, C., Pyrolysis kinetics of wheat and corn straw; J. Anal. Appl. Pyrolysis, 1998, 44, pp. 181-192.

51. Branca, C., Di Blasi, C., Kinetics of isothermal degradation of wood in the temperature range 528-708K; J. Anal. Appl. Pyrolysis, 2003, 67, pp. 207-219.

52. Chan, W.-C.R., Kelbon, M., Krieger, B.B., Modelling and experimental verification of physical and chemical processes during pyrolysis of a large biomass particle; Fuel, 1985, 64, pp. 1505-1513.

53. Thurner, F., Mann, U., Kinetic investigation of wood pyrolysis; Ind. Eng. Chem. Process Des. Dev., 1981, 20, pp. 482-488.

54. Di Blasi, C., Branca, C., Kinetics of primary product formation from wood pyrolysis; Ind. Eng. Chem. Res., 2001, 40, pp. 5547-5556.

55. Shafizadeh, F., Chin, Peter P.S., Thermal deterioration of wood; ACS Symp. Series, 1977, 43, pp. 57-81.

63

56. Shafizadeh, F., Introduction to pyrolysis of biomass; J. Anal. Appl. Pyrolysis, 1982, 3, pp. 283-305.

57. Chan, W.-C.R., Kelbon, M., Krieger-Brockett, B., Single particle biomass pyrolysis: Correlations of reaction products with process conditions; Ind. Eng. Chem. Res., 1988, 27, pp. 2261-2275.

58. Hajaligol, M., Waymack, B., Kellogg, D., Low temperature formation of aromatic hydrocarbon from pyrolysis of cellulosic materials; Fuel, 2001, 80, pp. 1799-1807.

59. Rocca, P.A.D., et al., Pyrolysis of hardwoods residues: on kinetics and chars characterization; Biomass and Bioenergy, 1999, 16, pp. 79-88.

60. Bonelli, P.R., et al., Effect of pyrolysis temperature on composition, surface properties and thermal degradation rates of Brazil Nut shells; Bioresource Technology, 2001, 76, pp. 15-22.

61. Figueiredo, J.L., et al., Pyrolysis of holm-oak wood: influence of temperature and particle size; Fuel, 1989. 68, pp. 1012-1016.

62. Stenseng, M., Jensen, A., Dam-Johansen, K., Thermal analysis and kinetic modelling of wheat straw pyrolysis; In Progress in Thermochemical Biomass Conversion, Bridgwater, A.V., Ed., Blackwell Science, Oxford, UK, 2001, pp. 1061-1075.

63. Varhegyi, G., Szabo, P., Antal, M.J., Jr., Kinetics of charcoal devolatilzation; Energy & Fuels, 2002, 16, pp. 724-731.

64. Wojtowicz, M.A., et al., Modeling the evolution of volatile species during tobacco pyrolysis; J. Anal. Appl. Pyrolysis, 2003, 66, pp. 235-261.

65. Rostami, A.A., Hajaligol, M.R., Wrenn, S.E., A biomass pyrolysis sub-model for CFD applications; Fuel, 2004, 83, pp. 1519-1525.

66. Antal, M.J., Jr., Effects of reactor severity on the gas phase pyrolysis of cellulose and kraft lignin derived volatile matter; Ind. Eng. Chem. Prod. Res. Dev., 1983, 22, pp. 366-375.

64

67. Diebold, J.P., The cracking kinetics of depolymerized biomass vapors in a continuous tubular reactor; M.Sc. Thesis, Colorado school of mines, USA, 1985.

68. Liden, A.G., A kinetic and heat transfer modelling study of wood pyrolysis in a fluidized bed; Master's Thesis, University of Waterloo, Ontario, Canada, 1985.

69. Boroson, M.L., et al., Product yields and kinetics from the vapor phase cracking of wood pyrolysis tars; AIChE J., 1989, 35, pp. 120-128.

70. Boroson, M.L., Secondary reactions of tars from pyrolysis of sweet gum hardwood, Ph.D. Thesis, Massachusetts Institute of Technology, 1987.

71. Bamford, C.H., Crank, J., Malan, H., The combustion of wood, part I; Proc. Cambridge Philos. Soc., 1946, 42, pp. 166-182.

72. Roberts, A.F., Clough, G., Thermal decomposition of wood in an inert atmosphere; In 9th International Symposium on combustion, Pittsburg, USA, 1963.

73. Di Blasi, C., Heat, momentum and mass transport through a shrinking biomass particle exposed to thermal radiation; Chem. Eng. Sci., 1996, 51, pp. 1121-1132.

74. Di Blasi, C., Modeling intra- and extra-particle processes of wood fast pyrolysis; AIChE J., 2002, 48, pp. 2386-2397.

75. Di Blasi, C., A transient two-dimensional model of biomass pyrolysis; Developments in thermochemical biomass conversion, Bridgwater A.V., Boocock, D.G.B., Eds., Blackie Academic & Professional; London, UK, 1997, pp. 147-160.

76. Miller, R.S., Bellan, J, A generalized biomass pyrolysis model based on superimposed cellulose, hemicellulose and lignin kinetics; Combust. Sci. Tech., 1997, 126, pp. 97-137.

77. Kersten, S.R.A., Biomass gasification in circulating fluidized beds; Ph.D. Thesis, University of Twente, Enschede, The Netherlands, 2002.

78. Kothari, V., Antal, M.J., Jr., Numerical studies of the flash pyrolysis of cellulose; Fuel, 1985, 64, pp. 1487-1494.

79. Bliek, A., van Swaaij, W.P.M., van Beckum F.P.H., Effects of intraparticle heat and mass transfer during devolatilization of a single coal particle; AIChE J. 1985, 31, pp. 1666.

80. Bryden, K.M., Hagge, M.J., Modeling the combined impact of moisture and char shrinkage on the pyrolysis of a biomass particle; Fuel, 2003, 82, pp. 1633-1644.

81. Janse, A.M.C., Westerhout, R.W.J., Prins, W., Modelling of flash pyrolysis of a single wood particle; Chem. Eng. Proc., 2000, 39, pp. 239-252.

82. Pyle, D.L., Zaror, C.A., Heat transfer and kinetics in the low temperature pyrolysis of solids; Chem. Eng. Sci., 1984, 39, pp. 147.

83. Scott, D.S., Piskorz, J., The continuous flash pyrolysis of biomass; Can. J. Chem. Eng., 1984, 62, pp. 291-294.

84. Scott, D.S., Piskorz, J., Radlein, D., Liquid products from the continuous flash pyrolysis of biomass; Ind. Eng. Chem. Prod. Res. Dev., 1985, 24, pp. 581-588.

85. Scott, D.S., Piskorz, J, Radlein, D., The role of temperature in the fast pyrolysis of cellulose and wood; Ind. Eng. Chem. Res., 1988, 27, pp. 8-15.

86. Scott, D.S., et al., Flash pyrolysis of peat in a fluidized bed; Fuel Processing Technology, 1988, 18, pp. 81-95.

87. Agblevor, F.A., Besler, S., Evans, R.J., Inorganic compounds in biomass feedstocks: their role in char formation and effect on the quality of fast pyrolysis oils; Proceedings of biomass pyrolysis oil properties and combustion meeting; National Renewable Energy Laboratory, Estes Park, CO, USA, 1994.

88. Horne, P.A., Williams, P.T., Influence of temperature on the products from the flash pyrolysis of biomass; Fuel, 1996, 75, pp. 1051-1059.

89. Peacocke, G.V.C., et al., Effect of reactor configuration on the yields and structures of pine-wood derived pyrolysis liquids: A comparison between ablative and wire-mesh pyrolysis; Biomass and Bioenergy, 1994, 7, pp. 155-167.

66

90. Peacocke, G.V.C., et al., Comparison of ablative and fluid bed fast pyrolysis products: yields and analysis; In Developments in thermochemical biomass conversion, Bridgwater, A.V., Boocock, D.G.B., Eds., 1997, Blackie Academic & Professional, London, UK, 1997, pp. 191-205.

91. Hague, R.A., The pre-treatment and pyrolysis of biomass for the production of liquids for fuels and speciality chemicals; Ph.D. Thesis, Aston University, Birmingham, UK, 1998.

92. Bilbao, R., et al., Experimental and theoretical study of the ignition and smoldering of wood including convective effects; Combustion and Flame, 2001, 126, pp. 1363-1372.

93. Luo, Z., et al., Research on biomass fast pyrolysis for liquid fuel; Biomass and Bioenergy, 2004, 26, pp. 455-462.

94. Olazar, M., et al., Kinetic study of fast pyrolysis of sawdust in a conical spouted bed reactor in the range 400-500°C; J. Chem. Techn. Biotechn., 2001, 76, pp. 469-476.

95. Scholze, B., Hanser, C., Meier, D., Characterisation of the water-insoluble fraction from fast pyrolysis liquids (pyrolytic lignin) Part II. GPC, carbonyl groups, and ^{13}C -NMR; J. Anal. Appl. Pyrolysis, 2001, 58-59, pp. 387-400.

96. Scholze, B., Long-term stability, catalytic upgrading, and application of pyrolysis oils-improving the properties of a potential substitute of fossil fuels; Ph.D. Thesis, University of Hamburg, Hamburg, Germany, 2002.

97. Oasmaa, A., et al., Physical characterisation of biomass-based pyrolysis liquids: Application of standard fuel oil analyses; VTT, Technical Research Center of Finland: Espoo, Finland, 1997, pp. 87.

98. Oasmaa, A., Czernik, S., Fuel oil quality of biomass pyrolysis oils: state-of-the-art for the end users; Energy & Fuels, 1999, 13, pp. 914-921.

99. Minkova, V., et al., Effect of water vapor and biomass nature on the yield and quality of the pyrolysis products from biomass; Fuel Proc. Techn., 2001, 70, pp. 53-61.

100. Agblevor, F.A., Besler, S., Inorganic compounds in biomass feedstocks .1. Effect on the quality of fast pyrolysis oils; Energy & Fuels, 1996, 10, pp. 293-298.

101. Ghetti, P., Ricca, L., Angelini, L., Thermal analysis of biomass and corresponding pyrolysis products; Fuel, 1996, 75, pp. 565-573.

102. Encinar, J.M., et al., Pyrolysis of two agricultural residues: Olive and Grape bagasse, influence of particle size and temperature; Biomass & Bioenergy, 1996, 11, pp. 397-409.

103. Roy, C., et al., The pyrolysis under vacuum of Aspen-Poplar; In Fundamentals of Thermochemical Biomass Conversion, Overend, R.P., Milne, T.A., Mudge, L.K., Eds., Elsevier Applied Science Publisher, New York, 1985, pp. 237.

104. Kelbon, M., Bousman, S., Krieger-Brockett, B., Conditions that favor tar production from pyrolysis of large moist wood particles; In ACS Symposium Series 376; Pyrolysis oils from biomass producing, analyzing, and upgrading, Soltes, E.J., Milne, T.A., Eds., 1988, American Chemical Society, Washington, DC, 1988, pp. 41-54.

105. Pyle, D.L., Zaror, C.A., Heat transfer and kinetics in the low temperature pyrolysis of solids; Chem. Eng. Sci., 1984, 39, pp. 147-158.

106. Babu, B.V., Chaurasia, A.S., Heat transfer and kinetics in the pyrolysis of shrinking biomass particle; Chem. Eng. Sci., 2004, 59, pp. 1999-2012.

107. Di Blasi, C., Modelling the fast pyrolysis of cellulotic particles in fluid bed reactors; Chem. Eng. Sci., 2000, 55, pp. 5999-6013.

108. Seebauer, V., Petek, J., Staudinger, G., Effects of particle size, heating rate and pressure on measurement of pyrolysis kinetics by thermogravimetric analysis; Fuel, 1997, 76, pp. 1277-1282.

109. Nik-Azar, M., et al., Effects of heating rate and particle size on the products yields from rapid pyrolysis of beech wood. Fuel Sci. Techn. Intern., 1996, 14, pp. 479-502.

110. Bilbao, R., Millera, A., Murrilo, M.B., Temperature profiles and weight loss in the thermal decomposition of large spherical wood particles; Ind. Eng. Chem. Res., 1993, 32, pp. 1811-1817.

111. Altun, N.E., Hicyilmaz, C., Kok, M.V., Effect of particle size and heating rate on the pyrolysis of Silopi asphaltite; J. Anal. Appl. Pyrolysis, 2003, 67, pp. 369-379.

112. Chan, W.C.R., Kelbon, M., Kriegerbrockett, B., Single-particle biomass pyrolysis - Correlations of reaction-products with process conditions; Ind. & Eng. Chem. Res., 1988, 27, pp. 2261-2275.

113. Lede, J., et al., Fusion-like behavior of wood pyrolysis; J. of Anal. Appl. Pyrolysis, 1987, 10, pp. 291-308.

114. Lede, J., Reaction temperature of solid particles undergoing an endothermal volatilization. Application to the fast pyrolysis of biomass; Biomass and Bioenergy, 1994, 7, pp. 49-60.

115. Lede, J., Blanchard, F., Boutin, O., Radiant flash pyrolysis of cellulose pellets: products and mechanisms involved in transient and steady state conditions; Fuel, 2002, 81, pp. 1269-1279.

116. Liden, A.G., Berruti, F., Scott, D.S., A kinetic model for the production of liquids from the flash pyrolysis of biomass; Chem. Eng. Comm., 1988, 65, pp. 207-221.

117. Boroson, M.L., et al., Heterogeneous cracking of wood pyrolysis tars over fresh wood char surfaces; Energy & Fuels, 1989, 3, pp. 735-740.

118. Freel, B.A., Graham, R.G., Bergougnou, M.A., The kinetics of the fast pyrolysis (Ultrapyrolysis) of cellulose in a fast fluidized bed reactor; AIChE Symposium Series, 1987, 83, pp. 105-111.

119. Lathouwers, D., Bellan, J., Modeling of dense gas-solid reactive mixtures applied to biomass pyrolysis in a fluidized bed; Int. J. Multiphase Flow, 2001, 27, pp. 2155-2187.

120. Gerhauser, H., Bridgwater, A.V., Scale effects and distribution problems in fluid bed fast pyrolysis using CFD models integrated with reaction kinetics; In Expert meeting on Pyrolysis and Gasification of Biomass and Waste, Strasbourg, France, CPL Press, UK, 2002.

121.   Gerhauser, H., CFD applied to the fast pyrolysis of biomass in fluidized beds; Ph.D. Thesis, Aston University, Birmingham, UK, 2003.

122.   Prins, W., Draijer, W., van Swaaij, W.P.M., Heat transfer to immersed spheres fixed or freely moving in a gas-fluidized bed; In Heat and Mass Transfer in Fixed and Fluidized Beds, van Swaaij, W.P.M., Afgan, N.H., Eds., Hemisphere Publishing Corporation, Washington, USA, 1986, pp. 317-331.

123.   Gronli, M., A theoretical and experimental study of the thermal degradation of biomass; Ph.D. Thesis, Norweign University of Science and Technology (NTNU), Trondheim, 1996.

124.   Reid, R., The properties of gas and liquids; 2nd ed., McGraw Hill, New York, 1987.

125.   Borman, G.L., Ragland, K.W., Combustion Engineering. McGraw-Hill, New York, 1998.

126.   Ramakers, B.J., de Ridder, R., Kerkhof, P.J.A.M., Fluidization behavior of wood/sand mixtures; In Proceedings of the 14th International Drying Symposium, Sao Paulo, Brazil, 2004.

127.   Miller, R.S., Bellan, J., Numerical Simulation of Vortex Pyrolysis Reactors for Condensable Tar Production from Biomass; Energy & Fuels, 1998, 12, pp. 25-40.

128.   Carslaw, H.S., Jaeger, J.C., Conduction of Heat in Solids; 2nd Ed., Clarendon Press, Oxford, UK, 1959.

129.   Thiele, E.W., Relation between Catalytic Activity and Size of Particle; Ind. Eng. Chem., 1939, 31, pp. 916-920.

Chapter 3

Biomass Pyrolysis in a Fluidized Bed Reactor. Part II: Experimental Validation of Model Results

Abstract

Various types of cylindrical biomass particles (pine, beech, bamboo, demolition wood) have been pyrolyzed in a batch-wise operated fluid bed laboratory set-up. Conversion times, product yields and product compositions were measured as a function of the particle size (0.7 – 17 mm), the vapor's residence time (0.25 to 6 s), the position of the biomass particles in the bed (dense bed or splash zone), and the fluid bed temperature (250 - 800ºC). For pyrolysis temperatures between 450 and 550°C, the bio-oil yield appeared to be maximal (in this work: about 65 wt %) while the water content of the bio-oil is minimal. The position of the biomass particles in the fluid bed, either in the dense bed or in the splash zone, does not affect the conversion time and product yields to a large extent during pyrolysis at 500°C. In the small fluid bed used for this work, with a char hold-up of up to 5 vol. % (or 0.7 wt %), the residence time of the pyrolysis vapors is not that critical. At typical fast pyrolysis temperatures of around 500°C, it appeared sufficient to keep this residence time below 5 s to prevent significant secondary cracking of the produced vapors to non-condensable gas. Up to a diameter of 17 mm, the particle size has only a minor effect on the total liquid yield. However, for particles larger than 3 mm, the water content of the produced bio-oil increases significantly. The experimental results are further compared with predictions from a one-dimensional (1D) and a two-dimensional (2D) single-particle pyrolysis model. Such models appeared to have a limited predictive power due to large uncertainties in the kinetics and selectivity of the biomass decomposition. Moreover, the product quality cannot be predicted at all.

1.   Introduction

The first part [1] of this work was concerned with the literature review on biomass pyrolysis and pyrolysis modeling for the purpose of reactor design. In this companion paper, experimental results of lab-scale fluidized bed pyrolysis will be presented. The following parameters have been varied: the type of wood (beech, pine, bamboo, palletized demolition wood), the reactor temperature ($250 - 800^{o}$C), the particle size ($0.7 - 17$ mm), the vapor residence time in the gas phase ($0.25 - 6$ s), and the position of the biomass particles in the reactor (freeboard, splash zone, dense bed). Experimental results are compared with predictions of existing single particle models as described in the first part [1] of this research report. On basis of this comparison, the predictive potential, and the minimal level of modeling detail still giving sufficient accuracy for reactor design calculations, will be established. The significance of the presented work with respect to the design of a (fluid bed type) reactor for the pyrolysis of wood particles is discussed.

2.   Experimental Equipment and Procedure

Fluidized bed pyrolysis of cylindrical wood particles has been carried out at ambient pressure and temperatures in the range of $250 - 800^{o}$C. These particles were made from beech, pine, bamboo or demolition wood, and their diameters were varied from $1.5 - 17$ mm while keeping their length constant at 42 mm. In addition to these cylindrical particles, saw dust with an average diameter of 0.7 mm has been used. Other particle properties relevant for the interpretation of the experimental results are listed in Table 1.

Figure 1 shows a sketch of the experimental setup. The fluidized bed reactor was made of stainless steel and placed in an electric furnace for independent temperature control. A 45 mm long cylindrical bottom section (26 mm internal diameter) was connected with a 90 mm long wider top section (60 mm internal diameter) by a conical part with a height of 125 mm. The incoming gas (nitrogen) was preheated by passing it through a 400 mm long heating tube (10 mm internal diameter) coiled around the fluid bed reactor. A sintered metal plate underneath the bottom section served as a gas distributor.

74

Table 1. Elemental analysis and density of cylindrical particles

Species	Moisture wt %	Carbon[a]	Nitrogen[a]	Hydrogen[a]	Oxygen[a,b]	Density, kg/m^3
Beech	7.3	48.42	0.15	6.01	45.42	662
Pine	7.5	49.90	0.10	5.95	44.05	571
Bamboo	5.8	48.62	0.33	5.90	45.15	648
Demolition wood pellets	7.0	52.2	0.30	5.9	41.6	1240

[a] Dry basis; [b] By difference

Silica sand with an averaged particle diameter (d_{50}) of 258 μm was used as a fluidized bed material. Its minimum fluidizing velocity at room temperature and ambient pressure was found to be 0.032 m/s. The fluidized bed temperature was recorded continuously by a submerged chromel-alumel thermocouple.

Two sequential condensers, immersed in containers with iced water and dry ice/ethanol mixtures, respectively, were used to collect the pyrolysis liquid. Most of the pyrolysis vapors (80 - 90 wt %) coming from the fluidized bed reactor could be collected in the first copper-coil condenser where they were quenched to 5$^\mathrm{o}$C. Low boiling point fractions were accumulated in the second washing bottle condenser in which temperatures down to -79°C could be reached. Online infrared and TCD analyzers of Hartman and Braun (made in Germany), protected by additional paper filters, were used to measure the concentration of four main components in the product gases (CO, CO_2, CH_4, and H_2). The tubular cotton filter was meant to capture any residual liquid droplets formed downstream the condensation system. Finally, all the off-gases were sent to the main ventilation system.
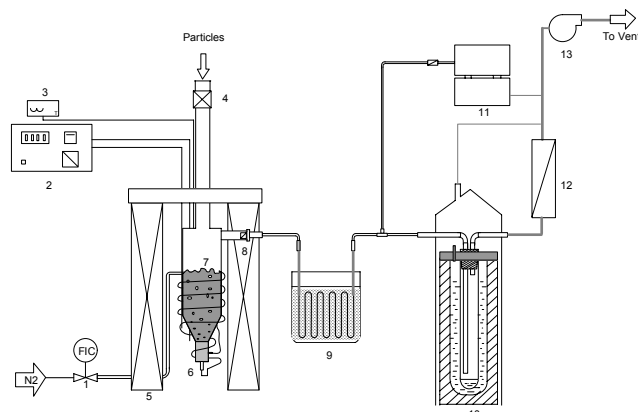
Figure 1. Scheme of the pyrolysis unit: (1) gas flow meter; (2) temperature controller; (3) reactor temperature monitor; (4) feedstock introduction; (5) electric furnace; (6) fluidized bed distributor; (7) fluidized bed reactor; (8) metal filter; (9) ice bath; (10) dry ice/ethanol mixture condenser; (11) gas analyzers; (12) cotton filter; and (13) ventilation system.

To achieve well reproducible, accurate results and a nearby full closure of the mass balance, a careful measurement procedure is of utmost importance. In the batch pyrolysis experiments of this work, this procedure consisted of a series of operations that are described here in detail.

1. The two condensers, the cotton filter, the paper filter of the gas analyzers, and the feedstock particles are weighed.

2. The fluidized bed reactor is filled with about 300 gram dry sand, installed in the furnace, and then connected to the nitrogen gas supply line. The feedstock introduction valve on top of the reactor is closed.

3. The nitrogen gas flow rate is fixed at 5 normal liters per minute, which yields a fluidization velocity between 2 to 3 times the minimum fluidization velocity, depending on the final operation temperatures. The reactor is heated to the desired temperature and stabilized for at least half an hour.

4. When the steady state is reached, the gas line to the analyzers is opened, approximately 10 g of biomass particles is rapidly fed to the reactor, in a series of typically three batches, and the computer program is initialized to record the gas concentrations. These operations are carried out at "time zero".

5. The pyrolysis time is defined as the time period from "zero" to the moment at which no more white smoke is visible in the top of first condenser, and obviously includes the heating time of the biomass particles.

6. A check on the visually observed pyrolysis time is obtained from the gas analysis. The pyrolysis process is completed when the gas analyzer readings are back on their base position. The response time of the analyzers has been determined separately with tracer gas injection. It appeared to be in the order of 1 s, which is at least 20 times shorter than the pyrolysis times observed experimentally (see Figure 3).

7. The furnace is switched off and left to cool.

8. The condensers, the paper filter, and the cotton filter are weighed again to determine the accumulated liquids.

9. To separate the produced char from the bed material, and determine its weight, the fluid bed inventory is carefully sieved.

10. Ethanol is used to clean the condensers.

11. Each experiment is repeated three times, and the measured values are averaged to create the data points included in the results presented. A mass balance closure over 95% is always considered necessary for accepting the results.

As shown in Figure 1, the biomass feed system is extremely simple. Each batch of wood particles is caused to fall on top of the bed by the opening of valve 4 in Figure 1 at time zero. Because the terminal falling velocity is always, even for the smallest wood particles, much higher (>1 m/s at 500 ^{o}C) than the applied fluidization velocity (about 0.05 m/s at 500 ^{o}C), there is no reason to believe that the wood particle will not reach the bed surface. Moreover, the falling time is always much less than 1 s. Therefore, the wood particles will be mixed into the splash zone and fluid bed interior before their pyrolysis vapors are added to the gas flow in the freeboard above the fluid bed.

In separate experiments, the mixing of wood particles with a fluid bed (of the same sand particles as used in the pyrolysis reactor) has been studied visually in a cold-flow glass model. At room temperature, the large wood particles (d_p > 5 mm) tend to float on the bed; small particles ($d_p \leq 3$), however, are mixed well with a fully fluidized bed.

Reported yields are based on the wet feedstock. The collected material in the first and second condenser plus the weight increase of the cotton and paper filter is defined as the liquid product. Typically, 80 - 90% was found in the first condenser, 10 - 20% in the second condenser, and about 1% on the filters.

Elemental analyses of solids (the original feedstock and residual char) and liquids samples were carried out (Flash EA 1112 ThermoQuest, Rodano, Italy). Carbon, hydrogen, and nitrogen were measured directly, while oxygen was determined by difference. The ash content of the feedstock was always very low, typically less than 1 wt %. The water content was determined by Karl-Fischer titration. It is important to mention that only the liquid collected in the first condenser has been analyzed. Liquids from the second condenser could not be analyzed, because of their small amounts.

The fluidized bed setup could not be used for temperatures below 350°C, because of the extremely long conversion time (24 h for 250°C). In this case, the condensation system suffers from continuous and prolonged re-evaporation of the liquid, resulting in a decreased recovery of bio-oil. To solve this problem, an autoclave reactor was used for the lowest temperatures. This autoclave was externally heated under good temperature control (heating jacket). It was divided horizontally into two parts by a stainless steel mesh. Wood particles of known mass were placed on the mesh. After an experiment, the autoclave was cooled in a nitrogen stream. Once at ambient temperature, first the autoclave reactor was flushed with a known volume of nitrogen; all the gases were collected in a sampling-bag and analyzed for its composition using a GC. On basis of the GC analysis and the known amount of nitrogen added, the produced permanent gases could be calculated. Afterward, the produced liquid was collected from the bottom part, and weighted. Finally, the char that remained on the mesh was weighted. The conversion time for T < 350°C was measured simply by putting the biomass particles in a controlled oven and weighing the mass of the sample every 15 min. Pressure built up during a pyrolysis experiment in the autoclave as a result of vapor, and gas production never exceeded the value of 1 bar (overpressure).

3.   Results

3.1.   Mass Balance

150 successful experiments were performed in total. Table 2 shows the mass balance of eight typical experiments at different conditions. It should be noticed that in this work the product yields are always based on the biomass "as received". Therefore, the liquid product includes the moisture present in the original biomass particle. The obtained closure of the mass balance was always between 94% and 104%. Experimental results outside this range have been rejected from the analysis. With this

78

criterion, the number of discarded experiments was about 15%. The reproducibility of the employed experimental method was checked by repetition of the experiments under identical conditions. It turned out that the relative error (defined as the standard deviation divided by the mean value) was always less than 2.5% (see Table 3).

Table 2. Mass balance of pyrolysis experiments at various conditions

Run No.	091803	090902	091701	091101	091801	091802	091001	091103
Temperature, ^{o}C	350	400	450	500	550	550	500	800
Feedstock	beech	beech	beech	beech	Beech	pine	bamboo	beech
Size (dp), mm	3	3	3	5	3	17	14	3
Yields, wt %, (on 'as received' basis)								
Liquids	57.2	55.7	67.5	65.0	64.6	58.9	56.6	33.8
Char	32.0	23.6	17.8	15.9	13.3	18.4	25.1	11.0
Permanent gas	10.0	18.4	10.1	17.7	20.5	17.9	19.1	56.9
Closure	99.2	97.7	95.4	98.6	98.4	95.2	100.8	101.7
Gas composition, vol. % (nitrogen free)								
H_2	0.9	1.4	0.8	2.3	3.4	6.9	1.5	13.8
CO	37.4	28.5	38.7	34.8	44.9	43.0	34.4	50.7
CO_2	60.5	68.6	58.5	54.3	37.2	33.2	54.0	13.5
CH_4	< 0.1	< 0.1	< 0.1	6.3	10.9	12.5	6.9	13.9
C_2H_4	0.5	0.7	0.8	1.1	1.7	1.8	1.2	5.8
C_2H_6	0.4	0.5	0.7	0.8	0.9	1.4	1.3	1.1
C_3H_6	0.2	0.3	0.3	0.4	0.7	0.9	0.5	1.0
C_3H_8	0.1	0.2	0.2	0.2	0.2	0.2	0.3	0.1

Table 3. Liquid yields (wt %) listed for various particle sizes[a].

	Size (d_p), mm					
	4.0	6.0	9.0	12.0	15.0	17.0
Test 1	64.4	64.7	62.9	64.0	62.2	62.3
Test 2	63.3	64.1	65.5	62.7	60.5	61.9
Test 3	64.9	65.0	63.5	62.5	61.0	60.9
Mean	64.2	64.6	64.0	63.0	61.2	61.7
Standard	0.9	0.4	1.4	0.8	0.9	0.7
$\sigma/<X>$, %	1.3	0.7	2.1	1.3	1.4	1.2

[a] Results of three identical measurements show the reproducibility of the experimental method. T = 500°C.

The water content of the liquid collected in the first condenser for 3 mm pine and beech wood particles was determined to be between 35% and 40% (see section 3.5). Assuming that the majority of water condenses in the first condenser, this results in a water content of the total liquid of 37.5% x 0.8 (fraction of liquid in the first condenser) = 30 wt %. This number corresponds to the water content of the oil produced by the main pyrolysis pilot plants [2,3].

3.2.   Position of Biomass Particles in the Fluid Bed Reactor

Because of their low density as compared to the sand particles, good mixing of biomass and char particles in the fluid bed is problematic, and segregation is likely to occur. Di Blasi and Branca [4] argued that in case of segregation, the biomass particles are decomposed mainly on top of the bed (splash zone) where the heat transfer rates are supposed to be low. This would lead to decreased yields. However, on top of the bed, there still is an intensive renewal of hot bed particles covering the biomass particle (a feature of splashing). To clarify this point, the present authors carried out separate heat transfer measurements according to the technique described by Prins et al. [5,6]. It appeared that the heat transfer coefficient from a spherical, 10 mm diameter particle in the splash zone of the fluid bed is just slightly lower than that in the dense phase (475 versus 400 W/m^2.K for the relevant conditions). This is further confirmed by the literature [7-10] concerning heat transfer from the fluid bed splash zone to a cooling tube. For instance, Pidwerbecki et al. [9] measured a value of 230 W/m^2.K in the splash zone against a value of 273 W/^{2}.K in the dense phase, for a vigorously fluidized bed of 1.1 mm particles (silica/alumina mixture), and a cooling tube of 51 mm outside diameter.

In addition to the separate heat transfer measurements, pyrolysis experiments were performed with particles that were forced to stay either in the dense bed or on top of the bed. Such particles were kept in the dense bed by either applying a sufficiently high gas velocity (intense mixing) or loading the particles with a massive metal weight attached to it by an iron wire. In case of the weight-loaded wood particle, a piece of metal had been connected to such particles with a thin flexible wire of about 3 cm length. While the metal piece descends to the bottom of the bed to stay there, the connected wood particle is allowed to move around, more or less freely, in the center region of the bed. Results of the latter method are placed within brackets in Table 4. This table shows that, with respect to the yields, there is hardly any difference between particles pyrolyzing on top or inside the fluid bed. Although, on top of the bed, the heat transfer appeared to be somewhat slower (resulting in a higher conversion time; see Table 4), apparently this difference in heating time is not enough to cause any significant variations in product yield. As there was no significant difference observed between experiments in the splash zone and in the dense bed, no further provisions were made for the rest of the experiments to ensure that the biomass particles are always completely submerged in the bed.

Table 4. Product yields of 42 mm long cylindrical beech wood particles pyrolyzed either on top of the bed in the splash zone (SZ), or in the dense bed (DB)[a].

Particle diameter:	Yield, wt %			
	3 mm	3 mm	15 mm	15 mm
Position	SZ	DB	SZ	DB
Reactor Temperature: 500°C				
Liquid	64.3	64.7 (64.8)	61.7	61.5 (62.4)
Char	15.2	15.8 (16.9)	19.1	19.4 (20.0)
τ, s	36	32	241	205
Reactor Temperature: 650°C				
Liquid	54.8	55.2 (57.5)	54.1	53.2 (51.8)
Char	13.4	13.4 (12.5)	17.0	16.7 (16.8)
τ, s	29	20	140	143

[a] Values between brackets refer to weight-loaded particles (see text).

3.3. Vapor Residence Time

For in-bed pyrolysis, the vapor residence time in the "high velocity" experiment is 1 s, while in case of a "weight loaded" particle it is 6 s. According to the results listed in Table 4, the vapor residence time does not affect the product yield to a large extent. With respect to that, it should be noticed that, at the end of the batch experiments referred to in Table 4, the char hold-up in the reactor was about 4 vol % .The corresponding specific external surface area of the char is estimated to be 10 m^2/m^3 ·bed for the 15 mm particles, and 70 m^2/m^3 ·bed for the 3 mm particles. This estimate is based on the observation that the particles stay intact during pyrolysis but are shrinking in volume by approximately 40%. Obviously the catalytic tar cracking effect of char is limited for the experiments described in this paper. Unfortunately, results reported in the literature concerning the effect of the vapor residence time are inconsistent (see part I [1]), which makes a comparison rather meaningless.

3.4. Effect of the Particle Aspect Ratio (l_p/d_P)

Model predictions show that increasing the aspect ratio above 2 does not result in a significant increase of the conversion time for otherwise identical conditions (see part I [1]). This is now confirmed by experimental results of pine wood cylinders shown in Figure 2.
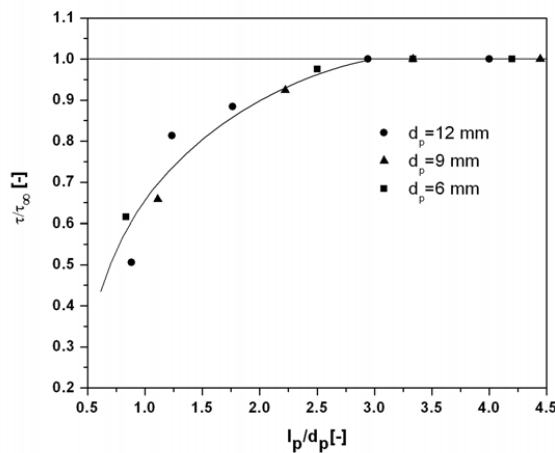
Figure 2. Effect of l_p/d_p on the conversion time, τ experimentally $\tau_{\infty} = \tau \big|_{l_p/d_p=4}$.

3.5. Effect of the Particle Size on the Pyrolysis Time at 500°C

In Figure 3, the measured pyrolysis time at a typical flash pyrolysis temperature of 500°C is plotted versus the particle size and compared with model predictions. The data were obtained from experiments with cylindrical beech wood particles, which all had a length over diameter ratio larger than 3; that is, they were one-dimensional with respect to heat transport. The one-dimensional single particle model was used for the simulations. The measured data (see Figure 3) show that, for beech, the kinetically controlled pyrolysis regime at 500°C reaches up to a particle size of ca. 2 mm. In the kinetically controlled regime, the pyrolysis time is independent of the particle size. For large particles, the conversion time becomes independent of the chemical kinetics. Instead the thermal diffusivity and external heat transfer (only for Bi < 50) are important variables [11,12]. The external heat transfer coefficient for most reactor types can be estimated with reasonable accuracy from available literature correlations. On basis of the overview on physical properties of woody biomass by Grønli [13], it can be recalculated that its thermal diffusivity ranges from 5×10^{-8} to 5×10^{-7} m^2/s (excluding Balsa wood with $\rho = 100$ kg/m^3). In fact, the density, the specific heat, and the thermal conductivity of almost any biomass type are available, so that a reliable estimate of the thermal diffusivity can be made.
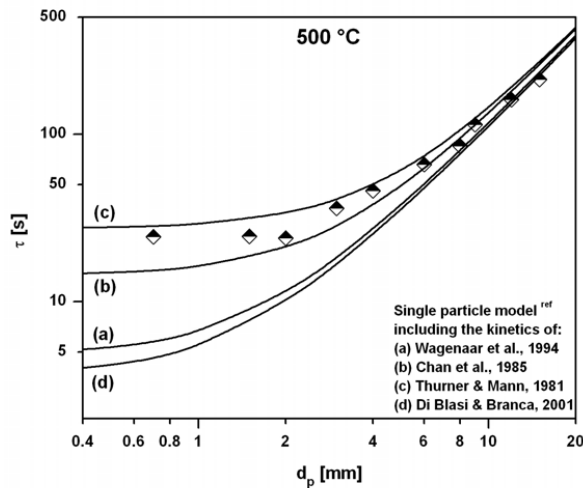
Figure 3. Pyrolysis time (at 500°C) of 42 mm long cylindrical beech wood particles versus the particle diameter. Experimental results ($\diamond$) are compared with predictions of the one-dimensional model (—) discussed in part I [1].

Detailed information on the chemical kinetics is required in single particle models for an accurate prediction of the conversion time for small particles (Figure 3: $d_p < 2$ mm). Contrary, in case of large particles (Figure 3: $d_p > 6$ mm), the pyrolysis time can be predicted quite precisely with a simple one-dimensional model irrespective of the used kinetics. For instance, for beech wood particles with a diameter of 12 mm, the measured conversion time was 161 s while the single particle model predicted a pyrolysis time of 159 s on basis of the kinetics derived by Wagenaar [14], 180 s for the kinetics of Chan [15]), 191 s for the kinetics of Thurner and Mann [16], and 152 s for the kinetics of Di Blasi and Branca [4]. For engineering purposes, that is, the design of a reactor for pyrolysis, these estimates are accurate enough. It is also worthwhile to note that for the biomass particle sizes applied in practical reactors, from 1 to 5 mm, the pyrolysis time is influenced by all three mechanisms: the pyrolysis kinetics, the heat transfer from the bulk of the reactor to the particle, and the intraparticle heat conduction.

3.6. Effect of the Particle Size and Biomass Type on the Product Yields at 500°C

Figure 4 shows the measured effect of the particle size ($l_p/d_p > 3$) on the product yield of fast pyrolysis of woody biomass at 500°C. In the same figure, results of computer simulations with a 1D single particle model are plotted. For the considered range of particle sizes (0.7 – 17 mm), the heating rate decreases from ca. 1000°C/s (0.7 mm), 50 °C/s (3 mm), 3°C/s (10 mm) to 1.5°C/s (17 mm), while the total liquid yield remains nearly constant. Both theory and experimental work show that the particle size has only a minor effect on the total liquid yield up to a diameter of 17 mm. The heating rates were calculated with the 1D single particle model. Although the pyrolysis process is usually related to the single-particle heating rate, the relevant heating rate has never been defined very well. The pyrolysis reactions of the 0.7 mm particle at 500°C take place at the reactor temperature, because the process is controlled by chemical kinetics. That means that, instead of the heating rate (here: the initial heating rate), the fluid bed temperature determines the pyrolysis rate and product distribution through the intrinsic reaction kinetics. In case of 10 and 17 mm particles, internal heat transport dominates the pyrolysis rate. The relevant heating rate is then defined as the one inside the penetrating reaction front, averaged over the particle's volume (see part I [1]).

84

Fluid bed pyrolysis of beech, bamboo, and pine gave nearly identical total liquid yields. Presumably, also as a consequence of a higher density and lower thermal diffusivity, significantly less liquid (and more char) was collected from 6 mm demolition wood particles. Concerning the char yields, a clear difference could be observed. For 3 mm particles, ca. 20 wt % of char was produced in case of bamboo, whereas pine had a char yield of only 10 wt %. Large-particle char and liquids yields are approximately the same for pine, beech, and bamboo.
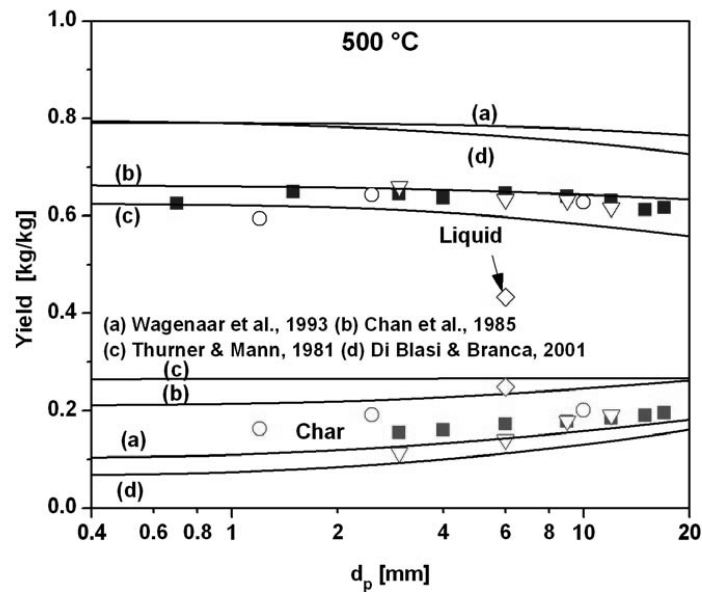
Figure 4. Total liquid and char yield of beech (■), pine (▽), bamboo (○), and demolition wood (◇) particles versus the particle size at 500°C. Experimental results are plotted for different kinetic data sets and compared with predictions (——) of the one-dimensional model discussed in part I [1].

As a consequence of the wide variation in the reported kinetic data (partly due to a variation in feedstock type), there is also quite some uncertainty in the model predictions regarding the product distribution, despite the high level of detail applied in the description of the mass and heat transfer processes (see model lines in Figure 4). However, contrary to the pyrolysis time, with respect to the product distribution the differences between the kinetic data sets remain over the whole range of particle sizes. In fact, it is still impossible to predict practical results regarding the product yields of biomass pyrolysis by combining detailed transport models with the available kinetics. Figure 4 shows that for the usual flash pyrolysis conditions, the calculated oil yield varies from 60 to 80 wt % depending on the kinetic data set used.

85

Figure 4 also shows the limited value of the published kinetic relations when used for the validation of experimentally observed product distributions. This is probably due to the different wood types used in kinetic studies and their numerous uncontrollable factors such as growth conditions and pretreatment. Thurner and Mann [16] measured for oak sawdust, Chan [15] for unspecified sawdust, Wagenaar [14] for pine and Di Blasi and Branca [4] for beech. Another aspect is the nature of the interpretation scheme being based on lumped components, which is known to be very sensitive to any applied experimental conditions and the type of reactor with its particular mixing state [17,18].

For the beech wood used in this work, none of the available kinetic data sets could describe the whole measured product yield satisfactorily (see Figure 4), not even the kinetic data of Di Blasi and Branca that were actually derived for beech. Model simulations including Wagenaar's reaction kinetics cannot predict our results of fluid bed pine wood correctly either, although they were actually measured for that wood type. The agreement between the measured liquid yield of beech, pine, and bamboo and the model predictions using the kinetics of Chan et al. is very good (see Figure 4). However, the amount of beech-char is overpredicted by a factor 1.75 for the same kinetics (see Figure 4). For beech-char, the model predicts the measured yield best when the kinetics of Wagenaar et al. are included.

3.7   Effect of the Reactor Temperature on the Product Yields

Next to the particle size, the reactor temperature is also an important design parameter. Figure 5 shows the measured product yields of relatively small particles versus the reactor temperature, which was varied over a wide range. At low temperatures (below 350°C), an autoclave instead of the fluidized bed reactor was used, because the condenser system of the FB setup was not suited to capture the liquids, due to the long pyrolysis time (2 - 3 days; see Experimental Section). Below 350°C, the conversion time is extremely long, up to 1.5 days for 250°C. The liquid yield shows a maximum between 450 and 550°C. Over the whole temperature range, yields of char and gas decrease and increase, respectively, upon increasing the reactor temperature. The results are in good qualitative agreement with the fluidized bed pyrolysis results of Scott and co-workers [19]. In Figure 5 also predictions of the 1D single particle model are plotted, and, again, like for the effect of d_p, the trends can be predicted quite well, whereas a quantitative mapping is not achieved. Only the kinetic data of Chan et al. [15] were used to calculate the model lines because these data

86

turned out to match the observed liquid yield data the best in the fast pyrolysis regime. For the other kinetic sets, the predicted trends are similar, however.
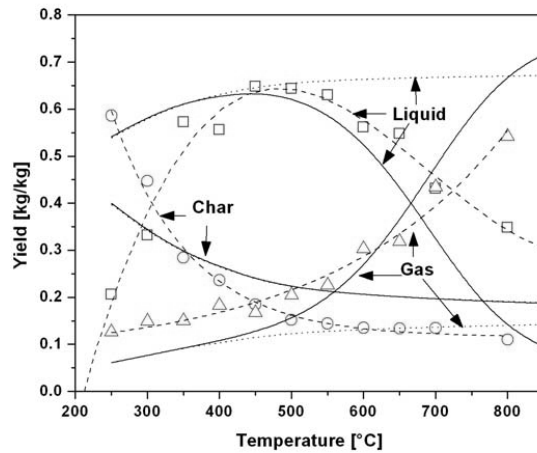

Figure 5. Product yields obtained from pyrolysis of pine wood particles (d_p = 3 mm and l_p= 42 mm) as a function of the reactor temperature. Dashed lines indicate the trends of measured values. Solid lines represent predictions of the one-dimensional model (see part I [1]) and include the effect of secondary cracking of vapors. Symbols used are: □ = liquid, Δ = gas, ○ = char.

It has been found that above 450°C cracking of primary tars inside the reactor to gases and refractory tar has to be included in the mathematical model in order to get the best possible agreement between model predictions and experimental results (compare dotted lines with solid lines in Figure 5). However, at 500°C the effect is still insignificant (for a vapor residence time of about 2 s). The reactor model used is very simple. It was assumed that the primary tars evolving from the pyrolyzing particle decompose according to a first-order decay reaction in a plug-flow reactor. The tar cracking kinetics of Boroson et al. [20] gave the best fit. When using the tar cracking kinetics of Diebold [21] and Liden et al. [22], the predicted effect of the reactor temperature on the liquid yield is too strong. This might be due to the limited opportunity in our reactor for contact between vapors and char, the latter being known to catalyze tar-cracking reactions.

3.8   Influence of the Reactor Temperature on the Product Quality

Up to now, most pyrolysis experiments have been interpreted on basis of kinetic schemes for lumped components classes (total liquids, char, and gas). In this way, only information on the yields of such products is available. However, next to the quantity of each product, also the quality (composition) of the products is a very important process parameter. Recently, the quality of the liquid main product has indeed become an item of research [23-26]. Usually, the research is focused on identification of the chemical species in the liquid product, the molecular weight distribution, physical properties, etc., while the investigations are limited to the analysis of oil samples obtained under more or less identical process conditions (500°C, small d_p). Hereafter, results with respect to the product composition (C, H, O, and water content) are presented for pyrolysis experiments conducted over a wide range of operating conditions. Only the liquids collected in the first condenser have been analyzed, which should be taken into account while considering the results discussed below.
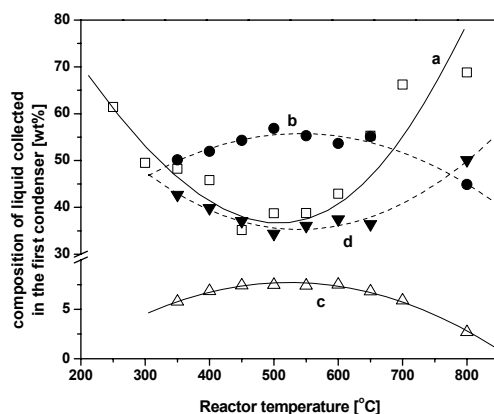
Figure 6. Effect of the reactor temperature on the composition of the liquid phase collected in the first condenser: (a) water content of the liquid, (b) carbon content of the organic fraction, (c) hydrogen content of the organic fraction, (d) oxygen content of the organic fraction. Pine wood, d_p= 3 mm, l_p = 42 mm.

Figure 6 shows the water content of the liquid product and the composition of the organic fraction collected in the first condenser, versus the reactor temperature. The water content of the liquid at typical fast pyrolysis conditions is higher than reported in the literature (range of water content [2,27,28]). It should, however, be noticed that only the liquid collected in the first condenser is considered here, which adds up only
88

to ca. 85% of the total liquid. The liquid collected in the second condenser contains hardly any water (less than 2 wt %). When corrected for this, the water content of the total liquid phase is about 30 - 35 wt %, which corresponds to the water content of, for example, BTG's pyrolysis oil [2]. Clearly, at torrefaction conditions [29-31] (T = 250 - 280°C) the produced liquid phase consists largely of water. This holds also for the produced liquids obtained at the highest temperature (800°C). The latter indicates that water is one of the main products of secondary cracking reactions. In the range of 450 - 600°C, the composition of the organic fraction collected in the first condenser varies hardly; it contains about 55 wt % carbon, 7.5 wt % hydrogen, 36 wt % oxygen, and 1.5 wt % nitrogen. This composition is in good agreement with results reported in literature [2,32,33]**.** It should be noticed, however, that addition of the liquid fraction collected in the second condenser (10 - 20%) could change the given numbers slightly. At higher and lower temperatures, the oxygen content increases while the carbon and hydrogen content decrease. It appears that just in the range of 450 - 550°C a liquid is produced that meets the characteristics of bio-oil [33]**.** The results presented in Figure 7 show that the solid product formed at low temperature is not really carbonaceous. In fact, only above approximately 500°C it seems justified to call the solid product char (more than 85 wt % carbon).
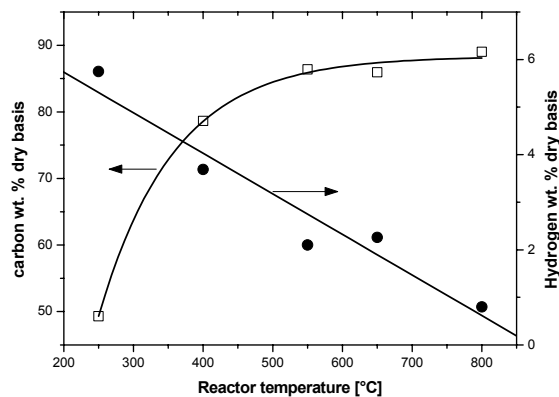

Figure 7. Effect of the reactor temperature on the composition of the solid phase. Pine wood, d_p= 3 mm, l_p = 42 mm.

3.9. Influence of the Particle Size on the Product Quality

In Figure 8, the water content of the liquid and the elemental composition of its organic fraction produced at 500°C are plotted versus the particle size. According to Figure 4, the total liquid yield (organics + water) is almost constant within the particle size range of 3 - 12 mm, just like the composition of the organic fraction (C, H, O; see Figure 8). However, Figure 8 shows that the water content of the liquid product increases from approximately 40 to 55 wt % when increasing the particle size from 3 to 12 mm. As a result of the increased water content, the heating value of the liquid product (wet oil) decreases. The increased water content for larger particles may be caused by a lower effective pyrolysis temperature (defined in part I [1]; see also Figure 6) and a longer residence of the vapors inside the particle (secondary cracking).
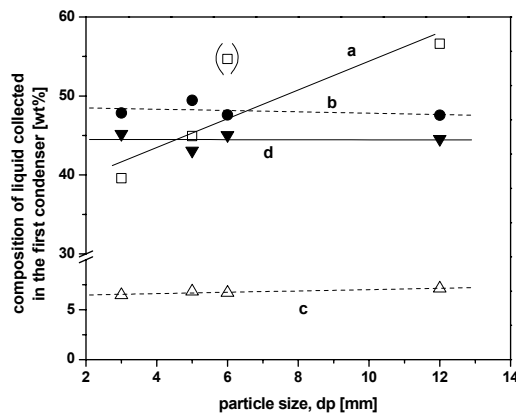
Figure 8. Effect of the particle size on the composition of the liquid phase collected in the first condenser: (a) water content of the liquid, (b) carbon content of the organic fraction, (c) hydrogen content of the organic fraction, (d) oxygen content of the organic fraction. Reactor temperature = 500°C. Beech wood, l_p = 42 mm.

Figure 9 shows the influence of the particle diameter on the carbon content of the produced solid phase. The carbon content decreases for larger particles, which can be explained again by a decreasing effective pyrolysis temperature (defined in part I [1]; see also Figure 6). At lower temperature, the produced char contains less carbon (see also Figure 7).

Product quality is indeed an important design variable. Optimal process conditions for a maximal liquid yield differ from those for a certain bio-oil quality. Especially the water content of the liquid product and the carbon content of the solid product are sensitive for the particle properties and pyrolysis conditions. Variations in product quality cannot be predicted by single particle models because the decomposition kinetics only include the three lumped product classes "gas", "tar" (total liquids, including water), and a carbonaceous solid indicated as "char".
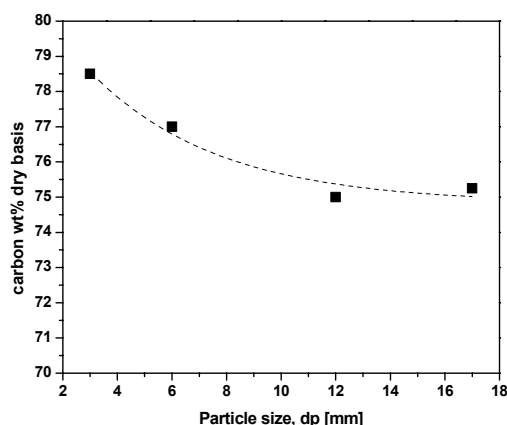
Figure 9. Measured effect of the particle size on the carbon content of the solid phase. Reactor temperature = 400°C. Beech wood, l_p = 42 mm.

4. Discussion

In this section, the reported results concerning the effect of the reactor temperature, the residence time of the vapors, the position of biomass in the FB, and the particle size are interpreted with respect to the use of models and reactor design.

For a variety of feedstock types, it has been observed by various other researchers[32, 34-40] that the maximum yield of bio-oil (up to 70 wt % on moisture-free basis) is obtained in small-scale laboratory equipment at a temperature of around 500°C. Also, the data presented in this paper show that for small particles (3 mm) the maximum oil yield is reached between 450 and 550°C. On basis of the wet feedstock, 65 wt % liquids with a water content of ca. 30 wt % were collected under typical pyrolysis conditions. Scott et al. [19] studied the product quality over a small temperature range and found that the best bio-oil quality in terms of caloric value and hydrogen over

carbon ratio is also achieved at the maximum-yield temperature. We measured over the temperature range of 250 - 800°C and found that the water content of the oil is minimal, and the heating value maximal between 450 and 550°C.

Regarding the maximal permitted residence time of the produced vapors in the hot section, the data reported in literature are contradictory. Some researchers found that residence times exceeding 0.5 s already cause the oil yield to decrease, whereas others found no effect of the residence time at all up to values of 2 - 3 s. Also, in the laboratory-scale experiments reported in this paper, the gas phase residence time has been varied. In a small fluid bed reactor at 500 °C, with a low char hold-up, the residence time of the vapor phase was varied from 1 - 6 s, which appeared to have no notable influence on the product yield. Especially at low temperatures, the contact with char has presumably more effect on secondary cracking reactions than the actual vapor residence time. While interpreting published results on secondary cracking of the primary pyrolysis vapors, and for future studies, the char hold-up of the pyrolysis reactor as well as the presence of entrained char in the hot parts between the reactor and the condenser should therefore be taken into account explicitly.

The experimental data obtained in this study have revealed that the total liquid yield is hardly affected by the particle size up to 17 mm. This effect can be explained on the basis of intrinsic kinetics and the heat penetration into the particle. For particles up to 20 mm, the decrease in effective pyrolysis temperature as defined in part I [1] is limited to 100°C for a reactor temperature of 500°C. In the range of 400 - 500°C, the majority of the total liquid yields (small d_p) reported in the literature are comparable.

The particle size, however, does have some effect on the oil quality. For increasing particle sizes, the moisture content of the produced liquid was found to increase. This can also be explained from the effective pyrolysis temperature, which is calculated to be notably lower for larger particles. This observation corresponds to the fact that for "kinetically controlled" pyrolysis of small particles, the moisture content of the liquid product also increases upon lowering the temperature (see Figure 6, for T < 500°C). The elemental composition of the organics in the oil does not change as a function of the particle size.

As stated before, the particle size has a large influence on the conversion time. For beech wood, the conversion time increases from 25 s for small particles (≤ 2 mm) up to 220 s for particles of 15 mm. While considering reactor design, the increased conversion time has two important consequences:

92

1) The residence time of biomass in the reactor should be increased to fulfill the criterion that the residence time of the feed particles must be larger than their conversion time to ensure complete conversion. In most reactors currently applied for fast pyrolysis [3], it is difficult to create a biomass residence time of more than 2 min as required for the pyrolysis of 1 cm diameter particles. For instance, large particles fed to the bottom of a fluid bed rise with a constant velocity and, once arrived at the top, do not mix back easily. This results in an undesired accumulation of partially converted feedstock on top of the bed. In such a case, most of the conversion takes place near the bed surface causing a nonuniform, local vapor production and heat demand in large-scale reactors.

2) A limit may be reached upon increasing the biomass particle throughput above which the specific hold-up of partially converted large particles becomes too high for acceptable fluidization of the (sand) bed. Therefore, the limit with respect to the maximum particle size for fast pyrolysis is imposed by the bio-oil quality (water content) and the restrictions for reactor design rather than by a loss in total liquid yield.

Finally, from the analysis reported in this paper, it has become evident that the value of advanced single particle modeling is limited. If the reaction kinetics and selectivity are known from special measurements, the conversion times of small particles, as well as the product yields for all particle sizes, can be predicted in principle. However, the variation in results of kinetic measurements is huge due to the facts that a) biomass is a natural material with always varying properties, even for a single type, b) results are always interpreted on basis of a lumped kinetic scheme, which is known for its sensitivity to experimental conditions and equipment configuration, and c) accurate measurement appears to be difficult. Mass balance closures are seldom good enough to clearly determine the real trends of the product yields as a function of temperature and biomass particle size.

Unfortunately, one has to conclude that the reaction kinetics reported until now cannot be used to predict the product distribution or the conversion time of small particles with sufficient accuracy. Only for large particles ($d_p > 6$ mm), the conversion time can be estimated quite well with single particle models. This is due to the fact of heat transfer control. External and internal heat transfer properties of biomass are known in sufficient detail. Future single particle models should focus more on the description of the quality of the product classes. To include quality aspects, a new kinetic scheme is required, for instance, starting from a molecular weight (MW)

93

distribution concept. It should be more consistent with the underlying chemistry of thermolytic bond cleavage, recombination reactions, and volatilization of low MW products. Such models are based on a continuous reaction and species spectra [41,42], which are characterized by MW and functional groups. Similar models are used to describe pyrolysis of synthetic polymers [43]. The challenge will be to find the chemical and physical processes that define the specific boundaries and restrictions for biomass pyrolysis. For instance, the model should account for the fact that a solid matrix always remains. Wagenaar et al. [36] and Landau et al. [44,45] proposed such a model already for biomass pyrolysis. Their early version, however, is too simple and shows many shortcomings.

5. Conclusions

Wood particles (pine, beech, bamboo, demolition wood) have been pyrolyzed batch-wise in a fluid bed laboratory setup. Conversion times, product yields, and product composition were measured as a function of the particle size (0.7 - 17 mm), the vapor's residence time (0.25 - 6 s), the position of the biomass particles in the bed (dense bed and splash zone), and the fluid bed temperature (350 - 800°C). The results are compared with single particle model calculations. The main conclusions can be summarized as follows:

- Wood particles stay intact during fluid bed pyrolysis but are shrinking in volume by approximately 40%.

- Product yields of pine and beech wood obtained are quite similar. The bio-oil yield is maximal (65 wt % on wet feedstock basis) for a wide temperature range of 450 - 550°C, while the water content of the bio-oil is minimal (30 - 35 wt %). More char is produced from bamboo particles (almost 20 wt %) and demolition wood particles of 6 mm (25 wt %).

- As long as excessive accumulation of biomass and char on the bed surface is avoided, the location of biomass particles in the fluid bed, either in the dense bed or in the splash zone, does not effect their pyrolysis time and yields to a large extent.

- In our fluid bed (with low char hold-up) at typical fast pyrolysis conditions, the residence time of the pyrolysis vapors is not very critical with respect to the possible loss of condensable products; $\tau < 5$ s seems to be acceptable at 500°C.

- While considering the risk of pyrolysis vapor cracking, the char hold-up of the reactor as well as the presence of entrained char in hot parts between the reactor and the condenser should be taken into account explicitly.

- Both, theory and experimental work show that the particle size has only a minor effect on the total liquid yield up to a diameter of 20 mm. However, for particles larger than 3 mm, the water content of the produced bio-oil increases substantially.

- The use of very small biomass particles as a feedstock for fast pyrolysis is not an intrinsic requirement. A choice to use small particles is more related to the desired oil quality and certain constraints concerning the reactor design.

- The pyrolysis time of biomass particles in the size range of 1 - 5 mm, usually applied in full-scale reactors at 500°C, is influenced by all three mechanisms: the pyrolysis kinetics, the heat transfer from the bulk of the reactor to the particle, and the intra-particle heat conduction.

95

- Existing single particle models have a limited predictive power with respect to the product distribution and the conversion time of small particles (< 3 mm), due to a wide variation in reported decomposition kinetics.
- Variations in bio-oil quality (e.g., water content of liquid) cannot be predicted by existing single particle models. Product quality is, however, an important design parameter. Optimal process conditions for a maximal liquid yield may differ from those for a certain desired bio-oil quality.

Acknowledgement

References

1. Kersten, S.R.A., Wang, X., Prins, W., van Swaaij, W.P.M., Biomass pyrolysis in a fluidized bed reactor: Part I. literature review and model simulations; Ind. Eng. Chem. Res., 2005, 44, pp. 8773-8785.

2. Scholze, B., Long-term stability, catalytic upgrading, and application of pyrolysis oils-improving the properties of a potential substitute of fossil fuels; Ph.D. Thesis, University of Hamburg, Hamburg, Germany, 2002.

3. Bridgwater, A.V., Peacocke, G.V.C., Fast pyrolysis processes for biomass; Renewable and Sustainable Energy Reviews, 2000, 4, pp. 1-73.

4. Di Blasi, C., Branca, C., Kinetics of primary product formation from wood pyrolysis; Ind. Eng. Chem. Res., 2001, 40, pp. 5547-5556.

5. Prins, W., Fluidized bed combustion of a single carbon particle; Ph.D. Thesis, University of Twente, Enschede, The Netherlands, 1987.

6. Prins, W., Draijer, W., van Swaaij, W.P.M., Heat transfer to immersed spheres fixed or freely moving in a gas-fluidized bed; In Heat and Mass Transfer in Fixed and Fluidized Beds, van Swaaij, W.P.M., Afgan, N.H., Eds., Hemisphere Publishing Corporation, Washington, USA, 1986, pp. 317-331.

7. Dyrness, A., Glicksman, L.R., Yule, T., Heat transfer in the splash zone of a fluidized bed; Int. J. Heat Mass Transfer, 1993, 35, pp. 847-860.

8.   Wood, R.T., Kuwata, M., Staub, F.W., Heat transfer to horizontal tube banks in the splash zone of a fluidized bed of large particles; In Fluidization, Grace, J.R., Matsen, J.M., Eds., Plenum, New York, 1980, pp. 235-243.

9.   Pidwerbecki, D., Welty, J.R., Heat transfer to a horizontal tube in the splash zone of a bubbling fluidized bed: an experimental study of particle size effects; Experimental Thermal and Fluid Science, 1995, 10, pp. 307-317.

10.   Pidwerbecki, D., Welty, J.R., Heat transfer to a horizontal tube in the splash zone of a bubbling fluidized bed: an experimental study of temperature effects; Experimental Thermal and Fluid Science; 1994, 9, pp. 356-365.

11.   Pyle, D.L., Zaror, C.A., Heat transfer and kinetics in the low temperature pyrolysis of solids; Chem. Eng. Sci., 1984, 39, pp. 147-158.

12.   Lede, J., Chemical engineering aspects of solid (biomass) particle pyrolysis: a review of the possible rate limiting factors; In Developments in thermochemical biomass conversion, Bridgwater A.V., Boocock, D.G.B., Eds., Blackie Academic & Professional, London, UK, 1997, pp. 104-116.

13.   Gronli, M., A theoretical and experimental study of the thermal degradation of biomass; Ph.D. Thesis, Norweign University of Science and Technology (NTNU), Trondheim, 1996.

14.   Wagenaar, B.M., Prins, W., van Swaaij, W.P.M., Flash pyrolysis kinetics of pine wood; Fuel Processing Technology, 1993, 36, pp. 291-298.

15.   Chan, W.-C.R., Kelbon, M., Krieger, B.B., Modelling and experimental verification of physical and chemical processes during pyrolysis of a large biomass particle; Fuel, 1985, 64, pp. 1505-1513.

16.   Thurner, F., Mann, U., Kinetic investigation of wood pyrolysis; Ind. Eng. Chem. Process Des. Dev., 1981, 20, pp. 482-488.

17.   Luss, D., Golikeri, S.V., Grouping of many species each consumed by two parallel first-order reactions; AIChE J., 1975, 21, pp. 865-872.

18.   Golikeri, S.V., Luss, D., Analysis of activation energy of grouped parallel reactions; AIChE J., 1972, 18, pp. 277-282.

19.   Scott, D.S., Piskorz, J., Radlein, D., The role of temperature in the fast pyrolysis of cellulose and wood; Ind. Eng. Chem. Res., 1988, 27, pp. 8-15.

20.   Boroson, M.L., Howard, J.B., Longwell, J.P., Peters, B., Product yields and kinetics from the vapor phase cracking of wood pyrolysis tars; AIChE J., 1989, 35, pp. 120-128.

21. Diebold, J.P., The cracking kinetcs of depolymerized biomass vapours in a continuous tubular reactor; M.Sc. Thesis, Colorado school of Mines, USA, 1985.

22. Liden, A.G., Berruti, F., Scott, D.S., A kinetic model for the production of liquids from the flash pyrolysis of biomass; Chem. Eng. Comm., 1988, 65, pp. 207-221.

23. Oasmaa, A., Czernik, S., Fuel oil quality of biomass pyrolysis oils: state-of-the-art for the end users; Energy & Fuels, 1999, 13, pp. 914-921.

24. Agblevor, F.A., Besler, S., Evans, R.J., Inorganic compounds in biomass feedstocks: their role in char formation and effect on the quality of fast pyrolysis oils; In Proceedings of biomass pyrolysis oil properties and combustion meeting, National Renewable Energy Laboratory, Estes Park, CO, 1994.

25. Minkova, V., Razvigorova, M., Bjornbom, E., Zanzi, R., Budinova, T., Petrov, N., Effect of water vapour and biomass nature on the yield and quality of the pyrolysis products from biomass; Fuel Process. Techn., 2001, 70, pp. 53-61.

26. Agblevor, F.A., Besler, S., Inorganic compounds in biomass feedstocks .1. Effect on the quality of fast pyrolysis oils; Energy & Fuels, 1996, 10, pp. 293-298.

27. Oasmaa, A., Leppamaki, E.A., Kopolen, P., Levander, J., Tapola, E., Physical characterisation of biomass-based pyrolysis liquids: Application of standard fuel oil analyses; VTT, Technical Research Center of Finland, Espoo, Finland, 1997, pp. 87.

28. Bridgwater, A.V., Czernik, S., Diebold, J., Meier, D., Oasmaa, A., Peacocke, C., Piskorz, J., Radlein, D., Eds., Fast pyrolysis of biomass: A handbook, CPL Press, 1999.

29. Bergman, P.C.A., Boersma, A.R., Kiel, J.H.A., Prins, M.J., Ptasinski, K.J., Janssen, F.J.J.G., Torrefaction for entrained-flow gasification of biomass; In The 2nd World Conference and Technology Exhibition on Biomass for Energy, Industry and Climate Protection, Rome, Italy, 2004.

30. Felfli, F.F., Luengo, C.A., Bezzon, G., Soler, P., Bench unit for biomass residues torrefaction; In 10th European Biomass Conference and Technology Exhibition, Biomass for Energy and Industry. Wurzburg, Germany: C.A.R.M.E.N., Rimpar, Germany, 1998.

31. Prins, M.J., Thermodynamic analysis of biomass gasification and torrefaction; Ph.D. Thesis, Technical University of Eindhoven, The Netherlands, 2005.

98

32. Peacocke, G.V.C., Ablative pyrolysis of biomass; Ph.D. Thesis, Aston University: Birmingham, UK, 1994.

33. Bridgwater, A.V., Ed., Fast pyrolysis of biomass. A handbook, CPL Press, 2002, vol. 2.

34. Scott, D.S., Majerski, P., Piskorz, J., Radlein, D., A second look at fast pyrolysis of biomass - the RTI process; J. Anal. Appl. Pyrolysis, 1999, 51, pp. 23-37.

35. Scott, D.S., Piskorz, J., The flash pyrolysis of Aspen-Polar wood; Can. J. Chem. Eng., 1982, 60, pp. 666-674.

36. Scott, D.S., Piskorz, J., The continuous flash pyrolysis of biomass; Can. J. Chem. Eng., 1984, 62, pp. 291-294.

37. Scott, D.S., Piskorz, J., Bergougnou, M.A., Graham, R., Overend, R.P., The role of temperature in the fast pyrolysis of cellulose and wood; Ind. Eng. Chem. Res., 1988, 27, pp. 8-15.

38. Horne, P.A., Williams, P.T., Influence of temperature on the products from the flash pyrolysis of biomass; Fuel, 1996, 75, pp. 1051-1059.

39. Luo, Z., Wang, S., Liao, Y., Zhou, J., Gu, Y., Cen, K., Research on biomass fast pyrolysis for liquid fuel; Biomass and Bioenergy, 2004, 26, pp. 455-462.

40. Bilbao, R., Mastral, J.F., Aldea, M.E., Ceamanos, J., Betran, M., Lana, J.A., Experimental and theoretical study of the ignition and smoldering of wood including convective effects; Combustion and Flame, 2001, 126, pp. 1363-1372.

41. McCoy, B.J., Distribution kinetics for temperature-programmed pyrolysis; Ind. Eng. Chem. Res., 1999, 38, pp. 4531-4537.

42. McCoy, B.J., Sterling, W. Jerome, Phase-Equilibrium Fraction of Continuous Distributions; AIChE J., 2000, 46, pp. 751-757.

43. McCoy, B.J., Madras, G., Discrete and continuous models for polymerization and depolymerization; Chem. Eng. Sci., 2001, 56, pp. 2831-2836.

44. Wagenaar, B.M., The rotating cone reactor: for rapid thermal solids processing; Ph.D. Thesis, University of Twente, Enschede, The Netherlands, 1994.

45. Landau, R.N., Libanati, C., Klein, M.T. Monte Carlo simulation of lignin pyrolysis: sensitivity to kinetic parameters; In Research in Thermal Chemical Biomass Conversion, Elsevier Applied Science, New York, 1988.

Chapter 4

Hydrodynamics of a Fluidized Bed with Immersed Filters for Extracting and Cleaning of Biomass Fast Pyrolysis Vapors

Abstract

In this chapter, the hydrodynamics of a fluid bed in which part of the ingoing gas flow is extracted via immersed filters are investigated. This is a model-system for a fluid bed pyrolysis reactor with immersed filters for extracting and cleaning of the produced vapors. It has been investigated, in two- and three-dimensional cold-flow fluid beds, how extraction of gas via filters influences intra-bed heat transport, and under which conditions a stagnant layer of bed-particles is formed around the filters (a so-called filter-cake).

If the velocity at the top of the fluid bed is used to correlate the data, heat transport in the tested fluid beds shows the same dependency of the superficial gas velocity, with or without extraction of gases through the filters. At equal top velocity the heat-dispersion coefficient with flow through the filter is ca. 2.5 times lower than without.

Form visual observation, it is has become clear that the filter-cake on horizontal filters is located primarily above the filter and is egg-shaped. By selecting a suitable filter and combination of particle size, gas velocity and filter-flow, filter-cake formation can be avoided in this model system while still removing large parts of the ingoing gas (up to 80%). The effect of the operating conditions on the filter-cake area can be explained with a simple force balance model including a drag and turbulent force.

1. Introduction

Fast pyrolysis is a promising technology that converts solid biomass into a transportable liquid energy carrier with a high energy bulk-density of ca. 20 GJ/m^3 [1] compared to ca. 6 GJ/m^3 [2] for e.g. wood chips. This is an advantage, especially when biomass resources are remote from the place where they are actually required. A "liquid" biomass can be readily stored, transported, and utilized at different sites [3,4]. Another advantage of fast pyrolysis is that the liquid product is cleaner than the original feedstock [5-7]. Minerals and metals in the feedstock are concentrated in the solid by-product (char) due to the relatively low process temperature (ca. 500°C). Because of this, the minerals remain in the production area with the possibility of recycling it back to the soil. However, due to entrainment, pyrolysis oil still contains between 0.1 - 1 wt % of char including minerals and metals. It is already known that char particles inside the bio-oil act as a catalyst for re-polymerization reactions of bio-oil components, making the oil unstable and subject to phase separation [4,8,9]. Metals inside the entrained char particles are believed to be a cause of problems in bio-oil applications like corrosion, and erosion of turbine blades, as well as of steam boilers and furnaces. However, char free bio-oil approaches the specifications of sophisticated end-use applications like furnaces, turbines and (catalytic) oil-gasifiers [10-12]. To produce such a clean product, it is crucial to separate the char from the oil. In-situ removal of ash/char may be an attractive option for producing particle free bio-oil (see Chapter 1). For this purpose, a fluidized bed with immersed filters for extracting pyrolysis vapors is proposed [13] (also see Chapter 1.). This concept is called the Filter Assisted Fluidized Bed (FAFB) pyrolysis reactor. The basic idea behind the FAFB is that the produced pyrolysis vapors are cleaned and extracted via immersed heat-resistant self-cleaning filters. In this chapter, results of cold-flow measurements concerning the hydrodynamics of this novel reactor will be presented. The measurements are indicative and are meant to support the concept of in-situ cleaning of pyrolysis vapors.

2. Other Particle Separation Techniques

Extensive overviews of flue gas cleaning systems have been presented by Clift and Seville [14], Thambimuthu [15], and Zevenboven and Kilpinen [16]. Because of restrictions imposed by the fast pyrolysis process, only a limited number of conventional cleaning devices are suitable for pyrolysis vapors. One typical problem is that biomass pyrolysis vapors start to condense around 300°C.

Pyrolysis char has a low density and, due to attrition, part of it is present as sub-micron particles. Traditionally, cyclones have been used to separate solid particles from the vapor streams because of their low cost and reliable design. However, the fraction of particles smaller than 5 micron can not be captured by cyclones [15]. In recent pilot-plant developments [5], electrostatic precipitators (EP) and hot gas filtration have been applied. EPs are very expensive [16], from both a capital and operating point of view. Tests with baghouse filters placed in the hot product line down stream of a pyrolysis reactor showed that their performance deteriorates in time [17]. During these tests, it became more difficult in time to remove the accumulated char. Generally, filters need complicated back-flushing systems to keep them clean. Alternatively to cleaning the vapors at high temperature, it is also possible to filter the condensed bio-oil. The main disadvantage of liquid filtration is that it generates a bio-oil/char sludge. Disposal and or utilization of this sludge may require costly secondary equipment. Besides, ashes dissolved in the bio-oil may slip through the filters.

Another type of in-situ particle removal pyrolysis reactor was introduced by Bramer and Brem et al. [18]. In their so-called PyRos process the pyrolysis is carried out in a cyclone reactor with an integrated hot gas filter to produce particle free bio-oil. Their hot gas filtration system is based on the principle of the rotational particle separator (US-patent No. 5073177). The PyRos reactor is still under development.

3.   Filter Assisted Fluidized Bed (FAFB)

Different from traditional downstream hot gas cleaning technology, the in-situ char/ash removal concept is based on the presence of self-cleaning heat resistant filters, submerged in a fluidized bed pyrolysis reactor (see Figure 1). The majority of the produced vapors are extracted through these filters. It is anticipated that due to the scouring action of the bed particles, the filters are permanently cleaned.

The filter assisted fluidized bed pyrolysis reactor has two intensification aspects: i) reaction and separation are integrated in a single apparatus and, ii) under flash pyrolysis conditions (that is a very high reaction rate) a higher throughput per unit volume reactor can be achieved, because the velocity in the bed is kept low by extraction of the produced vapors from the bed through the filters.

A final design of a FAFB pyrolysis reactor, including the filter bank arrangement, has not yet been made. Nevertheless, some design aspects are discussed in Chapter 6.
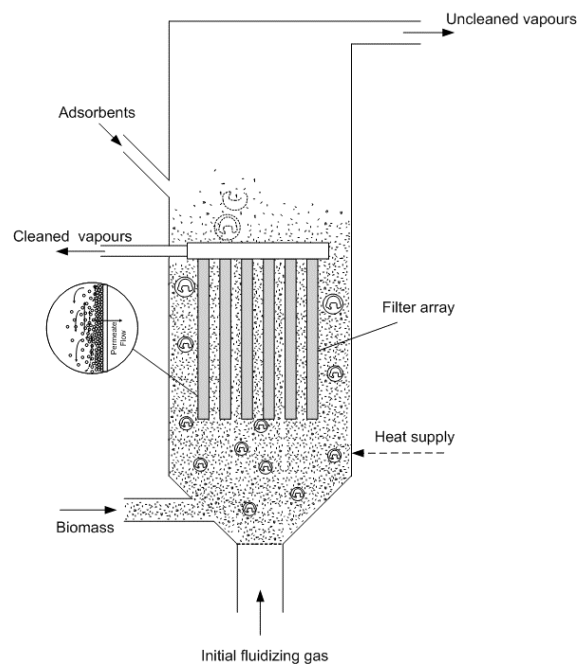
Figure 1. Principle of filter-assisted fluidized bed reactor.

To study the hydrodynamics, a single filter or an arrangement of three filters in two and three-dimensional fluid beds has been applied. In this chapter, cake formation and solids mixing experiments in cold-flow set-ups are presented and discussed. A filter cake is a stagnant area of bed particles around the filter. Characterization of cake formation is important, because it provides information on how much gas can be extracted without causing malfunctioning of the bed. Knowledge of the cake size is required to be able to predict bridging and stagnant zones between filters in case of a stack of filters. The additional flow-resistance caused by a filter cake is of less importance, because the dominant resistance to flow stems from the filters walls. The intensity of solids mixing determines the distribution of heat through the bed. Good mixing of the solids phase ensures a uniform temperature in the pyrolysis reactor. Pyrolysis requires a heat input of ca. 1.5 MJ/kg$_{feed}$ including heating of the cold feed [19,20]. When filters extract considerable amounts of gas, which occupy part of the bed, heat transport through convective currents in the dense phase may be hampered and undesired intra-bed temperature gradients can occur. Moreover, heat transfer to the biomass particles and between bed-particles may be lower.

4.   Experimental Set-up and Measurement Techniques

4.1.   Filter-Cake Formation

The goal of these measurements is to get a first impression of filter-cake sizes and the effect of the operating conditions on cake formation. Cold-flow 2-dimensional fluid bed experiments were carried out to study the effects of different operating parameters, such as filter's location and pore size (permeability), particle diameter, filter flow rate, and fluidizing velocity on filter cake formation. The 2-dimensional fluidized bed shown in Figure 2 (12 cm wide, 60 cm high and 3 cm deep) was made of plexiglass. Spherical glass beads (ρ = 2600 kg/m^3) of 132, 172, and 288 μm (d_{50}) were used as bed material. The minimum fluidization velocities under ambient conditions were found to be 0.019, 0.031, 0.061 m/s, respectively.

Cylindrical filters of different pore size (10 - 30 μm, Glasfilter-geräte GmbH, Germany) could be placed horizontally at three different positions at the centre-line (5, 10, and 15 cm above the gas distributor) in the fluidized bed. The filters were 12 mm in diameter and 25 mm long. Part of the fluidization gas could be extracted, at a controlled flow rate, from the bed through these filters by making use of a vacuum pump.
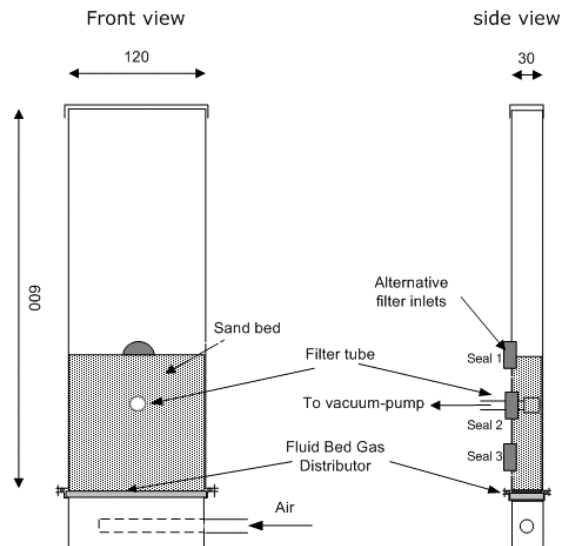

Figure 2. Experimental set-up for the measurements of the filter cake size (dimensions in mm).

Two different methods were used to measure d_{cake}:

1) The first method, which can only be applied in quasi 2-dimensional beds, consisted of the addition of a small fraction of fine colored tracer particles to the bulk bed material. Typically, 1 to 2 wt % of tracer particles were added. The tracer particles had a particle size (d_{50}) that was half the diameter of the bulk glass particles. Before the filters were turned on, the colored tracer particles were mixed with the bed particles at high fluidization velocities. For conditions at which a filter cake was present, a concentrated band of colored particles clearly indicated its boundaries. Apparently, at the stagnant filter cake boundary, these fine particles are filtered out of the fluid bed and form a thin fine additional cake. This phenomenon was not further investigated but Figure 3 shows a typical example of such a boundary.
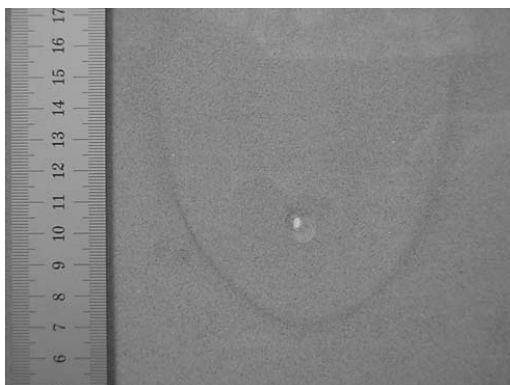
Figure 3. Example of a filter-cake contour indicated by colored tracer particles.

2) The second method used a heat flux probe (PT-1000 element), which was designed to discriminate between a bed in the fluidized or in the stagnant state. Werther [21] made an extensive review of this kind of technique. The technique is based on the temperature difference required to realize the rate of heat transfer of the probe to its surroundings at a certain electrical power input. Two probes of different dimensions were used, a probe with a cylindrical tip with a diameter of 5 mm and length of 20 mm and a probe with a flat film as tip (5 mm x 2 mm x 1.1 mm = length x width x thickness). The vast majority of the experiments were carried with the cylindrical probe.

106

It is assumed that the electrical power put into the probe is transferred to the fluid bed.

$$E \times I = A_{PT}\alpha(T_{PT} - T_{bed})$$ (1)

The temperature of the probe is related to the current because the resistance of the PT-1000 element, R_{PT}, is well defined (see Equation 2). In our case the probe operated at a constant direct current (DC) voltage of 20 V.

$$E = I \times R_{PT}, R_{PT} = 1000 + 3.85T_{PT} \rightarrow T_{PT} = \frac{E - 1000I}{3.85I} \qquad (20^{\circ}C \leq T_{PT} \leq 80^{\circ}C)$$ (2)

With T_{PT} in Celsius. Combination of Equations 1 and 2 leads to an expression of the heat transfer coefficient (α).

$$\alpha = \frac{3.85E \times I^2}{A_{PT}\left[E - I(1000 + 3.85T_{bed})\right]}$$ (3)

The equation above holds for the ideal case that only the probe's resistance is significant. If also other elements of the measuring system have a significant resistance, the equation for α becomes.

$$\alpha = \frac{3.85E \times I^2}{A_{PT}\left[E - I(1000 + R_{system} + 3.85T_{bed})\right]}$$ (4)

Equation 4 shows that by measurement of the current (I) the heat transfer coefficient can be calculated, because A_{PT}, E, R_{system}, and T_{bed} can be determined separately. The maximal (asymptotic) current of the electrical system, corresponding to infinitely fast heat transfer, is:

$$I_{asym} = \frac{E}{1000 + 3.85T_{bed} + R_{system}}$$ (5)

The current could be measured with a precision of 0.01 mA. Figure 4 shows the curves of I versus α for the cylindrical probe.
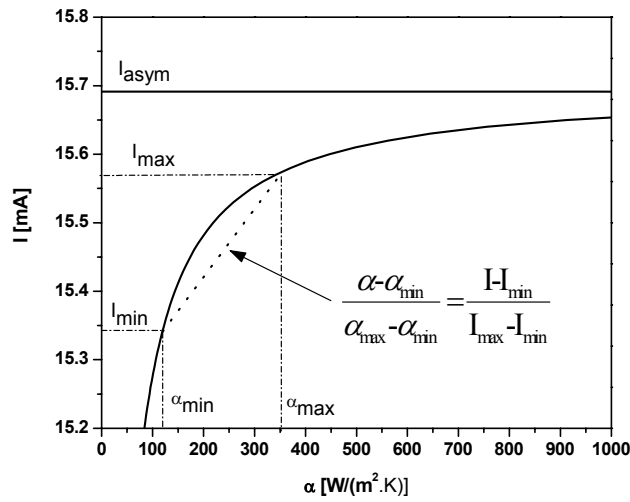
Figure 4. Example of α versus I for the cylindrical probe. R_{sys} = 195 Ohm, d_p = 197 μm, I_{min} and I_{max} are measured values (see Figure 5 for their definitions), E= 20 Volt.

The method to characterize the fluidizing state using the heat flux probe was tested in a fluidized bed under various superficial gas velocities. As shown in Figure 5, the point where minimum fluidization is reached (u_{mf} = 1.9 cm/s) clearly corresponds to a step increase in the electric current measured by the probe from I_{min} to I_{max}. This indicates that this method is able to discriminate between a fixed and a fluidized bed and therefore can be used to indicate stagnant zones (filter-cake) in a fluid bed. Figure 5 shows that once above $1.5u_{mf}$, the current measured does not change to a large extent at increasing gas velocity. It should be noted however, that in this region a small increase in the measured current represents a large increase in the calculated α value (see Equation 4 and Figure 4). After this test, the probe was used for the measurement of the cake diameter in a FAFB (see later). In these measurements intermediate levels between the minimum (I_{min}) and maximum (I_{max}) electrical current were observed. This was most likely caused by the finite size of the PT-1000 element (5 mm in diameter by 20 mm length in case of the large probe tip), which allowed the probe tip to be covered by both a stagnant and a fluidized zone. In experiments as described in Figure 5, intermediate current levels were never observed for $u_g > 1.5u_{mf}$.
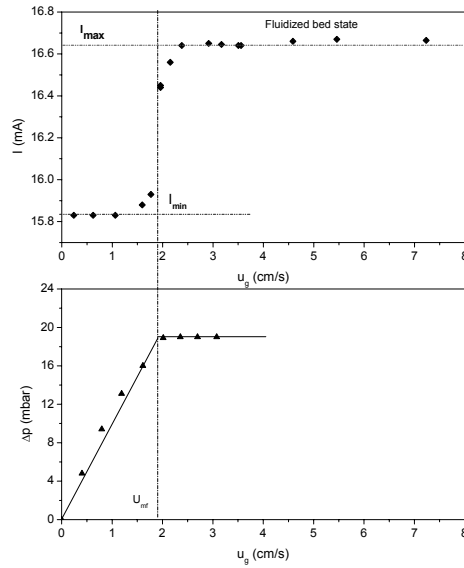
108

Figure 5. Comparison of the strength of the current measurement by the flat film heat flux probe (a) with the pressure drop over the bed (b) at different superficial gas velocities.

Fortunately, the currents measured never lay in the steep part of I versus α curve (see Figure 4 for a typical example). In fact, against the background of the screening character of these measurements it is sufficient to assume a linear relation of α in the range of I_{min} to I_{max} (see Figure 4).

$$\frac{\alpha\text{-}\alpha_{min}}{\alpha_{max}\text{-}\alpha_{min}} = \frac{I\text{-}I_{min}}{I_{max}\text{-}I_{min}} \tag{6}$$

This equation is used to assign an "averaged" heat transfer coefficient to a measurement in the intermediate current zone, that is in measurements in which the probe tip was surrounded by both fixed and fluidized zones (partly fluidized state). The predicted values of α (by Equation 4) for fluidizing conditions were in good agreement with the predictions of literature correlations for horizontal and vertical tubes in a fluid bed [22-27].

A grid of 17 cells of 1 cm x 1 cm was created around the filters (see Figure 6) to measure the size and shape of the filter-cake. The position of the probe with respect to its distance from the front wall was fixed. The position of the probe in the y and x

direction could be precisely set with a specially designed slide duct. On account of the fact that it was observed that always a "more or less" symmetrical filtration cake was formed, only 10 points were actually measured, assuming symmetry filled the others in. As mentioned before the chosen grid was 1 cm x 1 cm, while the most used probe had a length of 2 cm. Of course in this way an error is introduced, but for these first indicative experiments it was assumed that the measured current could be ascribed to the middle grid point through which the probe tip passed (see Figure 6).
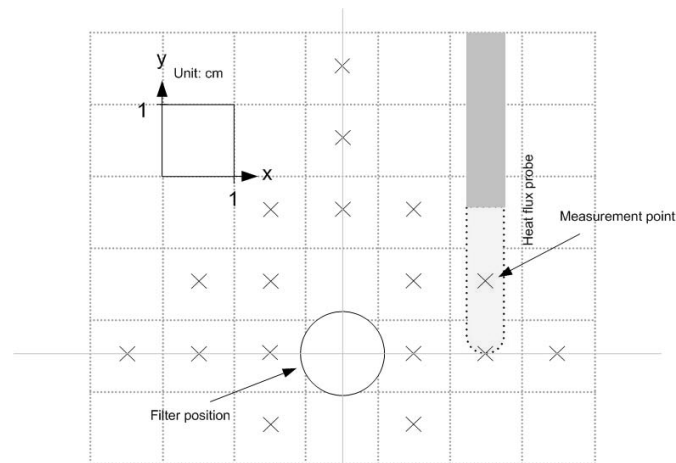

Figure 6. Grid for the determination of the cake area.

The total filter-cake area was defined as the sum of the areas ascribed to the individual grid cells. Every grid cell represents a potential filter-cake area of 1 cm^2. The following procedure was employed for the individual cells:

- If I was lower or equal than I_{min}, it counted for 1 cm^2 (stagnant zone).
- If I was between I_{min} and I_{max} (partly fluidized zone), the area was calculated by:

$$A=(1-\frac{I-I_{min}}{I_{max}-I_{min}}) \text{ cm}^2 \tag{7}$$

hereby we assumed a linear dependence between the area and the measured current (heat transfer coefficient).

- If I was above I_{max} (fluidized zone), it counted for 0 cm^2.
- The cell just above the filter could not be measured. The cell was considered stagnant (1 cm^2) if one of surrounding cells was stagnant or partly fluidized. If the surrounding cells were all fluidized ($I \geq I_{max}$), the cell was counted as 0 cm^2.

110

- The cells just underneath the filter could not be measured. The cell was considered stagnant (0.5 cm^2) if one of surrounding cells was stagnant or partly fluidized. If the surrounding cells were all fluidized ($I \geq I_{max}$), the cell was counted as 0 cm^2.
- For some conditions all grid cells were stagnant. In this case the actual filter-cake area could not be determined. To be on the safe side with respect to under-estimating the filter-cake area only total areas of less than 10 cm^2 were taken into account in the analysis.

The cake diameter was calculated from the determined area plus the area the filter self while assuming a circular cake. The area of the filter was added to remain consistent with the interpretation model (see section 5.1). An example of a calculated filter-cake area is shown in Figure 7.
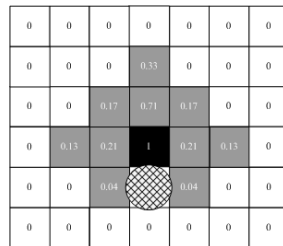

Figure 7. Numerical evaluation of the filter-cake area.

Comparing the Results of Method 1 and 2

In Figure 8 the comparison between the two methods is visualized. The colored particles (dark spots in the picture) clearly indicate the boundary of the cake, which is pointed out with the dashed line. The fluidization states as measured with the heat flux probe are divided into three categories: completely stagnant (S), partly stagnant (fluidized) (P) and fully fluidized (F). It can be seen from Figure 8 that the methods are quite comparable. Also the equivalent cake diameters coincide with each other reasonably well: 3.2 cm from the colored particle method versus 2.9 cm using the heat flux probe.
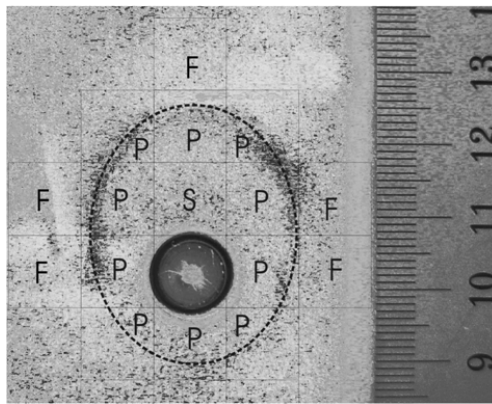

Figure 8. Comparison of the measurement of the filter-cake by visual observation using colored particles and the heat flux method. "S": fully stagnant, "P": partially stagnant, "F": fully fluidized.

After cross-checking both methods, the heat transfer method was selected, as it turned out to be a quantitative technique which can also be applied in 3-dimensional beds.

4.2. Solids Mixing

Solids mixing, with and without filter flow, was studied using heated particles as tracer material in a fluidized bed. Dispersion of heat through the fluidized bed was deduced from dynamic temperature profiles at different locations. The method using heated bed particles was, amongst others, used by Valenzuela and Glicksman [28] and Shen and Zhang [29]. An advantage of this method is that the tracer particles are identical to the bed material as a result of which there is no tendency of segregation

112

due to size, shape or density differences. Furthermore, the method enables rapid repetition of the experiments, as the tracer particles are indistinguishable from the rest of the bed material within several minutes.
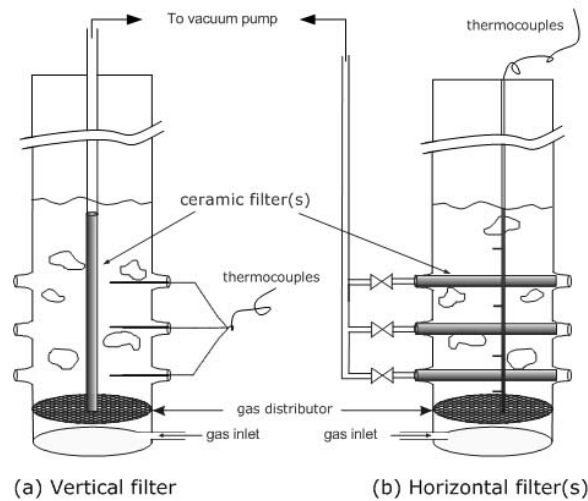

Figure 9. Set-up for the solid phase mixing experiments. a) Vertical filter, b) Horizontal filters.

The experiments were carried out in a cylindrical 3-dimensional bubbling fluidized bed (70 cm in height, 10 cm in diameter), which is shown in Figure 9. The initial bed height, including the additional tracer particles, was 19 cm. The bed was constructed of glass, which permitted visual observation. The fluidization gas (air) was added through a porous plate distributor, which had sufficient pressure-drop to ensure the gas to be distributed uniformly. Ceramic filters (pore size 6 μm) were placed vertically (Figure 9a) as well as horizontally (Figure 9b) and could be closed or opened individually. The temperature was measured at different lateral and axial positions in the bed using fast responding miniature thermocouples. The pressure drop over the filtering system was measured with a manometer.

In a typical experiment, glass beads (d_{50} = 163 μm) of ca. 100°C were added at the start of the experiment by quickly emptying a beaker glass. The amount of hot particles added corresponded to 6% of the total bed weight. At the same time the recording of temperature at different locations in the bed started. The hot tracer particles were evenly distributed over the top of the bed by making use of two

distributors in the particle free zone above the bed. It was verified that the time necessary for the addition of the hot beads did not influence the obtained mixing rates to a large extent. To convert the obtained temperature profiles into mixing rates, a model describing the particle motion was applied (see section 5.2).

5.   Interpretation Models

In this section, the models are described which have been used to interpret the experimental results.

5.1.   Filter Cake Force Balance Model

A simple force balance model is used to investigate the influence of the operating conditions and filter characteristics on filter-cake formation. The model considers a packed single particle layer at the border of the filter-cake (see Figure 8), which is subject to two forces: the drag force and a turbulent force (see also Huizenga et al. [30,31] for a somewhat similar problem). The gravitational force is not taken into account, because for the fluidized particles the drag force of the fluidization force balances it. Forces between the particles are neglected. This simple model assumes that the cake has a circular shape. Obviously this will not be the case in reality. Wake formation behind the immersed object will cause deviations from the cylindrical geometry.

The drag force experienced by the particle due to the suction of the filter can be formulated as:

$$F_D = C_D \left(\tfrac{1}{2} \rho_g v_e^{\ 2} \right) \left(\tfrac{1}{4} \pi d_p^{\ 2} \right) \tag{8}$$

The drag coefficient (C_D) can be expressed as a function of the particle Reynolds number (Re_p) according to (Schiller and Naumann [32]) but corrected for the presence of the other particles ($f(\varepsilon)$):

$$C_D = \frac{24}{Re_p} \left(1 + 0.15 Re_p^{\ 0.687} \right) f(\varepsilon) \qquad Re_p < 1000 \tag{9}$$
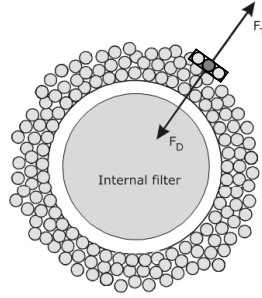
Figure 10. Schematic representation of the force balance model.

At low Reynolds numbers, $(Re_p) < 0.1$, Stokes's law is valid and the drag coefficient can be described with $24f(\varepsilon)/Re_p$. In the experiments in the present study Re_p never exceeded 1, which indicates that using the Stokes regime results in an underestimation of the drag force of maximally 15%. This error was found to be acceptable in the derivation of an analytical expression of the cake diameter below, as it enhances the insight in the influence of the different operating parameters. However, in the actual calculations Equation 9 was applied.

The filter velocity, v_e, in Equation 8 is the velocity of the gas around the particle at the border of the cake (at distance d_{cake} from the center of the filter), due to the suction of the filter and can be expressed as:

$$v_e = \frac{Q_f}{\pi d_{cake} L_f} \tag{10}$$

in which Q_f is the flow rate through the filter and L_f the filter length. It is relevant to notice that d_{cake} includes the diameter of the filter. Making use of $Re_p = \rho_g v_e d_p / \eta_g$, the following expression for the drag force on the single particle layer at the edge of the cake-cake can be derived:

$$F_D = \sum_N \frac{3\eta_g d_p Q_f f(\varepsilon)}{d_{cake} L_f} \tag{11}$$

Bubbles in the vicinity of the filter causes re-suspension of the particles from the edge of the filter-cake via dense phase convective eddy like currents. This "turbulent" force counteracts the drag force and is given by the product of the pressure of the turbulent eddies and the particle cross-sectional area:

$$F_T = \sum_N \left(\tfrac{1}{4} \pi d_p{}^2 \right) \left(\rho_{fb} (u')^2 \right) \tag{12}$$

The pressure of the turbulence force is estimated with the density of the fluid bed.
The eddy fluctuation velocity, u', is given for a pure fluid by Davies [33]:

$$u' = \left(\in \lambda \right)^{\frac{1}{3}} \tag{13}$$

The energy dissipation rate, $\in$, is equal to the product of the gas flow rate and the pressure drop over the fluid bed per unit of mass and equals: u_g. Dense phase movements only occur at velocities higher than the minimum fluidization and therefore we will describe the energy dissipation rate, since no better knowledge is currently available, as:

$$\in = \left(u_g - u_{mf} \right) g \tag{14}$$

Equating the drag force and the turbulence force at the border of the filter cake yields the following expression for the cake diameter:

$$d_{cake} = \frac{12 \eta_g Q_f f(\varepsilon)}{\pi \rho_{fb} d_p L_f \left((u_g - u_{mf}) g \lambda \right)^{\frac{2}{3}}} \tag{15}$$

The choice of the length scale of the eddies (λ) is by no means trivial. It is difficult to estimate the length scale of the eddies responsible for the turbulent force. For liquid slurries, Huizinga et al. [31] proposed to use the Kolmogorov length scale or the particle size. In a fluidized bed also a direct proportionality to the bubble diameter, which is the main cause of the eddies, is a possibility. The bubble size is described by the correlation of Werther [34] for Geldart B solids:

$$d_b = 0.00853 \left(1 + 27.2(u_g - u_{mf}) \right)^{\frac{1}{3}} \left(1 + 6.84 h \right)^{1.21} \tag{16}$$

In this way the equation for the cake diameter becomes:

$$d_{cake} = \frac{12 \eta_g Q_f}{\pi \rho_{fb} d_p L_f \left((u_g - u_{mf}) g (C_b d_b) \right)^{\frac{2}{3}}} \tag{17}$$

116

The influences of Q_f, u_g, d_p and the height of the filter above the distributor (h) on the filter-cake cross sectional area including the filter as predicted by the model, are listed in Table 1. The filter cake cross sectional area is defined as:

$$A_s = \frac{1}{4}\pi d_{cake}^2 \qquad\qquad\qquad (18)$$

Table 1. Predicted influence of Q_f, u_g, d_p, and h on the filter-cake area using Equation 17

Parameter	Filter-cake size	Relation
$Q_f \uparrow$	$A_s \uparrow$	$Constant = \dfrac{Q_f}{\sqrt{A_s}}$
$u_g \uparrow$	$A_s \downarrow$	$Constant = \sqrt{A_s}\,(u_g - u_{mf})^{\frac{2}{3}}$
$d_p \uparrow$	$A_s \downarrow$	$Constant = \sqrt{A_s}\,d_p$
$h \uparrow$	$A_s \downarrow$	$Constant = \sqrt{A_s}\,h^{\frac{4}{5}}$

In section 6.1. it is investigated if this simple model predicts the experimentally observed trends correctly.

5.2. Solids Mixing

Due to the high particle-over-gas heat content ratio (ρC_p), intra-bed heat transport in a gas blown fluidized bed is mainly caused by movement of the particles. Therefore, a model describing particle motion is required to convert the measured dynamic temperature profiles into mixing rates. Early studies [35-38] on solids mixing in fluidized beds used the phenomenological axial dispersion model to interpret the results. As the understanding of the fluidized bed hydrodynamics grew, more mechanistic models were proposed like the counter flow solids circulation model of Van Deemter [39-41] and the two-dimensional convection-dispersion model of Shen et al. [42]. These models are based on the observation that solids movement is induced by rising gas bubbles and predict that vertical heat transport in a fluidized bed is not symmetrical [29,43]. Upward transport is faster and characterized by the bubble diameter, whereas down flow is more uniform at a lower velocity. Obviously, the dispersion model does not predict asymmetric axial solids motion. The mechanistic

models, however, contain parameters that are difficult to asses by direct and independent measurements. In Van Deemter's model [40], for instance, there are the velocities and the fractions of the artificial upward and downward phases and the exchange coefficient between them. Kunii et al. [44-46] proposed to use Davidson's bubble model for the exchange coefficient. The convection-dispersion model of Shen at al. [42] has 7 parameters of which they fixed 6 by correlations derived to describe the hydrodynamics of regular fluid beds (e.g. Darton et al. [47] for the bubble diameter and Shi and Fan [48] for the radial dispersion coefficient), yielding, like the axial dispersion model, a one-parameter fit equation. Such a model cannot be used for the FAFB, because it has been observed that the fluidization pattern with gas extraction via immersed filters differs significantly from the one of the same bed without filter flow under otherwise identical conditions (see section 6.2).

The axial dispersion model is used here to quantify the difference between solids mixing in a FB with and without extraction of gas via filters. It is recognized that the axial dispersion model is not really suitable to characterize solids motion in a FB with a small aspect ratio, it does, however, provide a direct comparison of the solids mixing rate irrespective of the actual behavior of the bed. In this way the mixing intensity of the bed with and without filter flow can be compared. Because in the experimental method applied actually back mixing is measured, the obtained D_s values should be interpreted as conservative estimates of the mixing power.

Because of the high specific area and heat transfer coefficient, the solids and gas temperature are equal at all locations in the bed. The resulting combined energy balance is then of the form:

$$(\varepsilon_s \rho_s C_{p,s} + \varepsilon_g \rho_g C_{p,g})\frac{dT}{dt} = (D_s \varepsilon_s \rho_s C_{p,s} + D_g \varepsilon_g \rho_g C_{p,g})\frac{d^2T}{dz^2} - u_g \rho_g C_{p,g}\frac{dT}{dz} - \frac{4\alpha_w}{d_c}(T - T_w) \qquad (19)$$

The solids motion is described by the dispersive term (1st term RHS). This term describes the redistribution of the added hot particle layer over the rest of the bed. The bed is cooled by the cold inflowing gas (2nd term RHS) and heat through the reactor wall (3rd term RHS). At the start of the experiment (t = 0) the bed is at its initial temperature, which is measured using thermocouples. The following boundary conditions [49] apply:

$$\text{at } z = 0: \qquad u_g T_{g,in} = u_g T - (D_s \varepsilon_s + D_g \varepsilon_g)\frac{dT}{dz} \qquad (20)$$

118

at z = h: $$\frac{dT}{dz} = 0 \tag{21}$$

In these equations, h is the total bed height, which was determined by visual observations. From this value and the total weight of the particles, the void fraction, ε_g, was calculated. To obtain the solid phase dispersion coefficient from an individual experiment, an optimization routine was used, in which the measured temperature profiles were compared with the model predictions. In this routine, both the solids dispersion coefficient and α_w are fit parameters. The dispersion coefficient of the gas is set to be one order of magnitude bigger than the one of the solids, as has been indicated by the work of Van Deemter. Anyway, because of its low heat content the state of mixing of the gas-phase does not affect the results much. Figure 11 shows a typical example of measured temperature responses together with the best model fit. In the lower part of the bed (2 and 7 cm) the temperature profiles of a single experiment are reasonably reproducible. The profile at a higher point in the bed (12 cm) is much more scattered, due to the fact that the local mixing effects have not be averaged out. For this reason, only the bottom two temperature profiles are taken into account in the optimization routine. The dynamic temperature profiles are built up clearly out of two parts, the quick response of the solids mixing and the much slower effect of heat removal via gas convection and losses through the reactor wall. When neglecting the heat removal mechanism in the fitting procedure, (i.e. by setting $\alpha_w = 0$) the obtained dispersion coefficients are somewhat smaller (maximal 10 %).
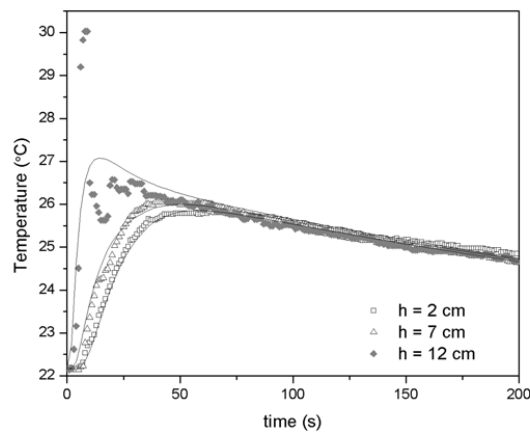

Figure 11. Example of temperature profiles in time at different heights in the bed (u_g = 9 u_{mf}, d_p =172 μm, Q_f = 31 liter/min). Solid lines represent the best model fit (D_s = $3.1\cdot10^{-4}$ m^2 s^{-1}).

119

6.   Results

In this section the obtained experimental results will be presented and interpreted with the models described in section 5.

6.1.   Filter Cake Formation

Figures 3, 7, and 8 shows that the observed filter-cakes are egg-shaped and are positioned more above than below the filter. This is contradictory to the interpretation model that assumes a circular filter-cake concentrically orientated around the filter (see Figure 10). The actual form of the filter-cake is probably caused by wake formation above the filter-cake. In this wake, turbulence is low and therewith also the force responsible for destruction of the cake. This leads to a larger filter-cake area above the filter as observed.

The effect of different operating conditions, viz. fluidizing velocity, filter flow, filter position and particle size of the bed material on the filter-cake area are shown in Figure 12.
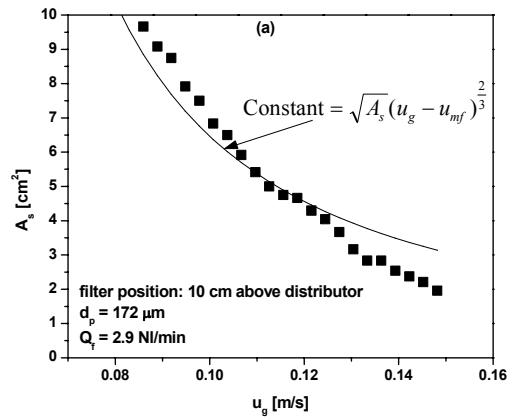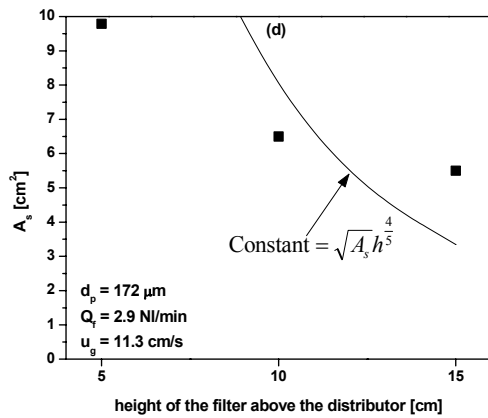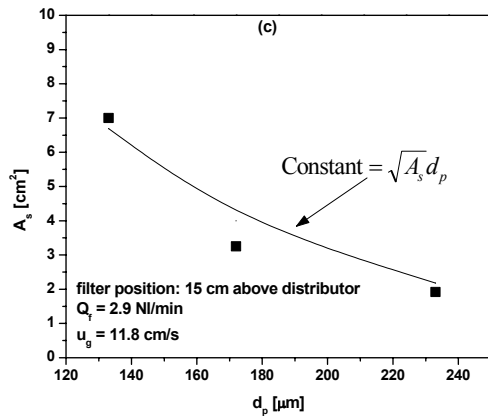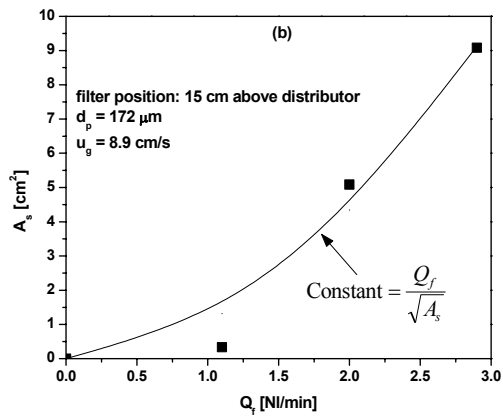

$$\text{Constant} = \sqrt{A_s} \, (u_g - u_{mf})^{\frac{2}{3}}$$

Figure 12. Effect of the operating conditions (at otherwise constant conditions) on the filter-cake area, a) superficial gas velocity, b) flow through the filter, c) bed particle size, and d) height of the filter above the distributor. In the graphs also the trend lines as predicted by the force balance model are plotted (see Table 1).

120

(b)

filter position: 15 cm above distributor
d_p = 172 μm
u_g = 8.9 cm/s

$$Constant = \frac{Q_f}{\sqrt{A_s}}$$

(c)

$$Constant = \sqrt{A_s}\, d_p$$

filter position: 15 cm above distributor
Q_f = 2.9 Nl/min
u_g = 11.8 cm/s

(d)

$$Constant = \sqrt{A_s}\, h^{\frac{4}{5}}$$

d_p = 172 μm
Q_f = 2.9 Nl/min
u_g = 11.3 cm/s

121

From Figure 12a, it is made clear that an increasing superficial velocity diminishes the filter-cake area. The force balance model also predicts this trend; the increase in fluidizing velocity increases the amount of turbulence around the filter, which decreases the built-up of filter cake. A higher flow through the filter at otherwise constant conditions leads to an increase of the filter-cake area (see Figure 12b). When the filter face velocity increases as a result of a higher flow though the filter, more suction is applied on the particles around the filter, which enlarges the stagnant zone. In Figures 12c and 12d the influence of the bed material particle size and the height of the filter in the bed are presented. The filter cake is significantly larger when the particles of the bed material are small. Furthermore, a higher filter position in the bed diminishes the cake size. These effects can also be explained with the force balance model. In the case of bed particle size, it is explained by noting that the turbulent force that is responsible for "breaking down" the filter-cake is proportional to d_p^2 (see Equation 12) while the drag force that "builds up" the filter cake is only proportional to d_p (see Equation 11). This leads to an overall effect of decreasing filter-cake for larger bed particles. The filter-cake area decreases when the filter is placed at a higher position in the bed (see Figure 12d) because the bubble diameter increases and therewith increasing the turbulent force.

Figure 12 show that when a suitable combination of particle size, gas velocity and filter flow is chosen, filter-cake formation can be avoided in this model system while still removing large parts of the ingoing gas (up to 80%). Quantitative mapping of the model predictions with the measured cake size did not succeed unless unexplainable large C_b factors (see Equation 17) were introduced. Probably, the model applied is too much simplified for this purpose. Accurate quantitative predictions might be achieved with computational fluid dynamic models.

Although the model seems to predict trends, care must be taken in applying and extrapolating it, because i) of the difference between the assumed and observed filter-cake geometry and ii) some parameters were varied only over a limited range. For instance, the bubble diameter varied only between 1 and 4 cm and will be completely different in larger reactors. More research on this topic in terms of scaling up is therefore required, but as a first approximation and in combination with a limited amount of experiments in reactors of different scale, these results are useful.

6.2. Solids Mixing

In order to be able to make a good comparison, several solids mixing experiments at different superficial gas velocities were performed without filtering. The size of the

122

used glass beads was 163 µm in all the experiments. The results are presented in Figure 13 and 14. It has been verified that the presence of the filter itself (without extracting gas) does not affect the solids dispersion coefficient. Furthermore, it has turned out that the radial position of the thermocouples does not influence the measured D_s, as long as their position is not inside the filter cake. The measured solid dispersion coefficient is therefore representative for the solid particles that are moving, which means that knowledge of both the filter-cake size and the dispersion coefficient is required in order to describe the complete system.

The solid dispersion coefficients can be well described using a correlation of the form: $D_s = \text{Constant} \cdot (u_g - u_{mf})$, which was also suggested by Lee and Kim [51]. The constant was in their work a function of bed material particle diameter, gas phase density and viscosity and column diameter, which were not varied in the present study. The results are quantitatively in good agreement with the data of Lewis et al. [52] who used a steady state heat transfer method and a similar size of glass beads (155 µm).

Visual observations have shown that the extraction of part of the fluidization gas by in-situ filtering changed the bubbling behavior of the bed to a large extent. Already at a low filter flow, much more large bubbles are observed at the reactor wall. At higher amounts of extracted gas, the regime changes from bubbly flow into slug flow. This is most likely caused by the presence of stagnant zones in the center of the vessel, which result in a larger part of the gas to flow up in the vicinity of the wall and thereby creating larger bubbles.
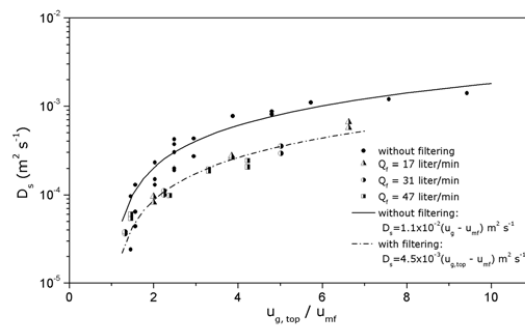

Figure 13. Solid phase axial dispersion coefficient as a function of the superficial gas velocity with and without filtering (vertical filter).

For the system in which the filter is placed vertically in the reactor, the dispersion coefficient versus the superficial gas velocity at the top of the reactor is shown in Figure 13.

In principle, three different superficial gas velocities could be used to correlate the data when the filter is present, the velocity at the bottom of the bed, at the top of the bed or the average axial velocity. The velocity at the top has been chosen, as it is the only velocity to give a continuous trend in the data points in which the filter flow varied. When this velocity is chosen to correlate the data, the dispersion coefficient is on average approximately a factor 2.4 lower than compared to the case without filtering.

The solids mixing experiments with horizontal filters were more difficult to perform compared to experiments in which the filters were placed vertically. Due to the non-symmetrical nature of the filter surroundings - from the top view the ends of the filter are close to wall, while the middle part of the filter is further from the wall - the bed behaves very non-uniform at larger filter flows. At the ends of the filter, the wall stabilizes the cake and the solids phase is at those positions completely stagnant. In the center part, a sort of spouted bed arises, in which the solids move relatively fast.
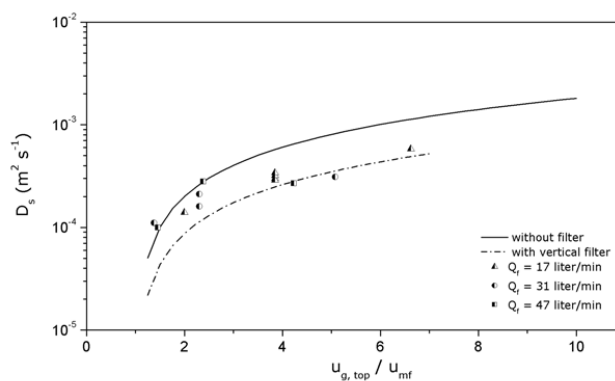

Figure 14. Solid phase axial dispersion coefficient as a function of the superficial gas velocity with and without filtering (horizontal filter).

These effects are due to the small scale of the set-up and they will therefore have less impact on a larger scale. The results are shown in Figure 15 and are less consistent compared to the results with the vertical filter. The influence of the number of filters, from which gas was extracted, on the dispersion coefficient is also indicated in Figure 13 and 14. Experiments were performed with 1, 2 and 3 filters at a filter flow of 17

124

liter/min and $u_{g,top}/u_{mf} = 3.8$. Although the fluidized beds were very different in nature for these cases, a large variation and a trend in D_s was not found.

7.   Conclusions

The hydrodynamics of a fluid bed, in which part of the ingoing gas flow is extracted via immersed filters, have been investigated. This system serves as a model-system for a fluid bed pyrolysis reactor with immersed filters for extracting and cleaning of the produced vapors. It must be noted, however, that the model-system is operated with clean gases while in a real pyrolysis reactor fine char particles and aerosols are presented, which may cause problems other then the ones discussed here. In this chapter, it has been investigated under which conditions a stagnant layer of bed-particles is formed around a filter (a so-called filter-cake), and how extraction of gas via filters influences intra-bed heat transport. The results can be summarized as follows:

- For horizontal filters the filter-cake is located primarily on top of the filter and is egg-shaped.
- An increase in flow through the filter (Q_f) increases the filter-cake cross sectional area (A_s). An increase in the superficial fluidizing velocity (u_g), the particle diameter (d_p) and the height of the filter in the bed (h) decreases the filter-cake cross sectional area. These trends are also predicted by simple force balance model including a drag force and a turbulent force.
- By selecting a suitable filter and combination of particle size, gas velocity and filter-flow, filter-cake formation can be avoided altogether in this model system while still removing large parts of the ingoing gas (up to 80%). The superficial gas velocity is the most important parameter; at $u_g > 7u_{mf}$ filter-cake formation was never observed (u_g is local velocity).
- If the velocity at the top of the fluid bed is used to correlate the data, heat transport in the tested fluid beds shows the same dependency on the superficial gas velocity, with or without extraction of gases through the filters. At equal top velocity the heat dispersion coefficient with flow through the filter is ca. 2.5 times lower than without.
- Horizontal, vertical and a stack of filters have been tested. No effect on the heat dispersion coefficient has been found at otherwise identical conditions, although the fluidization behavior changed significantly.

Acknowledgement

List of Symbols

A_s	Cross sectional area filter-cake	m^2
a_s	Interfacial area of the solid phase	$m^2 \, m^{-3}$
C_b	Bubble proportionality constant (in Equation 12)	-
C_D	Drag coefficient	-
C_p	Heat capacity at a constant pressure	$J \, kg^{-1} \, K^{-1}$
C_v	Heat capacity at a constant volume	$J \, kg^{-1} \, K^{-1}$
D	Dispersion coefficient	$m^2 \, s^{-1}$
d_c	Column diameter	m
d_{cake}	Cake diameter	m
d_f	Filter diameter	m
d_p	Particle diameter	m
E	Potential difference	Volt
$\in$	Energy dissipation rate	$m^2 \, s^{-3}$
F_D	Drag force	$kg \, m \, s^{-2}$
F_T	Turbulent force	$kg \, m \, s^{-2}$
g	Gravitational constant	$m \, s^{-2}$
h	Height of the filter in the bed	m
I	Electrical current	A
L_f	Filter length	m
N	Number of particles in of outer particle layers	-
N_{exp}	Number of experiments	-
Δp	Pressure drop	bar
Q_f	Flow through the filter	$M^3 \, s^{-1}$
R	Resistance	Ohm
t	Time	s
T	Temperature	K
u'	Eddy fluctuation velocity	$m \, s^{-1}$
u_g	Superficial fluidizing velocity	$m \, s^{-1}$
u_{mf}	Minimum fluidization velocity	$m \, s^{-1}$
v_e	Gas velocity at the edge of the cake (in the direction of the center of the filter)	$m \, s^{-1}$
v_f	Filter face velocity ($Q_f/\pi L_f d_f$)	$m \, s^{-1}$
z	Axial coordinate	m

Greek

α	Heat transfer coefficient	$W\ m^{-2}\ K^{-1}$
ε	Fraction	-
η_g	Gas phase viscosity	Pa s
λ	Length scale of the turbulent eddies	m
ρ	Density	$kg\ m^{-3}$
ρ_g	Gas phase density	$kg\ m^{-3}$

Dimensionless numbers

Re_p	Particle based Reynolds number ($\rho_g d_p v / \eta_g$)	-

Subscripts

B	Bubble
Fb	Fluid bed
G	Gas
In	Inlet
Min	Minimal: stagnant zone
Max	Maximal: fluidization zone
PT	PT-1000
S	Solid
Top	Top of the bed
W	Wall of the fluidized bed

References

1. Oasmaa, A., Leppamaki, E.A., Kopolen, P., Levander, J., Tapola, E., Physical characterisation of biomass-based pyrolysis liquids: Application of standard fuel oil analyses; VTT, Technical Research Center of Finland, Espoo, Finland, 1997, pp. 87.

2. Fengel, D., Wegener, G., Wood - Chemistry, Ultra structure, Reactions; Verlag Kessel, Germany, 2003.

3. Bridgwater, A.V., Bridge, S.A., A review of biomass pyrolysis and pyrolysis technologies; In Biomass pyrolysis liquids upgrading and utilisation, Elsevier Science Publishing Co., New York, 1991, pp. 11-92.

4. Bridgwater, A.V., Peacocke, G.V.C., Fast pyrolysis processes for biomass; Renewable and Sustainable Energy Reviews, 2000, 4, pp. 1-73.

5. Bridgwater, A.V., Czernik, S., Diebold, J., Meier, D., Oasmaa, A., Peacocke, C., Piskorz, J., Radlein, D., Eds., Fast pyrolysis of biomass, A handbook, CPL Press, 1999.

6. Agblevor, F.A., Besler, S., Evans, R.J., Inorganic compounds in biomass feedstocks: their role in char formation and effect on the quality of fast pyrolysis oils; In Proceedings of biomass pyrolysis oil properties and combustion meeting, National Renewable Energy Laboratory, Estes Park, CO, USA, 1994.

7. Peacocke, G.V.C., Ablative pyrolysis of biomass; Ph.D. Thesis, Aston University, Birmingham, UK, 1994.

8. Scholze, B., Long-term stability, catalytic upgrading, and application of pyrolysis oils-improving the properties of a potential substitute of fossil fuels; Ph.D. Thesis, University of Hamburg, Hamburg, Germany, 2002.

9. Diebold, J.P., A review of the chemical and physical mechanisms of the storage stability of fast pyrolysis bio-oils; National Renewable Energy Laboratory (NREL): Golden, CO, USA, 2004, pp. 59.

10. Wagenaar, B.M., Venderbosch, R.H., Prins, W., Penninks, F.W.M., Bio-oil as coal substitute in 600 MWe power stations; In Twelfth European Biomass Conference: Biomass for Energy, Industry and Climate Protection, Amsterdam, The Netherlands, ETA-Florence and WIP-Munich, 2002.

11. Venderbosch, R.H., van de Beld, L., Prins, W., Entrained flow gasification of bio-oil for synthesis gas; In Twelfth European Biomass Conference: Biomass for Energy, Industry and Climate Protection, Amsterdam, The Netherlands, ETA-Florence and WIP-Munich, 2002.

12. Van Swaaij, W.P.M., Kersten, S.R.A., van den Aarsen, F.G., Routes for methanol from biomass; In International 2-Day Business Conference on Sustainable Industrial Developments, Delfzijl, The Netherlands, 2004.

13. Wang, X., Kersten, S.R.A., Prins, W., van Swaaij, W.P.M., Biomass-syngas from fast pyrolysis vapors or liquids; In Twelfth European Biomass Conference: Biomass for Energy, Industry and Climate Protection, Amsterdam, The Netherlands, ETA-Florence and WIP-Munich, 2002.

14. Clift, R., Seville, J.P.K., Eds., Gas cleaning at high temperatures; Blackie Academic & Professional: London, UK, 1993.

15. Thambimuthu, K.V., Gas cleaning for advanced coal-based power generation; IEACR/53, IEA Coal Research, London, UK, 1993.

16. Zevenboven, R., Kilpinen, P., Control of pollutants in flue gases and fuel gases; 2nd Ed., Espoo/Turku, Finland, 2002.

17. Diebold, J.P., Czernik, S., Scahill, J.W., Phillips, S.D., Feik, C.J., Hot-gas filtration to remove char from pyrolysis vapors produced in the Vortex reactor at NREL; In Proceedings of biomass pyrolysis oil properties and combustion meeting, National Renewable Energy Laboratory, Estes Park, CO, USA, 1994.

18. Bramer, E.A., Brem, G. A., novel technology for fast pyrolysis of biomass: Pyros reactor; In Twelfth European Biomass Conference: Biomass for Energy, Industry and Climate Protection, Amsterdam, The Netherlands, ETA-Florence and WIP-Munich, 2002.

19. Daugaard, D.E., Brown, R.C., Enthalpy for pyrolysis for several types of biomass; Energy & Fuels, 2003, 17, pp. 934-939.

20. Rath, J., Wolfinger, M.G., Steiner, G., Barontini, F., Cozzani, V., Heat of wood pyrolysis; Fuel, 2003, 82, pp. 81-91.

21. Werther, J., Measurement techniques in fluidized beds; Powder Technology, 1999, 102, pp. 15-36.

22. Parmar, M.S., Hayhurst, A.N., The heat transfer coefficient for a freely moving sphere in a bubbling fluidised bed; Chem. Eng. Sci., 2002, 57, pp. 3485-3494.

130

23. Prins, W., Draijer, W., van Swaaij, W.P.M., Heat transfer to immersed spheres fixed or freely moving in a gas-fluidized bed; In Heat and Mass Transfer in Fixed and Fluidized Beds, van Swaaij, W.P.M., Afgan, N.H., Eds., Hemisphere Publishing Co., Washington, USA, 1986, pp. 317-331.

24. Pidwerbecki, D., Welty, J.R., Heat transfer to a horizontal tube in the splash zone of a bubbling fluidized bed: an experimental study of temperature effects; Experimental Thermal and Fluid Science, 1994, 9, pp. 356-365.

25. Rios, G.M., Gibert, H., Heat transfer between gas fluidized bed and big bodies: analysis and explanation of a big particle mobility effects;. In Proceedings of the Fourth International Conference on Fluidization, Kashikojima, Japan, Engineering Foundation, 1984.

26. Deshmukh, S.A.R.K., Volkers, S., van Sint Annaland, M., Kuipers, J.A.M., Heat transfer in a membrane assisted bubbling fluidized bed with immersed horizontal tubes; Int. J. of Chem. Reactor Eng., 2005, 3, pp. A1.

27. Grewal, N.S., Saxena, S.C., Maximum heat transfer coefficient between a horizontal tube and a gas-solid fluidized bed; Ind. Eng. Chem. Process Des. Dev., 1981, 20, pp. 108-116.

28. Valenzuela, J.A., Glicksman, L.R., An experimental study of solids mixing in a freely bubbling two-dimensional fluidized bed; Powder Technology, 1984, 38, pp. 63-72.

29. Shen, L., Zhang, M., Effect of particle size on solids mixing in bubbling fluidized beds; Powder Technology, 1998, 97, pp. 170-177.

30. Huizenga, P., Kuipers, J.A.M., van Swaaij, W.P.M., Hydrodynamics of the continuously filtering slurry reactor - the influence of the load of solids and particle size distribution; Chem. Eng. Sci., 1997, 52, pp. 3869-3882.

31. Huizenga, P., Kuipers, J.A.M., van Swaaij, W.P.M., A two-dimensional hydrodynamic model of a slurry system with immersed filters; Chem. Eng. Sci., 2003, 58, pp. 457-472.

32. Schiller, L., Naumann, A., Uber die grundlegenden Berechnungen bei der Schwerkraftaufbereitung; Z. Ver. Dtsch. Ing., 1935, 77, pp. 318.

33. Davis, J.T., Turbulence Phenomena; New York: Academic Press, New York, 1972.

34. Werther, J., Effect of Gas Distributor on the Hydrodynamics of Gas Fluidized Beds; Ger. Chem. Eng., 1978, 1, pp. 166-174.

35. Gilliland, E.R., Mason, E.A., Gas and solid mixing in fluidized beds; Ind. Eng. Chem., 1949, 41, pp. 1191-1196.

36. Mostoufi, N., Chaouki, J., Local solid mixing in gas-solid fluidized beds; Powder Technology, 2001, 114, pp. 23-31.

37. Abanades, J.C., Atares, S., Garasa, G. A comparative analysis of two solid mixing models suitable for coal fluidized bed combustors and gasifiers; In Proceedings of the 15th International Conference on Fluidized Bed Combustion., Savannah, Georgia, 1999.

38. Litka, T., Glicksman, L.R., The influence of particle mechanical properties on bubble characteristics and solid mixing in fluidized beds; Powder Technology, 1985, 42, pp. 231-239.

39. Van Deemter, J.J., Mixing and contacting in gas-solid fluidized beds; Chem. Eng. Sci., 1961, 13, pp. 143-154.

40. van Deemter, J.J., The counter-current flow model of a gas-solids fluidized bed; In Proceedings of international symposium on fluidization, Eindhoven, The Netherlands, University Press, Amsterdam, 1967.

41. van Deemter, J.J., Chapter 9: Mixing; In Fluidization, Davidson, J.F., Harrison, D., Eds., Academic Press, London, UK, 1985, pp. 331-353.

42. Shen, L., Zhang, M., Xu, Y., Model for solids mixing in a two-dimensional gas-fluidized bed; Chem. Eng. Sci., 1995, 50, pp. 1841-1844.

43. Shen, L., Zhang, M., Xu, Y., Solids mixing in fluidized beds; Powder Technology, 1995, 84, pp. 207-212.

44. Kunii, D., Levenspiel, O., Bubbling bed model, model for the flow of gas through a fluidized bed; Ind. Eng. Chem. Fundam., 1968, 7, pp. 446-452.

45. Kunii, D., Levenspiel, O., Bubbling model for kinetic processes in fluidized beds, gas-solids mass and heat transfer and catalytic reactions; Ind. Eng. Chem. Fundam., 1968, 7, pp. 481-492.

46. Kunii, D., Levenspiel, O., Fluidization Engineering; 1st Ed., New York, USA: John Wiley & Sons, Inc., 1969.

47. Darton, R.C., LaNauze, R.D., Davidson, J.F., Harrison, D., Bubble growth due to coalescence in fluidized beds; Transactions of the Institution of Chemical Engineers (Great Britain), 1977, 55, pp. 274-280.

48. Shi, Y.-F., Fan, L.-T., Lateral mixing of solids in gas-solid fluidized beds with continuous flow of solids; Powder Technology, 1985, 41, pp. 23-28.

49. Danckwerts, P.V., Continuous flow systems: Distribution of residence times; Chem. Eng. Sci., 1953, 2, pp. 1-13.

50. Johnsson, F., Andersson, S., Leckner, B., Expansion of a freely bubbling fluidized bed; Powder Technology, 1991, 68, pp. 117-123.

51. Lee, G.S., Kim, S.D., Axial mixing of solids in fluidized beds; Chem. Eng. J., 1990, 44, pp. 1-9.

52. Lewis, W.K., Gilliland, E.R., Girouard, H., Heat transfer and solids mixing in beds of fluidized solids; Chem. Eng. Progr. Symp. Series, 1962, 58, pp. 87-97.

Chapter 5

Pyrolysis Experiments in a Bench-Scale Filter-Assisted Fluidized Bed

Abstract

This chapter describes how the concept of extracting and cleaning pyrolysis vapors by means of filters immersed in a fluid bed (FAFB) has been tested experimentally. For this, a batch-wise fed lab-scale FB (20 g per batch) and a continuous bench-scale FB (1 kg/h) have been equipped with an immersed filter (pore size between 6 and 15 micron).

In short batch experiments of ca. 2 minutes, pyrolysis oils have been produced that did not contain any particles, magnesium and sodium.

While using the continuous bench-scale FB, approximately 5700 grams of non-filtered oil and 3000 g of filtered oil were produced. Filtered oil contained two times less particles and 5 times less ash components than the non-filtered oil. The ash content of the filtered oil was only 0.01 wt % resulting in a very low aging rate expressed as the increase in viscosity per unit time. Silica was found on the inner walls of the filter and the downstream tubing indicating that sand fines (bed material) slipped trough the filter during long-term operation. There is evidence that the particles found in the filtered bio-oil have different origins. Part of them slipped simply through the filter, while others were formed by secondary processes (polymerization of vapors) occurring after the filter.

With this preliminary work, the potential of the FAFB is shown, but at the same time some problems are identified. Further research is needed to develop the FAFB concept completely.

1. Introduction

Solid biomass, which is a difficult to handle material with a low bulk-density, can be converted into a convenient liquid (bio-oil) via fast pyrolysis [1]. At a relatively mild pyrolysis temperature of ca. 500°C, vaporization of metals and minerals is largely avoided and most of these components are concentrated in the solid char [2,3]. As a consequence, the oil produced contains less contaminants than the feedstock from which it originates (typically more then ten times less).

It has been long recognized that the physical properties of pyrolysis oil change in time during storage. This change is characterized primarily by an increase in average molecular weight and water content [4-6], and therewith by an increase in viscosity. The work of Czernik et al. [4,7] has linked the presence of char fines in the oil to this viscosity increase. Char has also been identified as the source of alkali metals in pyrolysis oil [8,9]. The presence of char fines (including ashes) degrades the quality of pyrolysis oils and weakens their ability to penetrate into the high-quality fuel market. Reported char (solids) contents lie typically between 0.1 and 2 wt % [1]. Typical contaminants of bio-oil are in listed in Table 5.1. together with the problems they are bound to cause.

Table 5.1. Main contaminants in the pyrolysis oils and subsequent problems.

Main contaminants	Caused problems
Water	Lower heating value, phase separation
Ash	Fouling; Erosion, destruction of the turbine blades, slagging
Char particles	Promote polymerization, entraining metals to the oil phase, blockage
Cl, S, N	Corrosion, catalysts poisoning, NO_x, SO_x, dioxin emissions
Alkali metals (K, Ca, Mg, Na, etc.)	Corrosion, fouling, slagging
Acid (low pH value)	Corrosion

Char fines originate from the solid biomass feedstock material. In most reactor designs employed to pyrolyze biomass, char is subject to some degree of attrition. In a typical pyrolysis process, the fines are entrained in the gas and vapor stream leaving the reactor. After condensation, the fines end up in the produced pyrolysis oil. Cyclone separators have been used to remove the char particles from the vapor stream because of their low cost and reliable design. However, a small but significant portion of the char is below 5 μm in particle size and consequently not captured by cyclones. Up to now several biomass pyrolysis pilot-plants and near-commercialized plants

136

have been installed, but a method to remove char particles efficiently from the oil has not been developed yet and filtration of the produced oil has several disadvantages (see Chapter 1).

To meet the specification requirements of the sophisticated end-user applications, high quality pyrolysis oil must have uniform and reproducible properties and be free of char fines and ashes. Pyrolysis oils should therefore be produced in such a manner that they will consistently meet the specifications required by the end-use application. For this purpose, a fluidized bed with immersed filters for extracting pyrolysis vapors is proposed in this thesis. This concept is called the Filter Assisted Fluidized Bed (FAFB) pyrolysis reactor. The concept and its hydrodynamic characteristics were presented in the previous chapters (Chapters 1, 3, and 4 of this thesis). In this chapter, first preliminary results of actual pyrolysis experiments in a FAFB reactor are presented. At this stage of development we will mainly focus on the solids and alkali content in the produced bio-oils. Tests were carried out in 3 different set-ups, i) a small batch-wise (20 gram per batch) operated FAFB reactor, ii) a continuous bench-scale plant (1 kg/h) and, iii) a pilot plant of BTG. The filtered bio-oils were compared with non-filtered oil produced in the bench-scale plant and with typical (non-filtered) bio-oils produced in BTG's pilot plant. Complete mass balances of tests carried out in the bench-scale plant are presented.

2. Experimental Set-up and Materials

2.1. Feedstock Materials

Two types of biomass were used as pyrolysis feedstock, beech wood provided by BTG and Lignocel 9, which is a small diameter ($d_p < 1$ mm) material, purchased from Rettenmaier and Söhne GmbH (Germany). The properties of these materials are given in Table 5.2.

Table 5.2. Properties of beech wood and Lignocel 9[a]

		Beech wood (hard wood)	Lignocel 9 (Pine, soft wood)
Organic components (wt %, dry)	Cellulose	34	35
	Hemicellulose	22	29
	Lignin	31	28
Ultimate analysis (wt %, daf)	C	44.50	46.58
	H	5.85	6.34
	O	49.29	46.98
	N	0.30	0.04
	S	0.06	0.06
	Ash	2.20	0.27
Alkali metals (mg/kg, dry)	K	164	34
	Mg	540	134
	Ca	6600	768

[a] Analysis was done by ENEA, Italy

2.2. Batch Laboratory-Scale Fluid Bed

To validate the in-situ filtering of the vapors by introduction of a filter under real process conditions, a series of preliminary tests were carried out in a batch laboratory fluid bed. The scheme of the batch laboratory reactor is shown in Figure 5.1. The fluid bed reactor was made from stainless steel and had a diameter of 60 mm. More details on this reactor can be found in Chapter 3 of this thesis. The experiments were performed batch-wise; beech wood cylinders with a length of 6 mm and a diameter of 3 mm (about 20 g) were introduced into the reactor per experiment. During an experiment, the produced vapors were extracted from the reactor through a single immersed filter and via a cyclone. Cylindrical filters with a pore size of 10 to 15 μm (ceramic) and 6 μm (metal) were used (length: 30 mm, diameter: 15 mm, wall thickness = 2.5 mm). Both the filter line and the condenser line were led to a condensation train from where the produced pyrolysis oils were collected (see Chapter 3). Nearly equal amounts (ca. 10 g per sample) of filtered and non-filtered oil samples were obtained for analysis.
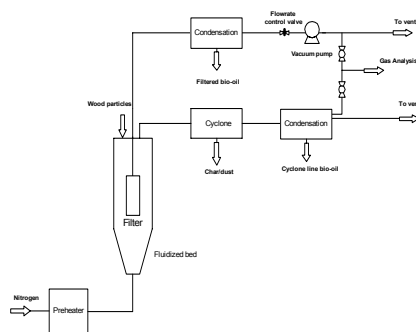
Figure 5.1. Flow sheet of the batch laboratory-scale set-up.

2.3.   BTG′s Pilot Plant

Some screening experiments were performed in BTG's pilot plant. See Prins et al. [12] for details on BTG's 200 kg/h pilot plant. The flowsheet is given in Figure 5.2. A segment of a commercial metal filter with pore size of 6 microns (GKN, Germany) was put into the exit line of the rotating cone reactor (see Figure 5.2). Using a vacuum pump and a bio-oil sampling system including condenser, approximate 10 g of filtered oil was obtained per run.
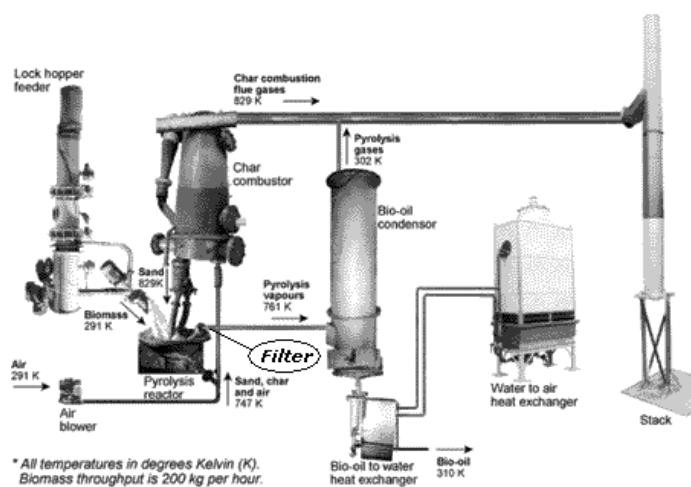
Figure 5.2. BTG pilot-plant BTG-200P.

2.4.   Bench-Scale Continuous Plant

In order to investigate the performance of the filter-assisted fluidized bed reactor under typical pyrolysis conditions for a longer time, a continuous bench-scale unit was designed and installed at University of Twente. Tests were carried out at atmospheric pressure and temperatures ranging from 450 - 600°C. The complete flow sheet is given in Figure 5.3. Biomass feedstock was introduced via a storage hopper (A). Plant operation was started with beech wood particles of 3 mm diameter. However, this feedstock caused a troublesome operation of the feeding system. Therefore, another feedstock (Lignocel 9) with a smaller particle size (1 mm) was used instead. The two-staged screw feeder (B) located under the storage hopper conveyed a controlled amount of feedstock into the FB reactor (E) through a constant speed injector screw. Good calibration of the feeding system appeared to be possible. The FB reactor was cylindrical with an inner diameter of 55 mm. However, the bottom section of the FB, with the feed entrance, had a conical shape. Typically, the feed rate was about 1 kg biomass per hour. A furnace (C) provided the heat to the bubbling fluidized pyrolysis reactor. The fluidizing gas (nitrogen) was preheated in a steel coil D before entering the fluid bed. The FB reactor had two exit streams (line 1 and line 2):

1)   The vapor/gas flow from the top of the bed passed through a knockout vessel (G) where most of the entrained char particles were removed. The remaining particles were further separated by a regular cyclone (I). The solids collected in the knockout vessel and cyclone receiver were considered as the char product.

2)   The product vapors could also be sucked off through a metal filter F immersed into the fluid bed. It was a cylindrical metal filter with an outside diameter of 20 mm, a height of 40 mm and pores of 10 to 15 microns. The vacuum pump (M) was adjusted to work at about 0.5 bar under pressure.

The hot vapor streams arrived in separate spray tower condensers (J-1 and J-2) where they were rapidly cooled to below 30°C. Trace heating was applied to keep the temperature above 350°C until just before the inlet of the condensers. Inside the condensers, the bio-oil itself was used as spraying liquid. To achieve this, the bio-oil was recycled by means of two pumps (K-1 and K-2). At set time intervals, bio-oil was collected from the bottom of the condensers by an overflow tube. In the first run, the condensers were started up with 1.5 liters of ethanol. As a result, the first batches of

140

produced ethanol contained large amounts of ethanol. After each experiment the condensers were completely emptied, while before every run the condensers were filled with oil obtained from the previous runs, up to the level of the overflow tube. The oil that was sent for analysis contained less than 8 wt % ethanol. Electrostatic precipitators (L-1 and L-2) were installed but not used in this preliminary work.

It appeared possible to operate the set-up with only the cyclone exit (line 1) open. When using the filter, line 1 had to be open as well, in order to keep the bed fluidized. The flow ratio through line 1 and 2 could be controlled by the applied vacuum and a control valve in line 1. The input gas flow rates of the reactor were measured and controlled by a set of mass flow controllers (MFC-1 and MFC-2), and the output gas (product) flow rates were measured by dry-gas-meters. In some cases, they were cross-checked based on the carrier gas (inert nitrogen) balance.

The temperatures in the reactor (4 axial equidistant points), transport lines and condensers were logged by the data acquisition system. The composition of the permanent gases was measured with a set of online gas analyzers. After an experiment, the char fractions of the knock-out vessel, cyclone receiver and the reactor were collected. The mass of net produced bio-oil and char was weighted and the produced gas was calculated based on the measured gas composition and flow rate.
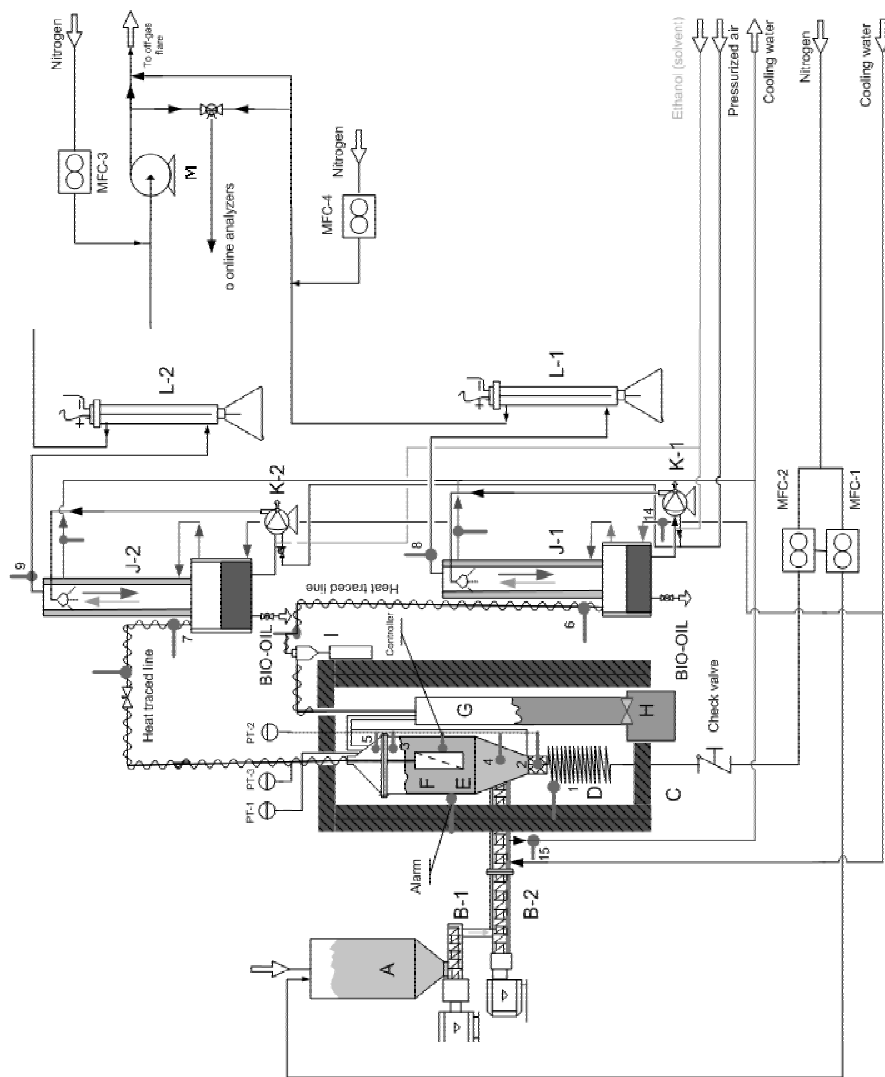
Figure 5.3. Flow diagram of the continuous bench-scale FAFB.

3.   Analysis

The Italian National Agency for new Technology, Energy and Environment (ENEA), and the Institute for Wood Chemistry (BFH) in Hamburg, Germany, have carried out the analyses of the produced oils. In the table below the most important analysis methods are listed together with the appropriate references.

Table 5.3. Analysis methods.

Analysis	Method	References
Solids content	Gravimetric	[6,13,14]
Ash content	EN ISO6245	[13,14]
Alkali metals	AAS	[6,13,14]
Viscosity	Capillary viscometers	ASTM D445

To characterize the aging of the pyrolysis oils its increase in viscosity per unit time was determined. This was done at room temperature (20°C), 40°C, and 90°C.

4.   Experimental Results

4.1.   Preliminary Testing in the Batch Lab-Scale FB and BTG′s Pilot Plant

For the batch lab-scale FB and BTG's pilot plant it was not possible to complete the mass balances. In these screening tests the focus was on the comparisons between filtered and non-filtered oils with respect to total solids and alkali metal contents.

Table 5.4 shows a comparison between the solids content of filtered and non-filtered oil. When feeding rather large beech wood particles (3 mm in diameter and 6 mm long), the non-filtered oil contained about 0.1 wt % solids (Table 5.4, UT-1 and UT-2). This is in agreement with results reported in literature [1]. In the filtered oil, no solids could be detected at all (Table 5.4, UT-1 and UT-2) by gravimetric methods (detection limit = 10^{-4} wt %). The same result was found for oil obtained via immersed filters in BTG's pilot plant (see Table 5.4, BTG plant).

To mimic the conditions of a real pyrolysis reactor, about 20 vol. % char was added to the fluidized bed in a separate experiment. The char contained quite some fines (smaller than 5 µm) and had an average particle size of 100 µm. With the additional char in the reactor, the collected non-filtered oil contained much more solids (see

143

Table 5.3, UT-3 and UT-4). However, the filtered oil remained completely solids free (see Table 5.3, UT-3 and UT-4).

Table 5.4. Solids and alkali content of filtered and non-filtered oils[a].

Exp. No.	Feed	U_g/U_{mf}	Filter pore size (micron)		Solids content (wt %)	Na (ppm)	Mg (ppm)	K (ppm)
UT-1	Beech	4	Filtered	10-15	$<10^{-4}$	0	0	5.72
			Non-filtered		0.11	3.05	7.40	34.60
UT-2	Beech	4	Filtered	6	$<10^{-4}$	0	0	5.49
			Non-filtered		0.07	0	0.34	9.37
UT-3	Beech and Char[b]	6	Filtered	6	$<10^{-4}$	0	0	14.43
			Non-filtered		2.2	25.81	20.93	66.46
UT-4	Beech and Char[b]	10	Filtered	6	$<10^{-4}$	0	0	7.89
			Non-filtered		>10	19.99	21.50	123.94
BTG plant	Beech wood hips		Filtered	6	$<10^{-4}$	n.d.	n.d.	n.d.
			Non-filtered		1.2	n.d.	n.d.	n.d.

[a] Analysis by BFH, Germany; n.d.: not determined.

[b] Wood was impregnated with Na, K an Mg salts and char fines were added to the bed.

The non-filtered oils UT-1 and UT-2 contained typical amounts of Na, Mg, and K. The beech wood particles used in UT-3 and UT-4 were impregnated with NaCl, KCl, and $MgCl_2$ solutions. As a result, the produced non-filtered oils contained more of these alkali metals (see Table 5.4, UT-3 and UT-4). However, the filtered oils did not contain any Na and Mg, but some K could be detected. This potassium could not originate from char because the oils were free of char (solids). It is assumed that K entered the filtered oil via the vapor phase. This is supported by the vapor pressures of the alkali metals analyzed, which are at reactor conditions (500°C) 10 Pa, 500 Pa, and 4000 Pa for Mg, Na, and K, respectively.

The above results indicate that particle free bio-oil with a low alkali content can in principle be produced in a filter assisted fluid bed reactor.

4.2.   Continuous Bench-Scale (1kg/h) FAFB

In the batch laboratory-scale fluid bed, described above, a typical experiment lasted ca. 2 minutes. To investigate the long-term performance of a filter assisted fluid bed pyrolysis reactor, experiments were performed in a continuous bench-scale facility. In this facility, an experiment lasted, on average, one hour.

144

Unfortunately, there were some operational problems. They were, however, not associated with using the immersed filter. Like often reported, blockage occurred at the inlet of the condenser at the point were the temperature gradient was largest.

The experimental campaign was started by performing regular fluid bed pyrolysis experiments, i.e. without filtering. Mass balances of five typical tests are presented in Table 5.5. The bed temperature in all five experiments was ca. 480°C. Table 5.5 contains the raw as well as the corrected (between brackets) mass balance. The correction is related to the loss of ethanol and bio-oil by vaporization from the condenser during operation. On average, the observed yields were 60, 18 and 17 wt % for respectively oil, char and gas. These yields are in good agreement with results reported for pine wood in literature.[1,15]. The closure of the uncorrected mass balance was ca. 95%, which increases after correction to 98%.

Table 5.5 also includes results of experiments in which vapors were extracted from the bed via an immersed filter (T ~ 500°C). During the first runs not many vapors were extracted via the filter (see run date 25-01-2005). The installation of a flow restriction in the tubing after the cyclone solved this problem. Hereafter, the ratio of oil obtained via the cyclone over oil obtained via the filter was ca. 2:1. With both oils obtained via the cyclone and the filter, the total (uncorrected) oil yield was ca. 50 wt %. The corresponding mass balance closure was about 84%, which is lower than in case the cyclone line was used only. This is ascribed to the extra loss of oil by vaporization in the second (filter-line) condenser. After correction the mass balance closure turned out to be approx. 88%.

For the purpose of this work, which is concerned with comparing filtered and non-filtered pyrolysis, the obtained mass balance closure is considered to be sufficient. Obviously, to investigate the influence of process conditions, like for instance the reactor temperature, the mass balance closure of the experiments with filtration should be improved. To achieve this in future experimentation, the electrostatic precipitator will be used.

Table 5.5. Overall mass balances obtained in the bench-scale FAFB.

	Run date	03-11-2004	16-12-2004	20-12-2004	23-12-2004	05-01-2005
	Duration, min	60	140	43	72	89
	Bio-oil, wt %	50 (53)	56 (59)	59 (63)	60 (63)	59 (62)
without filtration	*Knockout char*	28	13	18	17	17
	Cyclone char	2	1	2	1	3
	Total Char, wt %	30	14	20	18	20
	Gas, wt %	15	17	16	19	17
	Closure, wt %	95 (98)	87 (90)	95 (99)	97 (100)	96 (99)

	Run date	25-01-2005	03-02-2005	08-02-2005	10-02-2005	17-02-2005
	Duration, min	110	155	51	143	
	Filter line	6 (9)	14 (17)	19 (21)	16 (19)	15 (18)
	Cyclone line	42 (45)	28 (30)	31 (33)	38 (41)	35 (38)
	Total bio-oil, wt %	48 (54)	42 (47)	50 (54)	54 (60)	50
with filtration	*Knockout char*	17.9	28.7	16.4	14.8	13.9
	Cyclone char	0.1	0.3	0.6	0.2	0.1
	Total Char, wt %	18	29	17	15	14
	Filter line	1	3	3	2	2
	Cyclone line	16	11	14	13	14
	Total Gas, wt %	17	14	17	15	16
	Closure, %	83 (89)	85 (90)	84 (88)	84 (90)	80 (86)

4.2.1. In-situ Filtered Versus Non-Filtered Oil

Before each experiment, the condensers were filled with oil obtained in previous runs whereas in the first experiment the condensers were filled with ethanol. After the experiment, the obtained oil from that experiment was mixed with the oil collected until that day. In this way 5700 g of accumulated non-filtered oil and 3000 g of accumulated filtered oil were obtained from Lignocel 9 as a feedstock material. This oil was sent for analysis to ENEA, Italy. The non-filtered oil contained 4 wt % and the filtered oil 8 wt % of ethanol. The ethanol contents in standard pyrolysis oil [16,17] typically varies from 0.1 to 2 wt %. The results obtained indicate that the accumulated oil samples are not too much diluted with ethanol from the first experiment and can be considered as useful oil samples. Apart from the comparison with non-filtered oil from the same setup, the filtered oil has also been compared with non-filtered beech, pine, and switch grass oil from BTG's pilot plant.

The total solids content (including char fines and ashes) in the produced oils are 2.68 wt % and 1.47 wt % for non-filtered and filtered oils, respectively. A solids content of 2.68 wt % in the non-filtered bio-oil is a rather high number indicating that the knock-out vessel and cyclone were not performing optimal. The particle size distribution is presented in Figure 5.4. In the non-filtered oil sample the majority of solids are relatively large (char) fines (> 25 micron) whereas in the filtered oil the larger part of the particles is smaller than 25 microns. The latter observation is in agreement with the pore size of the filter used, which was between 10 and 15 μm. However, it is not known yet if the particles in the filtered oil are particles that slipped through the filters (char and/or sand) or that they are formed by secondary processes such as polymerization of vapors.
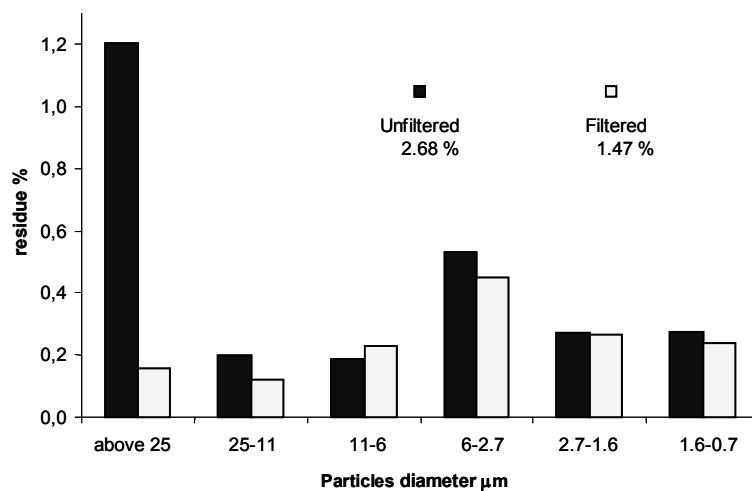
Figure 5.4. Particle size distributions in bio-oils as determined by ENEA, Italy.

In Table 5.6 the ash content of the oils are presented. The ash content of the non-filtered bio-oil from the bench-scale FAFB is in good agreement with oils produced in BTG's pilot plant. Knowing the particle content in the filtered and non-filtered oil, it is not surprising that the ash content in the filtered bio-oil is lower than in the non-filtered one (see Table 5.6). However, the ratio of the ash contents is not equal to the ratio of solids contents. The filtered oil contains about 2 times less particles, but approx. 5 times less ashes. When assuming that the primary char particles formed by pyrolysis have about the same ash content independent of their size, the residual solids found in the filtered oil can only be formed by secondary processes (polymerization).

Table 5.6. Total ash content in different bio-oils as determined by ENEA, Italy.

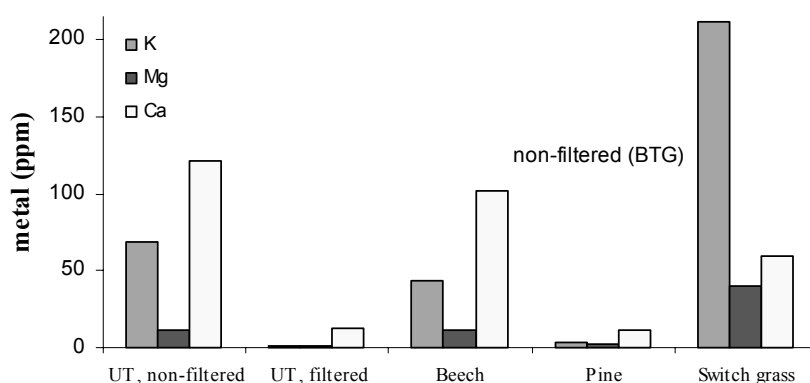| Oils	Ash content (wt %)
UT, filtered	0.0100 ± 0.0002
UT, non-filtered	0.054 ± 0.002
Beech, non-filtered	0.098 ± 0.001
Pine, non-filtered	0.16 ± 0.03
Switch grass, non-filtered	0.09 ± 0.02

Figure 5.5. Alkali metals in bio-oils, as determined by ENEA, Italy.

In line with the lower ash content, the filtered bio-oil contains less alkali metals than the non-filtered oil (see Figure 5.5). The alkali levels found in the non-filtered oil are in good agreement with values reported in literature [14] and those in the beech oil produced by BTG. The filtered oil still contains 15 ppm calcium. Such amounts of calcium can not have entered the oil via the vapor because the vapor pressure of Ca is less than 1 Pa at the reactor temperature. This indicates that some char fines slipped through the filter as a result of which calcium ended up in the oil.

Bio-oil contains compounds that, during storage or handling, can react with each other to form larger molecules. The main chemical reactions observed are polymerization of double-bonded compounds, as well as etherification and esterification occurring between hydroxyl, carbonyl, and carboxyl group components, in which water is formed as a byproduct. These reactions result in undesirable changes in physical properties, such as increase of viscosity and water content with a corresponding decrease of volatility. This process is called "aging" [5,14] and is quantified by measuring the increase in viscosity per unit time.
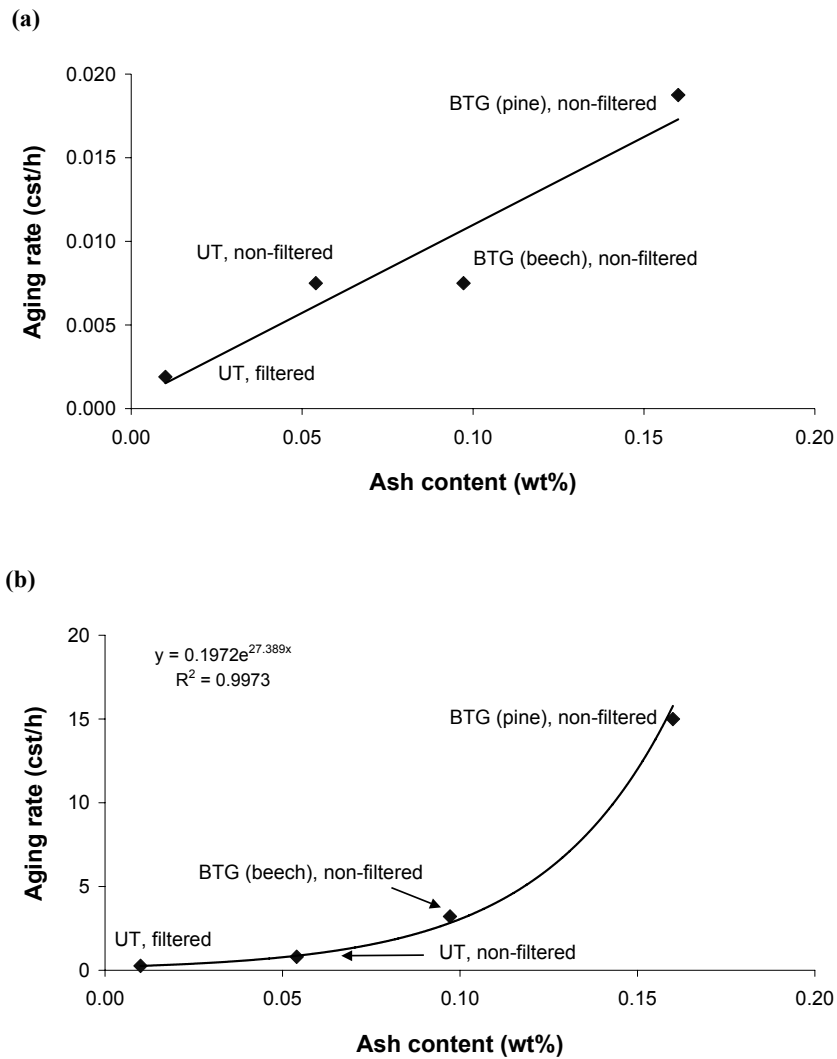
148

Figure 5.6. Aging rate at (a) room temperature, and (b) 90 ^{o}C as determined by ENEA, Italy.

In Figure 5.6 the aging rate is plotted versus the ash content in the oil, at room temperature and at 90°C. At both temperatures the aging rate can be related reasonably well to the ash content of the oil (see Figure 5.6). It was not possible to relate the aging rate to the solids content of the oils. Figure 5.6 clearly shows that the in-situ filtered oil has the lowest aging rate due to its low ash content. From the comparison of Figures 5.6a and 5.6b it appears that the temperature influences the aging rate drastically.

4.2.2. Deposits Inside the Filter and in the Tubing Downstream of the Filter

Upon cleaning of the set-up it was observed that the tubing after the filter contained black deposits. The filter was cleaned after every experiment. But after the last experiment, the filter was sawed in four pieces for visual inspection (see Figure 5.7). It appeared that some material was deposited on the inner walls of the filter. About 13 milligram of this material was scratched off the inside walls and sent for analysis. Ten milligram of the sample could be dissolved in an acid solution, which showed primarily the presence of Fe and Ni, being the metals out of which the filter consists. The three milligram that did not dissolve consisted out of carbon (20 wt %) and silica (80 wt %), materials that are not present in the filter. The fact that Si has been found on the inner wall of the filter indicates that sand (bed material) slipped trough the filter. The carbon deposits are supposed to be caused by either primary char particles that slipped through, or particles formed secondary condensation reactions.

Figure 5.7. Photograph of the filter after 1.5 hours of experimentation

5.   Discussion and Conclusions

The concept of in-situ extraction and cleaning of pyrolysis vapors through a filter immersed in a fluidized bed reactor has been tested in various setups. By performing batch pyrolysis experiments (10 g feedstock in 2 minutes), oils have been produced that were free of solid particles, magnesium and sodium. These oils still contained some potassium, which entered the oil presumably via the vapor phase.

About three liters of in-situ filtered pyrolysis oil have been collected in 8 tests with

the bench-scale FAFB at ca. 1 kg/h feeding rate. With respect to the filtering, no severe operational problems have been encountered. The filtered bio-oil has been compared with non-filtered oil produced in the same set-up. The filtered oil contained two times less particles but 5 times less ashes than the non-filtered oil. The ash content of the filtered oil was only 0.01 wt % resulting in a very low aging rate expressed as the increase in viscosity per unit time. The fact that the ratio of solids in the filtered oil over solids in the non-filtered oil (0.55) is much larger than the ratio of ashes in the oils (0.19) indicates that some solids in the filtered oil are formed by secondary processes, i.e. they are formed after the filter. There is strong evidence that char fines and bed material fines slipped trough the 10 to 15 μm filter during 13 hours of operation. This slip seems inevitable as the use of filters with a much smaller pore size is unpractical because it would lead to either a high pressure drop or a large required filter area.

With this work, the potential of the FAFB is shown but at the same time some problems have been identified. Further research is needed to develop the FAFB concept fully, with special attention to the filter design.

Acknowledgement

References

1. Bridgwater, A.V., Czernik, S., Diebold, J., Meier, D., Oasmaa, A., Peacocke, C., Piskorz, J., Radlein, D., Eds., Fast pyrolysis of biomass; A handbook, CPL Press, 1999.

2. Helsen, L., van den Bulck, E., Mullens, S., Mullens, J., Low-temperature pyrolysis of CCA-treated wood: thermogravimetric analysis; J. Anal. Appl. Pyrolysis, 1999, 52, pp. 65-86.

3. Hansen, U., Strenziok, R., Meier, D., Achenbach, D., Energy from contaminated waste wood; In Twelfth European Biomass Conference: Biomass for Energy, Industry and Climate Protection, Amsterdam, The Netherlands, ETA-Florence and WIP-Munich, 2002.

4. Czernik, S., Johnson, D.K., Black, S., Stability of wood fast pyrolysis oil; Biomass and Bioenergy, 1994, 7, pp. 187-192.

5. Diebold, J.P., A review of the chemical and physical mechanisms of the storage stability of fast pyrolysis bio-oils; National Renewable Energy Laboratory (NREL), Golden, CO, USA, 2000, pp. 59.

6. Scholze, B., Long-term stability, catalytic upgrading, and application of pyrolysis oils-improving the properties of a potential substitute of fossil fuels; Ph.D. Thesis, University of Hamburg, Hamburg, Germany, 2002.

7. Czernik, S. Storage of Biomass Pyrolysis Oils; In Proceedings of Biomass Pyrolysis Oil, Properties and Combustion Meeting, National Renewable Energy Laboratory, Estes Park, CO, USA, Golden, CO, NREL-CP-430-7215, 1994, pp. 67-76.

8. Bridgwater, A.V., Cottam, M.-L., Opportunities for biomass pyrolysis liquids production and upgrading; Energy & Fuels, 1992, 6, pp. 113-120.

9. Oasmaa, A., Czernik, S., Fuel oil quality of biomass pyrolysis oils: state-of-the-art for the end users; Energy & Fuels, 1999, 13, pp. 914-921.

10. Elliott, D.C., Comparative analysis of gasification/pyrolysis condensates; In Proceedings of the 1985 Biomass Thermochemical Conversion Contractors Meeting, Minneapolis, Minnesota, USA, 1985.

11. Antonelli, L., Improvement of pyrolysis products: bio-oil and bio-carbon/emulsion and slurries; In Energy from Biomass 4, Proceedings of the Third Contractors Meeting, Paestum, London, Elsevier Applied Science, 1989.

12. Prins, W., Wagenaar, B.M., Review of the rotating cone technology for flash pyrolysis of biomass; In Biomass gasification and pyrolysis: state of the art and future prospects, Kaltschmitt, M., Bridgwater, A.V., Eds., CPL Press, Newbury, UK, 1997, pp. 316-326.

13. Oasmaa, A., Meier, D., Analysis, characterization and test methods of fast pyrolysis liquids; In Fast pyrolysis of biomass. A handbook, Bridgwater, A.V., Ed., CPL Press, 2002, pp. 23-40.

152

14. Oasmaa, A.,Peacocke, C., A guide to physical property characterisation of biomass-derived pyrolysis liquids; VTT, Technical Research Center of Finland, Espoo, Finland, 2001, pp. 102.

15. Meier, D., Faix, O., State of the art of applied fast pyrolysis of lignocellulosic materials - a review; Bioresource Technology, 1999, 68, pp. 71-77.

16. Piskorz, J., Scott, D.S., Radlein, D., Composition of oils obtained by fast pyrolysis of different woods; In ACS Symposium Series 376: Pyrolysis oils from biomass producing, analyzing, and upgrading, Soltes, E.J., Milne, T.A., Eds., American Chemical Society, Washington, DC, 1988, pp. 167-178.

17. Aguado, R., Olazar, M., San Jose, M.J., Aguirre, G., Bilbao, J., Pyrolysis sawdust in a conical spouted bed reactor: Yields and product composition; Ind. Eng. Chem. Res., 2000, 39, pp. 1925-1933.

Chapter 6

Preliminary Design Calculations for an Industrial (10 ton/h Intake) Fluid Bed Pyrolysis Reactor with In-Situ Cleaning of the Product Vapors (FAFB)

Abstract

Based on knowledge, gained in Chapters 2 to 5 of this thesis, an engineering model has been developed to estimate the volume of a FAFB reactor for pyrolysis. Calculations have been done for a system with a throughput of 10 tonnes biomass per hour. For small particle sized feedstocks ($\leq$ 1 mm), the required reactor volume of a FAFB is 13 m^3 including the freeboard, compared to 22 m^3 for a regular FB. For larger sized feedstocks intensification is hardly possible, because the lower reaction rate and therewith the hold-up of reacting particles dominates the reactor design. Extracting large parts of gases and vapors through the immersed filters does not result in significantly large intra-bed temperature gradients due to less intense solids mixing.

1.   Introduction

A wide variety of reactor designs have been proposed and tested for fast pyrolysis of biomass (see Chapter 1) after the first investigations concerning a fluidised bed reactor by Scott and Piskorz [1-6]. In various connected papers [7-15], these concepts are described in detail. While presenting their specific advantages, usually no results are given of a proper reactor design including calculations.

Reactor design for the fast pyrolysis process is based on solving mass and energy balances, first on a particle scale and subsequently on the scale of the entire reactor. A variety of assumptions may be connected to the model in order to keep it simple and soluble.

Reactor design simulations are meant primarily to decide on the size/shape of the reactor and to evaluate its performance for the design conditions. But they are also used to predict the effects of a change in operating parameters (like temperature and particle size of the feed) and eventually to define the possible operation window.

As discussed in Chapter 2, the number of publications concerning pyrolysis reactor design and modelling is limited. The models, developed and discussed so far, were meant rather to understand some specific aspects of the reactor operation than to design a reactor completely in relation to a full-scale process.

In this chapter, a model of the proposed fluid bed pyrolysis reactor with in-situ cleaning of the produced vapors is described. This system is further indicated by the abbreviation FAFB (Filter-Assisted Fluid Bed). The intention is to determine the required reactor volume and to evaluate the performance as a function of the size of the feed particles for a plant with an intake of 10 ton biomass per hour. The FAFB systems are compared with regular fluid beds without filtering. An intake of 10 ton per hour is chosen on the basis of economical/logistic reasons related to the transport costs of raw biomass to the plant in the oil producing countries.

2.   FAFB Design Criteria

The proposed reactor is based on fluid bed technology. Up to now, many reactor types have been applied in biomass pyrolysis processes. Fluidized beds are suitable for biomass pyrolysis because of the following advantages:

156

- High feedstock flexibility, especially in particle size and sorts;
- Intensive heat transfer rate, leading to nearly isothermal conditions;
- Rapid removal of produced pyrolysis vapors from the reaction zone.

Of course, in a regular fluidized bed a large amount of gas (inert or recycled product gas in most cases) is needed to fluidize the solid particles. This dilutes the gaseous products and consequently increases the load of the bio-oil condensation system. A practical solution employed in the FAFB concept is to use a conical bottom section to decrease the amount of the fluidization gas as much as possible. When doing so, in principle, no additional gas supply is required during steady state operation, because the bed is fluidized by the produced vapors and permanent gases.

Below, the main choices made in this preliminary design are discussed per item:

Particle Size of the Feedstock

The rising velocity of wood particles (ρ = 600 kg/m^3) of different size has been measured in a fluid bed (h=30 cm). It has been observed that large particles (ρ = 600 kg/m^3, d_p > 7 mm) fed to the bottom of a lab-scale fluid bed rise with a constant velocity and once arrived at the top, do not mix back easily. The rising velocity of these particles lies in the range of 10 to 30 cm/s. Although measured in a lab-scale fluid bed, these values are also used for the industrial size as a conservative estimate. This leads to a rising time in an industrial scale reactor (3 – 4 meters high) of 10 to 40 s, which is much less than the conversion time of larger particles (see Chapters 2 and 3). As a result, an undesired accumulation of partially converted feedstock on top of the bed occurs. In this case, most of the conversion takes place near the bed surface causing a non-uniform, local vapor production and heat demand. It has been observed visually that wood particles with a size of up to 5 mm mix rather well with the fluid bed particles under pyrolysis conditions (see Appendix 1). In this case, the vapors are produced more or less uniformly over the bed's volume and consequently also the heat demand is spatially uniform. For these reasons the particle size of the feedstock is limited to 5 mm in this design.

Velocity at the Top of the Bed

According to the results presented in Chapter 4, the superficial velocity at the top of the bed must be larger than 7 x U_{mf} to provide a good solids mixing (is important for a

spatially uniform temperature) and to minimize the formation of stagnant zones around the filters.

Bed Particle Size

Is in principle left free as design variable. However, the choice depends on the velocity at the top of the bed: in case of a high velocity large particles will be chosen to keep U/U_t limited, for a rather low velocity small particles will be selected to satisfy the $U_{top}/U_{mf} > 7$ criterion.

Fluid Bed Layout and Dimensions

The biomass feedstock enters the reactor in the bottom, which has a conical design to assure fluidization while minimizing the use of additional fluidizing gas. The L/D of the cylindrical part of the bed is 2 (not in conflict with industrial practice). The height of the freeboard is half the height of the bed level and its diameter is 1.5 times the bed diameter. Cone dimensions are one third of the dimensions of the cylindrical section. In Figure 1, the fluid bed system is presented schematically.
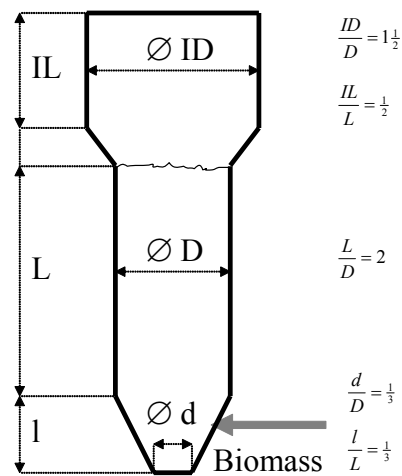

$$\frac{ID}{D} = 1\tfrac{1}{2}$$

$$\frac{IL}{L} = \tfrac{1}{2}$$

$$\frac{L}{D} = 2$$

$$\frac{d}{D} = \tfrac{1}{3}$$

$$\frac{l}{L} = \tfrac{1}{3}$$

Figure 1. Schematic drawing of the fluid bed.

Hold-up of Reacting Particles

The following particles in the fluidized bed can be defined as reacting: fresh feed particles, particles in the transition towards char, and char. Earlier experiments [16]

have shown that a maximum of 20 vol % of the bed can consist of reacting particles in order to retain good mixing. As a conservative estimate, this maximum is also adopted for the large scale design.

Heat Provision

Heat is supplied to the pyrolysis reactor via a circulation loop of sand (bed particles). The sand is heated in a combustor where the non-filtered permanent gases and vapors are oxidized. Sand plus char are extracted out of the pyrolysis reactor by means of an overflow tube. Before this stream enters the combustor char has to be separated from the sand (to be developed).

Filters

Horizontal filters are selected with a diameter of 5 cm and permeability of 1.5×10^{-12} m^2. The pressure inside the filters is ca. 1 bara. This choice is merely based on keeping the required volume of filters limited (less than 0.2 m^3 filter volume per 10 ton intake required). The selection of the filters (material) and the spatial arrangement of the filters in the bed has not been subject of this investigation.

Vapor Residence Time

This is expected to be not an important issue because the vapors are extracted immediately after being formed.

Pressure

The pressure at the bottom of the fluid bed is kept at about 1.7 bara. In this way there is enough pressure available for pressure drop over the filters.

Temperature

Ca. 500^0C for the pyrolysis reactor and ca. 550 for the combustor. 500^oC gives for most feedstock materials a maximal oil yield, while the water content of the oil is minimal (see Chapter 3). Keeping the temperature of the combustor as low as 550^oC allows the use of standard (cheap) construction materials. Besides, it avoids ash-meting and agglomeration of bed particles. If char combustion is applied to provide the energy for the process, a relatively low combustor temperature keeps the concentration of alkali's (metals) in the exhaust gas limited.

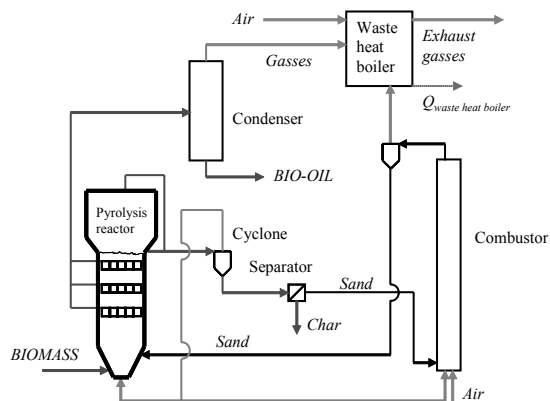In Figure 2, the layout of the whole design is sketched.

Figure 2. Layout of the whole design.

3.   FAFB Reactor Model

Basically only the pyrolysis reactor is modelled, the combustor is included by assuming a constant temperature in it and setting the sand circulation rate. The pyrolysis reactor model consists out of several sub-models. These sub-models are described in detail below. After these descriptions, the overall algorithm for the design calculations is given.

3.1.   Overall Energy Balance

The energy balance calculations are based on the experimental results obtained for beech wood (7.3 wt % moisture) pyrolysis at a reactor temperature of $500^{\circ}C$ (see Chapter 3, Table 2). In Table 1 the product yields and heating values, used in the calculation, are listed.

Table 1. Product yields and heating values for beech wood pyrolysis at 500°C.

	Yield [kg/kg]	LHV [MJ/kg]
Beech Wood	-	16.3
Char	0.16	31
Oil	0.65	15.5
Permanent Gas	0.19	4.9

The pyrolysis process is overall endothermic, because energy input is required to heat the cold feedstock material to the reactor temperature. Besides, there may be a net reaction enthalpy for the multitude of individual chemical reactions occurring during pyrolysis. However, the effects of heating the feedstock and the reaction enthalpy are impossible to measure independently. The combined effect of heating the feed and the reaction enthalpy is defined as the heat for pyrolysis in the handbook of A.V. Bridgwater et al. [17] and is also adapted here. Reported values for the heat for pyrolysis lie in the range of 0.8 MJ to 3.5 MJ per kg dry wood. Reed and Gaur [18] measured the time a plume was present above a wood particle when placed in a flame of 2000°C. By performing these tests for dry and wetted particles they could deduce the heat for pyrolysis from the difference in time that the plume was visible, under the assumption that heat transfer from the flame to the particles was equal for the dry and wet particles. With this method they found values between 2.9 and 3.5 MJ/kg. These numbers turn out to be rather high, which is probably caused by the measurement technique. Based on measurements of Martin et al. [20], Cottam and Bridgwater [19] derived a value of 1.4 MJ per kg dry wood.

The heat for pyrolysis can also be estimated from operational data of pilot and demonstration plants. In case sand recirculation is used as a heat source, Q_p can be calculated from the measured values of the feed rate, the sand circulation rate, the temperatures of the pyrolysis (T_{out}) and combustor (T_{in}) reactors and the estimated heat losses.

$$F_{bio}\dot{Q}_p + Q_{loss} = \Theta_{sand}Cp[\langle T_{in}\rangle - \langle T_{out}\rangle] \rightarrow$$
$$\dot{Q}_p = \frac{\Theta_{sand}Cp[\langle T_{in}\rangle - \langle T_{out}\rangle] - Q_{loss}}{F_{bio}} \tag{1}$$

Operational data from BTG's 200 kg/h intake pilot plant [20] have been used to estimate the heat for pyrolysis. For a typical throughput of 120 kg/h of dried (~ 10 wt

161

% moisture) pine or beech wood, the sand circulation rate is 3600 kg/h and the temperature difference between the combustor and the pyrolysis reactor is 50°C. When neglecting the heat losses (the plant is well isolated), these data indicate that the heat for pyrolysis for dry pine or beech wood is 1.2 MJ/kg.

The heat for pyrolysis is an essential property for the design of a pyrolysis plant. It affects the choice of reactor system and the degree of heat integration in terms of selecting the by-products to be burned for heat generation. Results will be presented for a range of 1.0 - 2.5 MJ/kg. For a more detailed analysis a conservative estimate from the pilot plant data of 1.5 MJ/kg is used, which is also used further in the design calculations.

Energy balance calculations have been done for three process alternatives:

a)   Char is burned to deliver the heat for pyrolysis and the produced permanent gases are fed to a waste heat boiler ($Q_{waste\ heat\ boiler}$). In the combustor, steam pipes are installed to produce steam from the energy surplus (Q_{steam}). The vapors leaving the reactor via the cyclone are either considered to be a different product or are recycled (with the permanent gases) and fed back to the reactor;

b)   All produced permanent (non-condensable) gases are burned to deliver the heat for pyrolysis. Char is collected and considered as a product of the process that is sold on the market just like pyrolysis oil. The vapors leaving the reactor via the cyclone are either considered to be a different product or are recycled (with the permanent gases) and fed back to the reactor;

c)   The part of the permanent gases and vapors that is not extracted via the filters from the reactor is burned to deliver the heat for pyrolysis. If the amount of energy in the permanent gases and vapors leaving the cyclone exceeds the required heat for pyrolysis, the surplus is recycled to the reactor. The permanent gases leaving the condenser are fed to a waste heat boiler. Char is collected and considered as a product of the process.
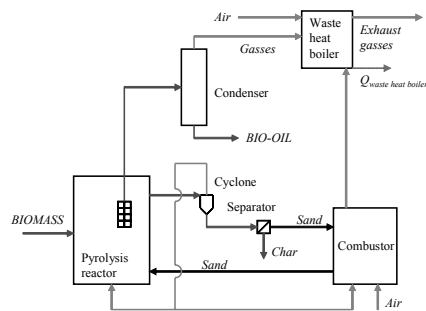
These cases are also schematically drawn in Figure 3.

162
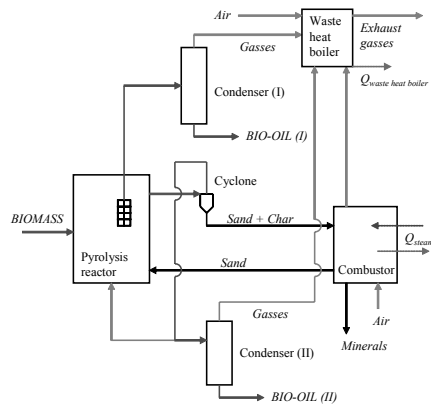
(a)
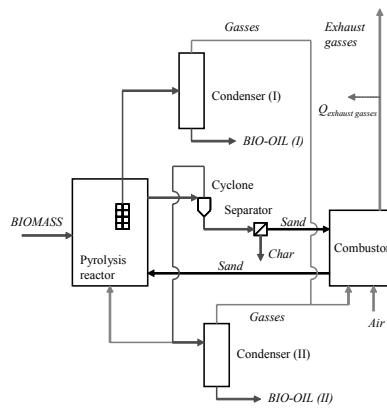
(b)

(c)

Figure 3. Schematic drawings of the considered process alternatives (a, b and c).

In the energy balance calculations it is assumed that the efficiency of the combustor system is 80%, that is 80% of the LHV of the fuel is transferred to the pyrolysis reactor and/or the inserted steam pipes. Burning of only the gases is not a preferred mode of operation because it can only deal with feedstock materials with a very low heat for pyrolysis (< 1 MJ/kg). For feeds with a higher heat demand, additional (external) heat has to be supplied to the process. Consequently, this alternative is not robust with respect to a changing feedstock. The results of these energy balance calculations for alternatives (a.) and (c.) are shown in Figure 4. The faction of the LHV of the feedstock that ends up in the products ($Y_{energetic}$) oil, char, steam, and waste-heat, is plotted in Figure 4.
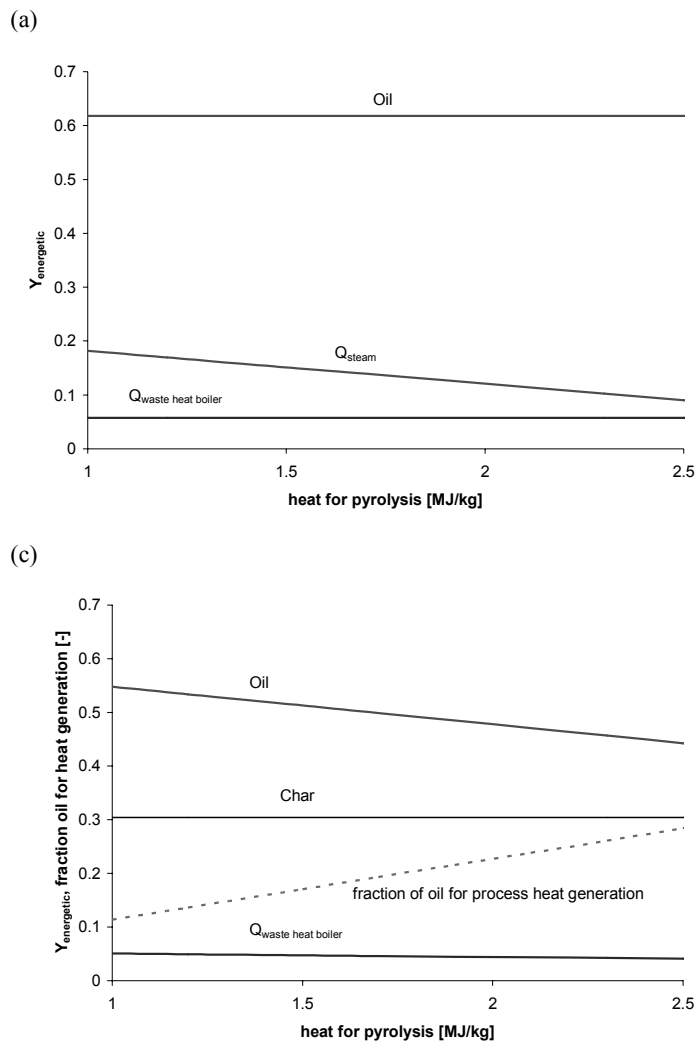
(a)

(c)

Figure 4. Energy balance of process alternatives (a and c).

164

The energy balances of the process alternative are assessed according to the following criteria:

– Value of the <u>energetic yields</u> of the products being in increasing order of value $Q_{waste\ heat\ boiler}$, Q_{steam}, char and oil;

– <u>Robustness</u> with respect to the delivery of heat for pyrolysis. This criterion evaluates if the heat for pyrolysis can also be delivered if the feedstock and/or the product distribution changes;

– <u>Technical feasibility</u>.

Burning the char gives the highest oil yield and is very robust. The amount of heat generated by combustion of the char is more than enough to run the endothermic pyrolysis process. Therefore any changes in the feedstock (composition, moisture content) and/or product distribution can be easily dealt with from an energy balance point of view. Also the technical feasibility of this process is good. The only expected problem is the accumulation of minerals in the system.

Using the part of the vapors and permanent gases that is not extracted via the filters to provide the energy required for the pyrolysis process is an interesting alternative. Obviously, the oil yield is lower compared to the alternative (a: combustion of char) but not drastically. In this alternative, next to oil, a second high-valued product (char) is produced, increasing the value of the total product slate. For an estimated heat for pyrolysis of 1.5 MJ/kg, the yield of oil plus char adds up to 82% on energy basis (oil = 51%, char 31%). Under these conditions, 83% of the produced vapors and permanent gases have to be extracted via the filters. On lab-scale, it has been found that this does not cause malfunctioning of the fluid bed as long as the velocity at the top of the bed exceeds 7 x U_{mf} (see Chapter 4). With respect to robustness of heat supply this scheme has no problems. When the heat for pyrolysis increases for instance, auto-thermal operation can be easily attained by increasing the amount of extracted vapors and gases. Another benefit of this scheme is that the combustor can be relative small because gases are combusted instead of char. Char combustion rates are very low compared to gas combustion rates because they are controlled by mass transport when using particles larger than 2 mm [21]. A drawback of this system is that it requires a dedicated device to remove char from the system

Concluding, burning char gives the highest oil yield and its technology is developed. Burning part of the vapors and the permanent gases, as in the proposed fluid bed with in-situ filtering, lowers the oil yield a bit but gives a second high-valued product, namely char. Char is an interesting side product in the oil producing countries, where it is used as fertilizer. However, from a technological point of view, this alternative has some challenges.

In the investigated design, the vapors and gases that are not extracted via the filters are used to provide the heat. When assuming a heat for pyrolysis of 1.5 MJ/kg this results in extracting 83% of the produced vapors and gases via the filters.

3.2 Energy Balance of the Pyrolysis Reactor

The system under consideration is large enough to assume a negligible relative heat loss to the environment. Therefore, the macroscopic energy balance over the reactor can be simplified to:

$$\dot{Q}_p = \Phi C p_{sand} \left[T_{in} - T_{out} \right]$$
$$\Phi = \frac{\Theta_{sand}}{F_{bio}}$$

(2)

In this equation, T_{in} is the temperature of the hot sand coming from the combustor and T_{out} the temperature of the sand leaving the pyrolysis reactor to the combustor. For the microscopic energy balance over the reactor, the following assumptions have been made:

– The biomass (reacting) particles are distributed spatial uniformly in the reactor leading to a spatial uniform volumetric heat for pyrolysis (Q_p);

$$Q_p = \frac{F_{bio}\dot{Q}_p}{V_{bed}}$$

(3)

– Hot sand enters the reactor at the bottom (x = 0) and the cooled-down sand leaves the reactor from the top of the bed level (x = L), or visa versa which comes down to a similar mathematical model;

– The flow of the sand through the reactor can be described with the standard axial dispersion model;

166

- The heat for pyrolysis is constant. Obviously this is not the case in practice, but the model is applied only for a pyrolysis reactor operated at ca. 500°C with an intra bed temperature gradient smaller than 50°C;
- Additional fluidization gas is not required during stationary operation due to the conical bottom section;
- The conical section is not modelled. This section is intensely mixed and is assumed to be of uniform temperature.

The microscopic energy balance becomes then:

$$\left(D\varepsilon\rho Cp\right)_{sand}\frac{d^2T}{dx^2} - \left(u\rho Cp\right)_{sand}\frac{dT}{dx} - Q_p = 0$$

$$u_{sand} = \frac{\Phi F_{bio}}{\rho A_r}$$

(4)

By introducing the following dimensionless numbers:

$$\theta = \frac{x}{L}, \quad Pe = \frac{Lu}{\varepsilon D}, \quad \overline{Q}_p = \frac{Q_p L^2}{D\varepsilon\rho Cp}$$

Equation 3 can be rewritten to:

$$\frac{d^2T}{d\theta^2} - Pe\frac{dT}{d\theta} - \overline{Q}_p = 0$$

(5)

Using the boundary conditions as proposed by Danckwerts [22]:

$$\frac{dT}{d\theta}(\theta = 1) = 0$$

$$T_{in} = T(\theta = 0) - \left(\frac{1}{Pe}\frac{dT}{d\theta}\right)(\theta = 0)$$

(6)

Equation 5 can be solved yielding:

$$T(\theta) = T_{in} + \frac{\overline{Q}_p}{Pe}\left[\frac{e^{Pe\theta}}{Pe \times e^{Pe}} - \theta - \frac{1}{Pe}\right]$$

(7)

167

With Equation 6, the axial temperature distribution inside the fluid bed can be calculated. The intra-bed temperature gradient defined as $[T(\theta=0)-T(\theta=1)]$ is then given by:

$$[T(\theta = 0) - T(\theta = 1)] = \frac{\overline{Q}_p}{Pe}\left[\frac{1}{Pe \times e^{Pe}} + 1 - \frac{1}{Pe} \right] \tag{8}$$

The axial averaged bed temperature can be calculated from:

$$\langle T(\theta) \rangle = \frac{\int_0^1 T(\theta)d\theta}{\int_0^1 d\theta} = T_{in} + \frac{\overline{Q}_p}{Pe}\left[\frac{1}{Pe^2} - \frac{1}{Pe^2 \times e^{Pe}} - \frac{1}{2} - \frac{1}{Pe} \right] \tag{9}$$

With Equations 2, 8 and 9, an intra-bed temperature gradient and the average pyrolysis bed temperature can be calculated for a given combustor exit temperature (inlet temperature of solids entering the pyrolysis FB, T_{in}), sand flux ratio (Φ) and pyrolysis reactor geometry. Alternatively, the required combustor exit temperature can be calculated for a certain desired average pyrolysis bed temperature.

In Figure 5, the temperature profiles inside a regular fluid bed pyrolysis reactor (without filtering) with an intake of 10 tons per hour are given as function of the mixing intensity (Pe-number). A very conservative estimate of 2 MJ/kg for the heat for pyrolysis is used. The volume of the bed is ca. 8 m^3 leading to a volumetric heat for pyrolysis (Q_p) of 0.72 MJ/m^3 bed. For the sand recirculation rate over the biomass feed rate ratio, Φ, 50 has been taken. The combustor operates at 550°C.
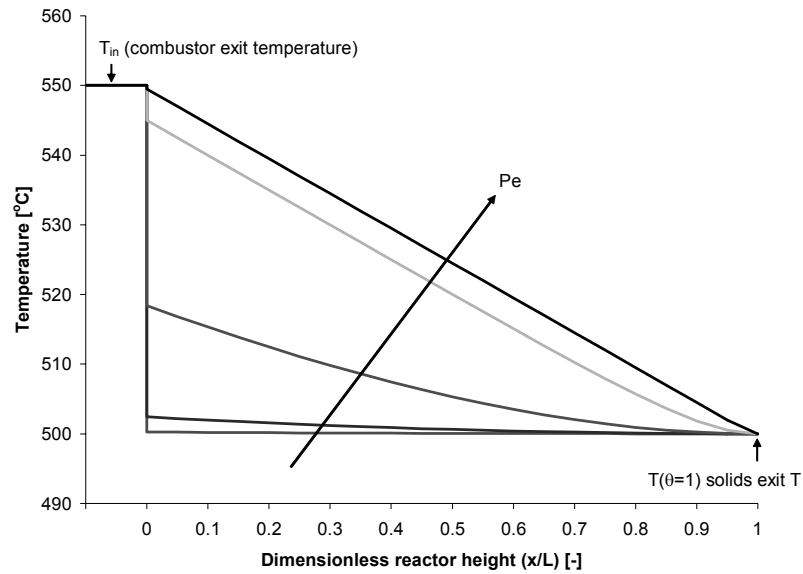
168

Figure 5. Axial temperature profiles in a fluid bed pyrolysis reactor with an intake of 10 ton per hour, other conditions and assumptions see text above. Pe = 0.01, 0.1, 1, 10, 100.

Using the data on solids mixing collected by Van Deemter [23], the Pe number for the reactor under consideration in Figure 1 can be calculated and is ca. 1.8. This Pe number results in an axial averaged bed temperature of $510^{\circ}C$ and an intra-bed temperature gradient of $27^{\circ}C$. These calculations indicate that when using relative small biomass particles to ensure good mixing, a regular fluid bed pyrolysis reactor can be operated at nearly isothermal conditions. How filtering and therewith possible process intensification affects the intra-bed temperature distribution, is discussed in the results section.

The influence of the sand recirculation rate over the biomass feed rate ratio (Φ) on the energy balance of a regular fluid bed pyrolysis reactor is explained in Figure 6. In Figure 6, the required combustor temperature, the intra-bed temperature gradient and the difference between the combustor temperature and the reactor exit temperature of solids from the pyrolysis reactor is plotted versus Φ. For these calculations the heat for pyrolysis is assumed to be 1.5 MJ/kg. The intake is 10 ton per hour and axial averaged pyrolysis bed temperature is set at $500^{\circ}C$. Solids mixing is calculated with the solids dispersion coefficient data collected by Van Deemter [23]. For design calculations on the FAFB system, the solids dispersion coefficient of Van Deemter is

169

multiplied with a correction factor accounting for the extraction of gases and vapors via filters. The correction factor has the value of 1 divided by 2.5 (see Chapter 4).
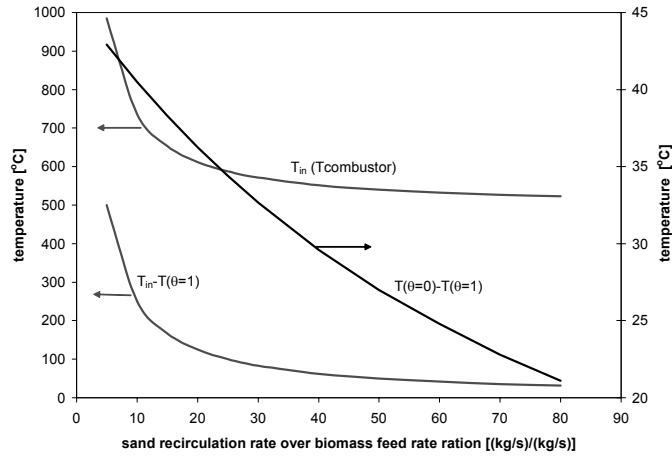

Figure 6. Effect of Φ on the required temperature of the combustor, the intra-bed temperature gradient and the difference between the combustor temperature and the exit temperature of circulating solids from the pyrolysis reactor. Pe = 1.8, Q_p = 0.72 MJ/m^3 bed.

The calculations show that above Φ =30, Φ hardly affects the required temperature of the combustor. For smaller values of Φ, the required combustor temperature increases quickly leading to more advanced and expensive construction materials and higher sensible heat losses. The intra-bed temperature gradient of the pyrolysis reactor is acceptable for all investigated cases and limited to 50°C. For the reactor design Φ =30 is selected.

3.3   Reacting Particle Hold-up Calculation

To estimate the required hold-up of reacting particles in the fluid bed, predictions of a single particle pyrolysis model (see Chapter 2) are combined with a population balance model. Reacting particles include the fresh feed, completely devolatized particles (char) and partly converted biomass. From the one-dimensional single particle pyrolysis model, information on the reaction rate is extracted. In the simulations, the kinetic data of Chan et al. [24] have been used. These kinetic data provide the best agreement with beech wood pyrolysis experiments concerning the conversion time (see Chapter 3), which indicates that also the reaction rate is predicted accurately. The population balance assumes that i) the feed consist of

170

particles of single density and particle size, ii) the size of the particles does not change during their conversion; only the density changes, iii) the reacting particles are ideally mixed in the fluid bed and, iv) the out flow of a certain class of reacting particles is proportional to its mass fraction. A fluid bed pyrolysis reactor with an overflow to transport the sand-char mixture to the combustor (see Figure 7) tends to comply to the third and fourth assumption provided that relatively small biomass particles are used. Mixing tests have shown that wood and char particles with a diameter up to 5 mm can be mixed rather well in a sand fluid bed operated at above 5 x U_{mf} (see Appendix 1). For this system the population balance, with the particle density as independent variable, is given by Kuni, Levenspiel and Fitzgerald [25]:

Equation numbers

$$0 = F_0 - F_1\Psi_1(\rho) - MR(\rho)\frac{d\Psi_1(\rho)}{d\rho} - M\Psi_1(\rho)\frac{dR(\rho)}{d\rho} + \frac{MR(\rho)\Psi_1(\rho)}{\rho} \qquad (10)$$

With boundary condition:

$$\Psi_1(\rho_f) = -\frac{F_0}{MR(\rho_f)} \qquad (11)$$

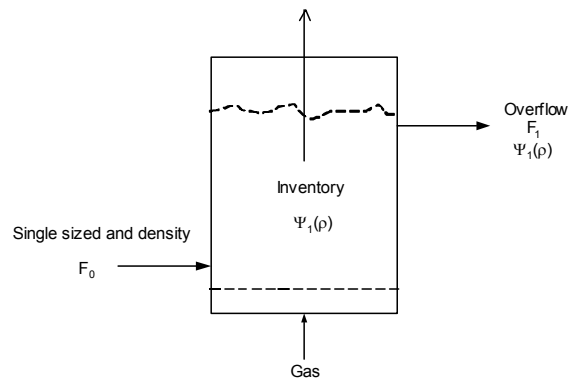Figure 7 is a schematic presentation of the reacting particle hold-up model.

Figure 7. Schematic representation of reacting particle hold-up model. F_o is the feed rate of single sized biomass particles. F_1 is the rate at which reacting particles (fresh feed, particles in transition from biomass to char and char) are removed from the reactor.

The first and second terms of the right hand side of this equation represent the flow of particles in (F_0) and out ($F_1\Psi_1$) the fluid bed. The changing position of particles within the density distribution is described by the terms three and four. The decrease in density of a particle due to the pyrolysis reaction is described by the fifth term. In Equations 10 and 11, $\Psi_1(\rho)$ (m^3/kg) is the particle density distribution function, F_0 the flow rate of the ingoing biomass particles (kg/s), F_1 the flow rate of the outgoing particles, $R(\rho)$ the reaction rate of a single particle, ρ the density and M the total mass of reacting particles in the bed. F_1/F_0 is the overflow ratio and is defined as mass flow of reacting particles that leaves the system via the overflow over the feed rate (mass basis).

In case of very small particles, the pyrolysis process is kinetically controlled and the reaction rate, $R(\rho)$, is described by:

$$R(\rho) = -k(\rho - \rho_\infty) \tag{12}$$

For this limiting case, the equations can be solved analytically. The expressions for Ψ_1, M (mass of reacting particles) and V_{rp} (volume of reacting particles) are then given by:

$$\psi_1(\rho) = \frac{F_0}{Mk(\rho - \rho_\infty)} \frac{\rho}{\rho_f} \frac{\rho - \rho_\infty}{\rho_f - \rho_\infty}^{\frac{F_1}{Mk}} \tag{13}$$

$$M = \frac{1 - \dfrac{F_1}{F_0}}{(\dfrac{k}{F_0} - \dfrac{k}{F_1}\dfrac{\rho_\infty}{\rho_f})} \tag{14}$$

$$V_{rp} = \frac{-F_0(F_0 - F_1)}{k(F_0\rho_\infty - F_1\rho_1)} \tag{15}$$

In all other cases, the $R(\rho)$ function is obtained from the single particle pyrolysis model (see Chapter 2) and the population balance is solved numerically by the finite volume method.

172

Dry wood particles with $l_p/d_p > 3$ and a typical density of 600 kg/m$^3_{particle}$ have been used in the simulations. Other model parameters are listed in Table 2 of Chapter 2. With the single particle model, the reaction rate in kg/m$^3_{particle}$/s of a particle with certain size can be calculated at very point in its conversion trajectory. In Figure 8, the reaction rate is plotted versus the conversion for particles of various sizes. For the very small particle with a diameter of 0.1 mm heat transfer to and within the particle is much faster than the chemical kinetics. As a result, the whole conversion takes place at the reactor temperature (assuming $\Delta H = 0$, see Chapter 2) and the reaction rate can be described by a first order rate equation. Somewhat larger particles of 1mm are already not chemically controlled anymore. For these particles the conversion takes place partially in the heating phase, ranging from the temperature of the fresh feed to the reactor temperature. The reaction rate drops compared to particles of 0.1 mm, especially in the high density region close to the density of the feedstock (low conversion). Particles of 3 and 5 mm suffer even more from the fact that heat transfer to the particle is the dominant factor in the conversion process. In addition, particles of 3 and 5 mm also have significant intra-particle gradients lowering the overall reaction rate. The density averaged reaction rate of particles with diameters of 0.1, 1, 3, and 5 mm are 75.6, 60.0, 28.2, and 14.0 kg/(m$^3_{particle}$/s), respectively.

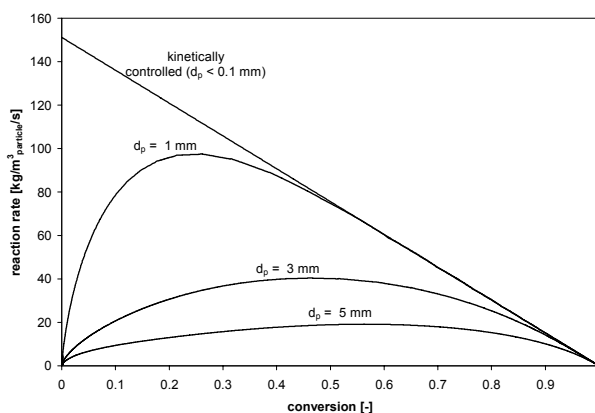**Figure 8** Calculated reaction rate of particles with diameters of 0.1, 1, 3, and 5 mm versus their conversion. Initial density = 600 kg/m$^3_{particle}$, moisture content = 0 wt %, for other parameters see Table 1 of Chapter 2.

With the population balance, it is investigated how the particle size and thus the reaction rate affects the required hold-up of reacting particles in the fluid bed. The equation to calculate the required hold-up has a positive pole at $F_1/F_0 = \rho_\infty/\rho_f$ (ρ_∞/ρ_f = char yield of individual particles at infinite time, Y_{char}). This means when the overflow ratio (F_1/F_0) approaches the char yield of individual particles, the required hold-up increases rapidly (see Figure 9a). In this region, the vast majority of the reacting particles in the fluid bed are char particles (see Figure 9b). For higher overflow ratios the required hold-up of reacting particles decreases. However, at higher overflow ratios a considerable part of the particles leaving the reactor are only partly converted (see Figures 9c and 9d).
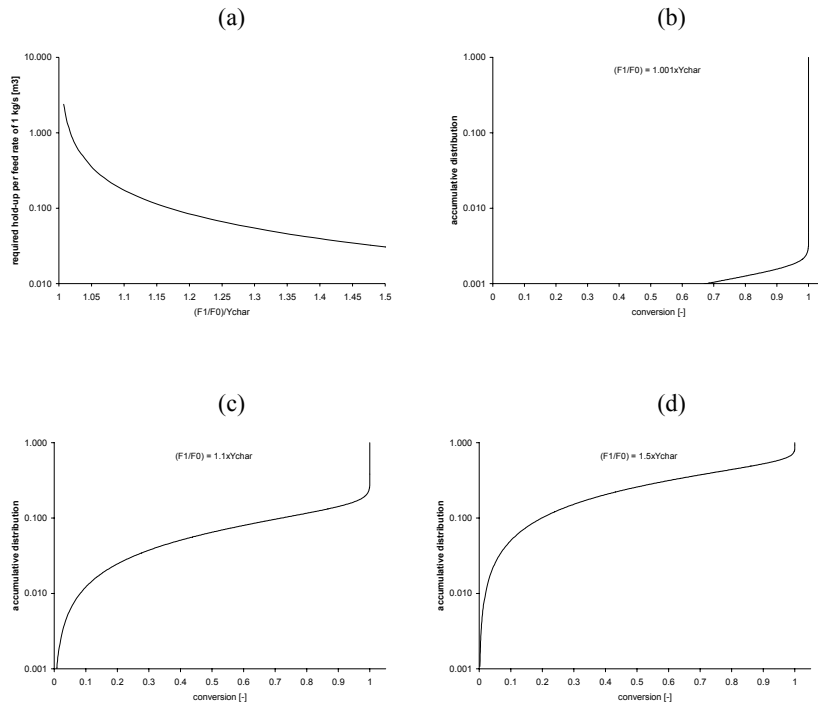

(a)

(b)

(c)

(d)

Figure 9 Reacting particles distribution function for kinetically controlled pyrolysis conditions. (a) Required hold-up of reacting particles per kg/s feed versus $(F_1/F_0)/Y_{char}$; (b) Accumulative distribution versus the particle's conversion for $(F_1/F_0)/Y_{char} = 1.001$; (c) Accumulative distribution for $(F_1/F_0)/Y_{char} = 1.1$. (d) Accumulative distribution for $(F_1/F_0)/Y_{char} = 1.5$.

174

Figure 10 shows the required hold-up of reacting particles in the fluid bed (for a feed rate of 1 kg/s) versus the over-flow ratio for particles of different diameter. The decreased reaction rate of larger particles has a profound effect on the required hold-up. At an overflow ratio of 1.2 times the ultimate char yield of the individual particles, the required hold-up is 0.08, 0.12, 0.3, and 0.54 m^3 per 1 kg/s feed for particles of < 0.1, 1, 3, and 5 mm in diameter. Concluding, when increasing the particle size from very small shreds to 5 mm the required hold-up increases by a factor 7. This has serious consequences for reactor design, because in order have an ideally mixed bed of sand and biomass particles the allowed fraction of reacting particles is limited.

Selecting the over-flow ratio is a trade-off between a low hold-up of reacting particles (high overflow ratio) and a low loss of not completely de-volatilized particles (low overflow ration). For the design of the FAFB, an overflow ratio of 1.1 has been selected.
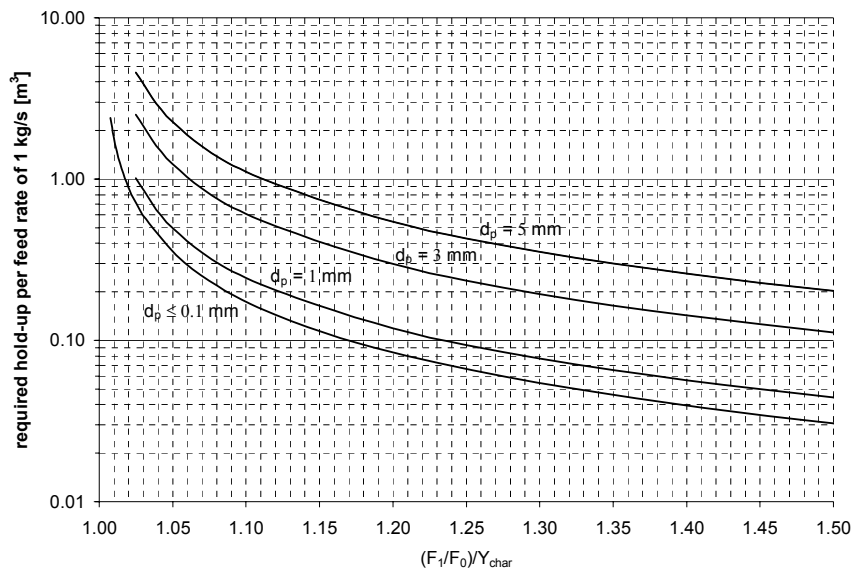

Figure 10. Required hold-up of reacting particles in the fluid bed (for a feed rate of 1 kg/s) versus the over-flow ratio for particles of different diameter.

Overall Design

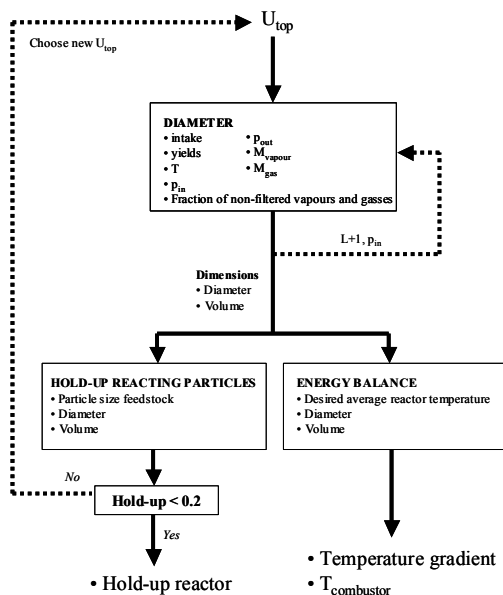The calculation scheme is given below.

Figure 11. Calculation algorithm flow diagram for overall design.

The reactor design calculations have been done for different feedstock particle sizes, viz. ≤ 0.1 mm, 1 mm, 3 mm, and 5 mm. With increasing feedstock particle size, the required volume of reacting particles in the bed increases (see Figure 12) because heat transport limitations lower the overall pyrolysis rate. Design choices and assumptions are listed in Table 2.

Table 2. Design choices and assumptions.

| Feedstock | – Dry wood, 10 ton/hour |
	– Single sized ($\leq$ 5 mm) and density particles
	– Decomposition kinetics of Chan [24]
	– Density : 600 kg/m^3
Products	– Yields and LHVs as in Table 1
	– Molar mass vapors = 150 g/mol
	– Molar mass gases = 35 g/mol
Bed geometry	– L/D = 2, l/L=1/3, d/D=1/3, ID/D=1.5,IL/L=1/2
	– Feeding in cone
	– Overflow ratio = 1.1 x Y char
Bed material Mixing	– Sand particles, 300 μm.
	– Reacting particles spatially uniform mixed
	– Particle motion described by SDM.
Process heat	– Heat for pyrolysis = 1.5 MJ/kg
	– Combustion of non-filtered vapors/gases
	– Φ = 30
Filtering	– 83% of vapors and permanent gases
	– Filter volume ~ 0.20 m^3
Temperatures, Pressure	– Reactor (average) temperature = 500°C
	– Combustor ~ 550°C
	– Pressure on top of bed = 1.2 bar

177
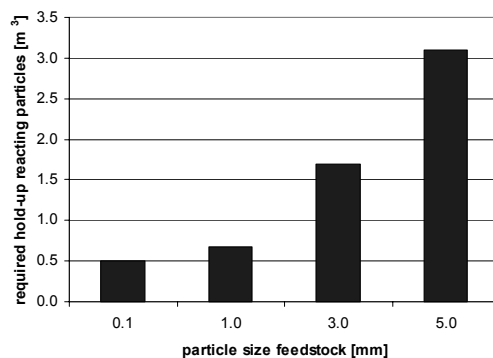
Figure 12. Required volume of reacting particles in the bed for different particle sizes of the feedstock.

Conventional FB (without filters)

As a reference point, calculations have been done for a system without filters, i.e. a conventional fluid bed pyrolysis reactor (with conical section). The first calculations were done for very small feedstock particles of less than 0.1 mm (see Table 3 and Figure 13a for the results). For such a system, the volume of the reactor is determined by the velocity at the top of the bed. In the design, the velocity at the top of the bed has been set to 0.5 m/s in order to keep the reactor volume limited. Bed particles of 300 mm have been selected, resulting in turbulent fluidization (U_{top}= 45 x U_{mf}), but remaining well below the terminal velocity (U_{top}=0.38 x U_t). The reactor volume is ca. 22 m^3 (L = 3.66 m, D = 1.83) and the hold-up of reacting particles has an acceptable low value of ca. 9 vol %. This reactor can also accommodate particles of up to 1 mm. The reactor of 22 m^3 cannot handle particles of 3 and 5 mm, because the hold-up of reacting particles becomes too high. To keep the hold-up below the upper limit, the reactor volume has been increased to ca. 37 and 62 m^3 for particles of 3 and 5 mm respectively (see Table 3 and Figure 13a). For all considered cases, the energy did not cause any problems; for the selected sand recirculation rate the intra bed temperature gradient is limited to ca. 20°C.

FAFB

If filters are placed in a fluid bed that extract the majority of the produced vapors and permanent gases (83%), the velocity at the top of the bed decreases if the reactor volume is kept equal. For instance, when filters would be placed in the conventional pyrolysis FB reactor of ca. 22 m^3 (small particles feedstock), the velocity at the top of bed reduces to 0.1 m/s. Intensification of the reactor can then be achieved by increasing again the velocity on top of the bed by reducing the bed diameter, while keeping the hold-up of reacting particles below the limit. For feedstock particles of 0.1 mm in size or smaller, the reactor volume can be reduced to 13 m^3 (see Table 4 and Figure 13b) being half the size of the conventional FB without filters. 1 mm feedstock particles cannot be processed in this 13 m^3 reactor, because the hold-up of reacting particles exceeds the upper limit. Increasing the reactor volume to 17 m^3 yields a design, which satisfies the upper limit of the hold-up of reacting particles (see Table 4 and Figure 13b). For particles of 3 mm or larger, intensification by side-wise extraction of vapors from the reactor is not possible anymore (compare Table 3 and 4). For these particles sizes, the reaction rate and therewith the hold-up of reacting particles dominates the reactor design. The actual design then comes down to selecting a reactor volume (and aspect ratio), which keeps the hold-up of reacting particles below the limit that ensures good mixing of feed particles while also respecting the criterion for having a sufficiently high velocity at the top of the bed to prevent malfunctioning of the bed with respect to isothermal operation.

In case of 5 mm particles, another bed particle size (200 μm instead of 300 μm) has to be selected in order to satisfy the $U_{top}/U_{mf} > 7$ criterion.

Table 3. Reactor designs for a conventional fluid bed (without filters).

	Particle size feedstock			
	≤ 0.1 mm	1 mm	3 mm	5 mm
$V_{reactor}$ (inc. freeboard), m^3	22.1	22.1	37.4	61.9
L_{cyl}, m	3.66	3.66	4.37	5.17
D_{cyl}, m	1.83	1.83	2.18	2.58
d_p, micron	300	300	300	300
U_{top}, m/s	0.50	0.50	0.35	0.25
U_{top}/U_{mf}, -	45.5	45.5	31.9	22.8
U_{top}/U_t, -	0.38	0.38	0.27	0.19
β, -	0.09	0.12	0.18	0.19
Combustor temperature, ^{o}C	550	550	553	555
Intra-bed ΔT, ^{o}C	20.8	20.8	17.5	14.5

Table 4. Reactor designs for a the FAFB.

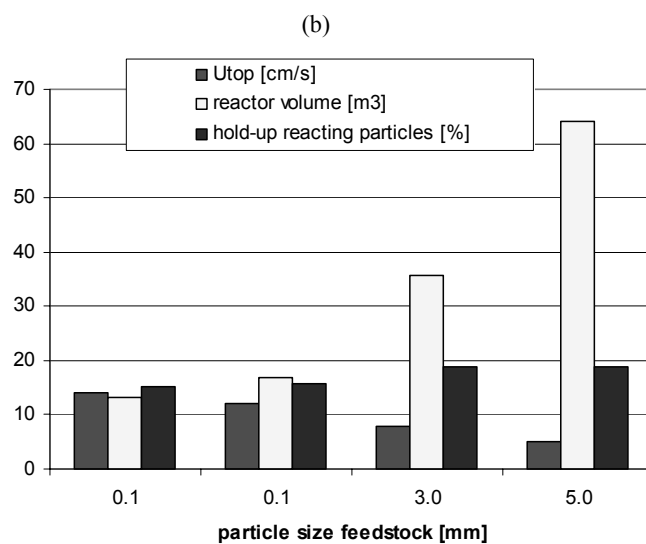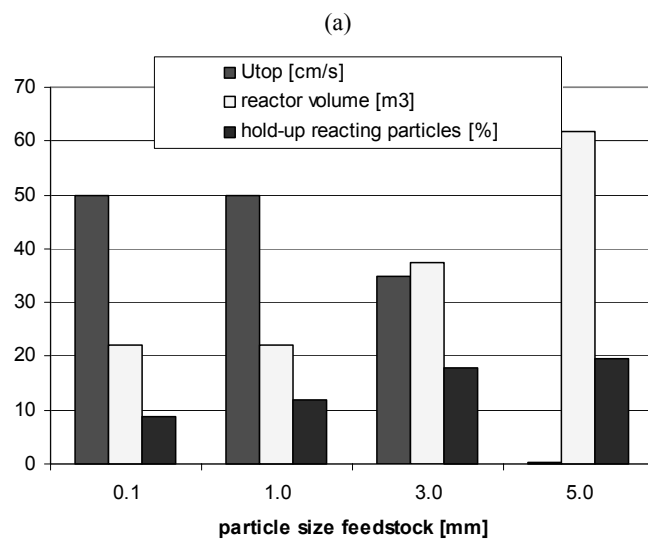|	Particle size feedstock			
	≤ 0.1 mm	1 mm	3 mm	5 mm
$V_{reactor}$, m^3	13.1	17.0	35.6	64.1
L_{cyl}, m	3.08	3.08	4.30	5.22
D_{cyl}, m	1.54	1.68	2.15	2.61
d_p, micron	300	300	300	200
U_{top}, m/s	0.14	0.12	0.08	0.05
U_{top}/U_{mf}, -	12.7	10.9	7.3	12.3
U_{top}/U_t, -	0.11	0.09	0.06	0.07
β, -	0.15	0.16	0.19	0.19
Combustor temperature, ^{o}C	543	544	545	547
Intra-bed ΔT, ^{o}C	37.0	34.0	27.0	22.0

180

(a)

(b)

Figure 13. Main results of the design calculations, a) conventional FB (without filters), b) FAFB.

Conclusions

Design calculations have been performed to estimate the volume of a FAFB pyrolysis reactor with an intake of 10 tonnes biomass per hour. Experimental data on the reaction rate and solids mixing while extracting large amounts of gases and vapors, obtained in Chapters 3 and 4 respectively, have been incorporated in the model. The conclusions can be summarized as follows.

- Burning the non-filtered gases and vapors (~17% of the totally produced amount) can provide the heat for pyrolysis. In this way the oil yield is somewhat lowered compared to the conventional case where char is burned (from 61 to 51%). However, char, which presents ca. 30% of the LHV of the feedstock, is added to the product slate;

- By feeding the biomass in the conical bottom section of the reactor, the use of additional fluidization gas can be limited to a large extent;

- The volume of the installed filters can be neglected relatively to the bed volume;

- Under filtering conditions, mixing of solids remains good enough to keep the intra-bed temperature gradient below 50°C;

- When feeding small particles of $d_p \leq 1$ mm and $\rho = 600$ kg/m^3 (typical for wood), the required FAFB reactor volume is 13 m^3 including the freeboard, compared to 22 m^3 for a regular fluid bed;

- For larger sized feedstocks intensification is hardly possible. The particle size of the feedstock influences the required reactor volume. Larger particles have a lower reaction (pyrolysis) rate, expressed in kg/m$^3_{particle}$, leading to a higher required absolute hold-up of reacting particles (m$^3_{reacting\ particles}$) to accommodate a certain intake. Because there is a maximum to the relative hold-up of reacting particles (β, m$^3_{reacting\ particles}$/m$^3_{total\ bed\ particles}$) to ensure good solids mixing, the required reaction volume increases for larger feedstock particles.

Appendix I: Mixing of Biomass Particles in a Fluid Bed under Pyrolysis Conditions

To visually verify that biomass particles mix well in a fluidized bed, combustion experiments were done at pyrolysis conditions (T $\approx$ 500 °C and atmospheric pressure). Wood particles (size up to 5 mm and a density around 600 kg/m$^3_{particle}$) and char fines (d_p < 1 mm) were introduced into a hot fluidized bed (U = 5 x U_{mf}), using air as fluidizing gas. The combustion was recorded in time using a video camera. Reacting particle bed mixing could be observed by the light being produced by the combustion. Figure 14 shows photos of both combustion of wood particles (a and b) and char fines (c and d).

Figure 14. Photos of the combustion of wood particles (a and b) and char fines (c and d) in a fluidized bed, using air as fluidizing gas. T $\approx$ 500 °C, U = 5 x U_{mf}, atmospheric pressure. The whole bed is visualized.

(a)　　　　　　　　　(b)

(c)　　　　　　　　　(d)
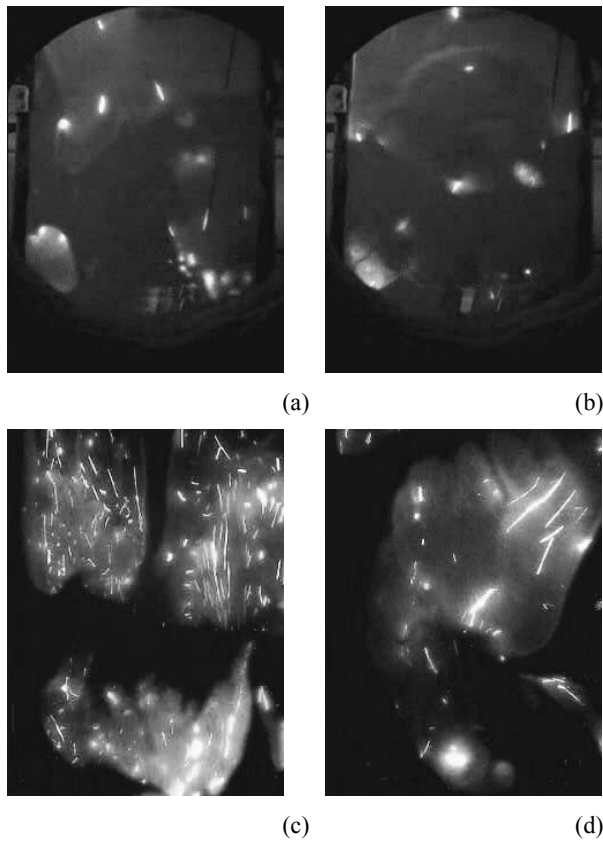
As can be seen in Figure 14, the light production (i.e. combustion of reacting particle) is distributed over the whole bed indicating good mixing of the reacting particles in the fluidized bed.

List of Symbols

A_r	Cross sectional area of the reactor	m^2
Cp	Heat capacity	$J\ kg^{-1}\ K^{-1}$
D	Dispersion coefficient bed material	$m^2\ s^{-1}$
D_{cyl}	Diameter of cylinder	m
d_p	Particle diameter	m
F_0	Reacting particle ingoing	kg/s
F_1	Reacting particle outgoing	kg/s
F_{bio}	Biomass intake	kg/s
h	Height fluid bed	M
k	Reaction rate of particle	s^{-1}
L	Total reactor length	m
L_{cyl}	Length of cylinder	m
l_p	Length particle	m
M	Mass of reacting particle	kg
$\dot{Q}_p$	Heat for pyrolysis	$J/kg_{biomass}$
$\overline{Q}_p$	Dimensionless heat for pyrolysis ($\dot{Q}_p\ L^2\ D^{-1}\ \varepsilon^{-1}\ \rho^{-1}\ Cp^{-1}$)	K
Q_{loss}	Heat losses	W
Q_p	Heat for pyrolysis	$W\ m^{-3}$
Q_{steam}	Heat available from steam production	W
$Q_{waste\ heat\ boiler}$	Heat available from waste heat boiler	W
R	Reaction rate single particle	$kg\ m^{-3}\ s^{-1}$
T	Temperature	K
t	Time	s
T_{in}	Temperature combustor	K
T_{out}	Temperature pyrolysis	K
U_{mf}	Minimal fluidization velocity	$m\ s^{-1}$
u_{sand}	Velocity of sand inside the reactor	$m\ s^{-1}$
U_t	Terminal velocity	$m\ s^{-1}$

184

U_{top}	Velocity at the top of the fluid bed	$m\ s^{-1}$
$V_{reactor}$	Volume of reactor	m^3
V_{rp}	Volume of reacting particles	m^3
x	Reactor length (from 0 to L)	m
Y_{char}	Char yield at infinite time	-
$Y_{energetic}$	Fraction of the LHV of the feedstock that ends up in the products oil, char, steam, and waste-heat	-

Greek

ε	Solids fraction	-
Φ	Ratio of sand recirculation rate over biomass intake	-
ρ	Density	$kg\ m^{-3}$
ρ_f	Density feed (biomass)	$kg\ m^{-3}$
ρ_∞	Density char (complete devolitization)	$kg\ m^{-3}$
Θ_{sand}	Sand circulation rate	kg/s
θ	Dimensionless length reactor ($x\ L^{-1}$)	-
Ψ_1	Particle density distribution function	-

Dimensionless Numbers

| Pe | Peclet number ($L\ u\ \varepsilon^{-1}\ D^{-1}$) | - |

References

1. Scott, D.S., et al., A second look at fast pyrolysis of biomass - the RTI process; J. Anal. Pyrolysis, 1999, 51, pp. 23-37.

2. Scott, D.S., Piskorz, J., The flash pyrolysis of Aspen-Polar wood; Can. J. Chem. Eng., 1982, 60, pp. 666-674.

3. Scott, D.S., Piskorz, J., The continuous flash pyrolysis of biomass; Can. J. Chem. Eng., 1984, 62, pp. 291-294.

4. Scott, D.S., Piskorz, J., Radlein, D., The role of temperature in the fast pyrolysis of cellulose and wood; Ind. Eng. Chem. Res., 1988, 27, pp. 8-15.

5. Scott, D.S., Piskorz, J., Radlein, D., Liquid products from the continuous flash pyrolysis of biomass; Ind. Eng. Chem. Prod., 1988, 24, pp. 581-588.

185

6.   Scott, D.S, et al., Flash pyrolysis of peat in a fluidized bed, Fuel; Process. Technol., 1988, 18, pp. 81-95.

7.   Agblevor, F.A., Besler, S., Evans, R.J., Inorganic compounds in biomass feedstocks: their role in char formation and effect on the quality of fast pyrolysis oils; Proceedings of biomass pyrolysis oil properties and combustion meeting; National Renewable Energy Laboratory, Estes Park, CO, 1994.

8.   Horne, P.A., Williams, P.T., Influence of temperature on the products from the flash pyrolysis of biomass; Fuel, 1996, 75, pp. 1051-1059.

9.   Peacocke G.V.C., Ablative pyrolysis of biomass; Ph.D. Thesis, Aston University, Birmingham, UK, 1994.

10.   Peacocke G.V.C., et al., Effect of reactor configuration on the yields and structures of pine-wood derived pyrolysis liquids: A comparison between ablative and wire-mesh pyrolysis; Biomass Bioenergy, 1994, 7, pp. 155-167.

11.   Peacocke G.V.C., et al., Comparison of ablative and fluid bed fast pyrolysis products: yields and analysis, Developments in thermochemical biomass conversion; Bridgwater, A.V., Boocock, D.G.B., Eds., Blackie Academic & Professional, London, UK, 1997, pp 191-205.

12.   Hague, R.A., The pre-treatment and pyrolysis of biomass for the production of liquids for fuel and specialty chemicals; Ph.D. Thesis, Aston University, Birmingham, UK, 1998.

13.   Bilbao, R., et al., Experimental and theoretical study of the ignition and smouldering of wood including convective effects; Combust. Flame, 2001, 126, pp. 1363-1372.

14.   Luo, Z., et al., Research on biomass fast pyrolysis for liquid fuel; Biomass Bioenergy, 2004, 26, pp. 455-462.

15.   Olazar, M., et al., Kinetic study of fast pyrolysis of sawdust in a conical spouted bed reactor in the range 400-500°C; J. Chem. Technol. Biotechnol., 2001, 76, pp. 469-476.

16.   Kersten S.R.A., Biomass gasification in circulating fluidized beds; Ph.D. Thesis, Twente University, Enschede, The Netherlands, 2002.

17.   Bridgwater, A.V., et al., Fast pyrolysis of biomass: a handbook; IEA Bioenergy, CPL Press, Berkshire, UK 1999.

18.   Reed, T.R., Gaur, S., The high heat of fast pyrolysis for large particles, Developments in thermochemical biomass conversion; Bridgwater, A.V., Ed., Blackie Academic & Professional, London, UK, 1993, pp 1343-1357.

19.   Cottam, M.L., Bridgwater A.V., Techno-economics of pyrolysis oil production and upgrading, Developments in thermochemical biomass conversion; Bridgwater, A.V., Boocock, D.G.B., Eds., Blackie Academic & Professional, London, UK, 1997, pp 97-103.

20.   Private communications with W. Prins.

21.   Janse A.M.C., A heat integrated rotating cone reactor system for flash pyrolysis of biomass; Ph.D. Thesis, Twente University, Enschede, The Netherlands, 1998.

22.   Danckwerts, P. V., Continuous flow systems; Chem. Eng. Sci. 1953, 2, pp. 1-13.

23.   Van Deemter, J.J., Chapter 9: Mixing; Proceedings of the international symposium on fluidization, Netherlands University Press, Amsterdam, The Netherlands, 1967, pp 331-355.

24.   Chan, W.C.R., Kelbon, M., Krieger, B.B., Modelling and experimental verification of physical and chemical processes during pyrolysis of a large biomass particle; Fuel, 1985, 64, pp. 1505-1513.

25.   Levenspiel, O., Kunii, D., Fitzgerald, T., The processing of solids of changing size in bubbling fluidized beds; Powder Technology, 1968, 69, pp. 87-96.

Acknowledgements

As early as in 2000, like many other young Chinese students, I was seeking an opportunity to study abroad. Today, five years later, I feel completely satisfied with this decision. It has been a wonderful experience working and meeting with people with diversified backgrounds.

Culmination of this project has resulted not only in this dissertation but also in sharpening the many facets of my personal and professional development. A great number of people have contributed to this thesis, some by making direct contributions and some by making life outside of my motherland more enjoyable. Herewith, I wish to express my gratitude to all of these wonderful people.

Firstly, I would like to thank my academic supervisor Prof. dr.ir. Wim van Swaaij for accepting me as an AIO student in his research group. His expertise in reactor engineering and biomass conversion has provided new insights and elucidations to many theoretical and practical problems during the course of this research. Next, I would like to extend my thanks to Dr. Sascha Kersten and Dr.ir. Wolter Prins, my daily advisors for their patience, guidance and moral supports. I still remember the countless times we had discussion in the office room A 1.12 of Langezijds (CT) building at the University of Twente. Their knowledge and enthusiasm have proven an invaluable contribution to this research.

I am also indebted to Mr. Akse, time flies, but I can not forget my correspondence with him during my application to the University of Twente in August, 2000. Later on when I arrived in Twente, it was you who gave me lots of practical help. Thank you Rik.

I was really fortunate to meet excellent undergraduate, graduate as well as many Ph.D. students whose valuable work contributed to the successful realization of this project. Nina Woicke from the University of Stuttgart, Germany, and Toine Cents did cold-flow experiments. We spent several months together in the laboratory, and without their support the comprehensive experimental program carried out in this part of the thesis would not have been possible.

Dr. Marco Rep and Dragan Knezevic also helped me in deciphering many Dutch documents. It was a great time working with Kim Jansen, Roel Westerhof, Evert

189

Leijenhorst, and particularly Daan Assink, an expert from BTG, who patiently performed the hot flow experiments of biomass pyrolysis.

Johan Agterhorst and Jeffry Kastenberg facilitated the development of critical experimental set-ups. Especially thanks to Bert Koning who helped me debugging the data acquisition system. Dr. Detlef Schmiedl at BFH, Germany and the staff at ENEA, Italy contributed to the analyses of the complicated bio-oil samples and various feedstocks.

I enjoyed the time spent together with our TCCB group members (Biljana Potic, Dragan Knezevic, Guus van Rossum, Mariken Bleeker, Marco Rep) as well as the HDL staff (Gert Banis, Fred ter Borg, Karst van Bree). The delicious barbecue foods and wonderful tours are unforgettable in my life.

It is important to acknowledge the secretarial support, provided in the most efficient and effective manner, by Yvonne Bruggert - ter Huurne and Wies Elfers.

During the last stage of thesis preparation Yvonne, Guus and Dragan gave me lots of help. Thanks a lot, Guys!

Because of the international character of my project, I had got opportunity to travel within the European zone and it was possible to meet many leading authorities in this research area.

During the hot summer of 2005 in Beijing, I was fortunate to get to know Mr. Jianjun Tian, Dr. Megan Clark and Ms. Colleen Walker at BHP Billiton and their support and encouragement is very much appreciated.

Last but not least, I wish to thank my family for their understanding and moral support.

Xiaoquan Wang
Enschede & Beijing
Winter, 2005

Curriculum Vitae

Xiaoquan Wang was born on July 15th, 1969 in Xishui, Hubei Province of China. He obtained his bachelors' degree in Chemical Engineering in 1992 from East China University of Science and Technology in Shanghai, China, followed by two years working as a process engineer at Huangmailing Phosphate Chemical Corp., China from August 1992 till August 1994.

After this he continued his studies in Chemical Engineering at Dalian University of Technology, Liaoning, China, and received his masters' degree in July 1997 with Prof. Jieshan Qiu on the subject of 'Pulverized coal pyrolysis in thermal plasma'.

From September 1997 till January 2001 he was a research assistant in the group of Prof. Jinghai Li and Prof Mooson Kwauk at Multiphase Reaction Laboratory, Institute of Chemical Metallurgy, Chinese Academy of Sciences in the field of fluidization application in clean coal technology.

In February 2001 MSc Wang started his Ph.D. work in the group of Prof. dr. ir. Wim van Swaaij at the University of Twente on the subject of 'In situ cleaning of flash-pyrolysis vapours'.

Since September 1st, 2005 Xiaoquan has been employed by BHP Billiton in Beijing, China as a senior scientist.